

# **Spintronics in Semiconductors**

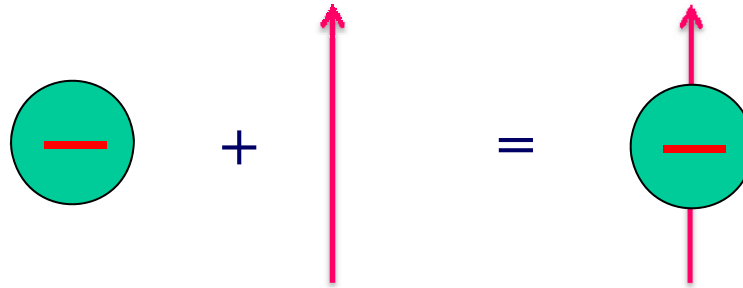
**C.S. Chu**

**Department of Electrophysics  
National Chiao Tung University**

# Outline

- Introduction
- Spin-orbit interaction in semiconductors
- Spin-Hall Effect (SHE)
- Spin Dipole
- Detection of spin current:
  - a nano-mechanical proposal
- Detection of spin current: by inverse SHE
- Spin injection
- Spin-Hall Effect in a non-uniform driving field
- Competition between Spin-orbit interactions
- Quantum Spin-Hall Effect
- Summary

An electron has a **charge  $-e$**  and a **spin  $1/2$**



Electronic industries have made good use of the **charge**.

But the **electron spin** has essentially been neglected.

**Quoted from the abstract of  
“Spintronics: Fundamentals and applications”**

**Spintronics, or spin electronics, involves the study of active control and manipulation of spin degrees of freedom in solid-state systems.**

**in Reviews of Modern Physics,  
vol. 76, p.323-410, 2004,  
by I. Žutić, J. Fabian, and S. Das Sarma.**



# Spintronics

**Where magnetic material and magnetic field is involved:**

- **GMR: giant magneto-resistive effect**
- **Memory / storage**
- **TMR, CMR**

**Spin-based Quantum Computing:**  
uses spin of nuclei as qubits

**All electrical means of generation and manipulation of spins:**

- **spin-polarized transport in semiconductors**
- **spin FET, spin filter**
- **logic / storage**

## **Why spintronics ?**

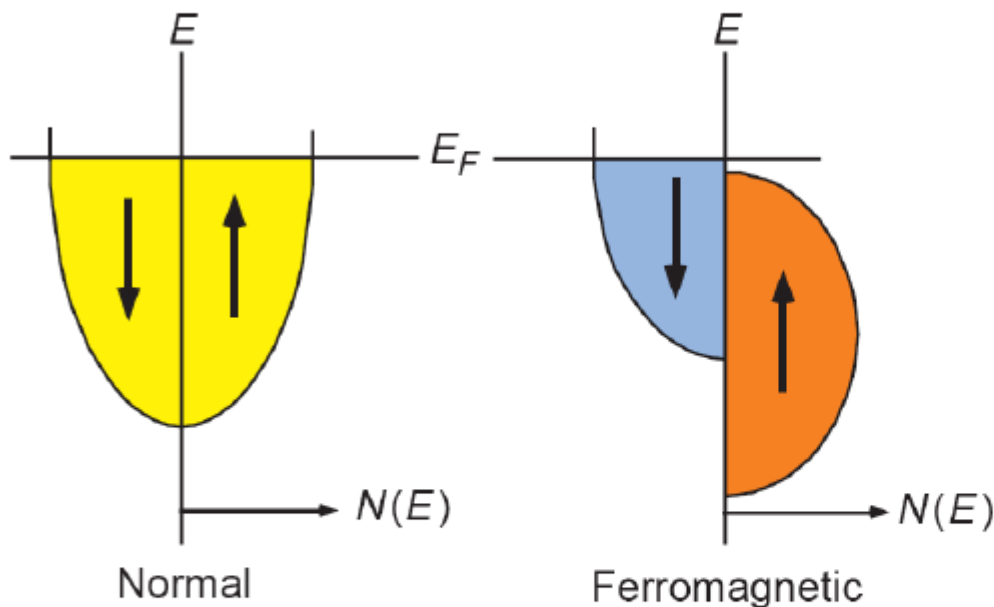
- **new physical principles**
- **new challenges**
- **new working principles for applications**
- **new devices for technologies**
- **potentially decreases electric power consumption**



# Spin-polarized transport

Magnetic materials  
are involved.

schematic DOS



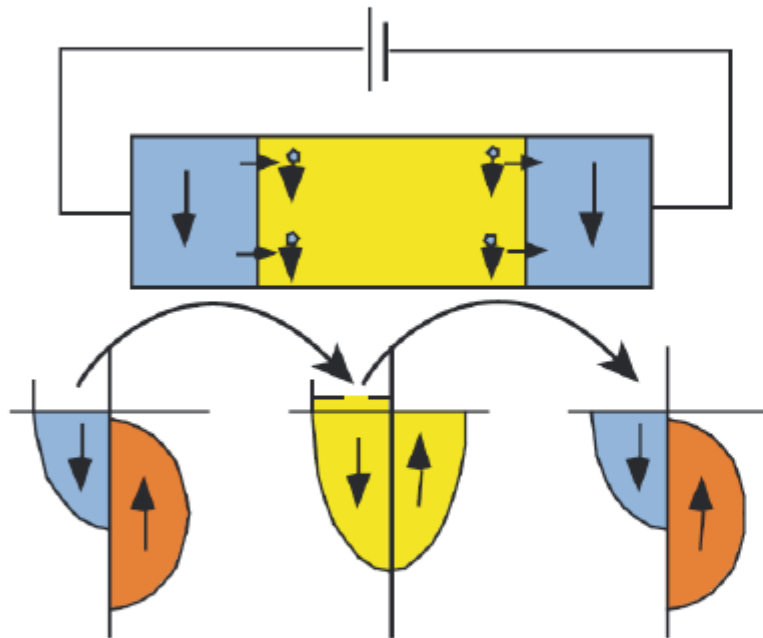
polarization:

$$P = \frac{n_{\uparrow} - n_{\downarrow}}{n_{\uparrow} + n_{\downarrow}}$$

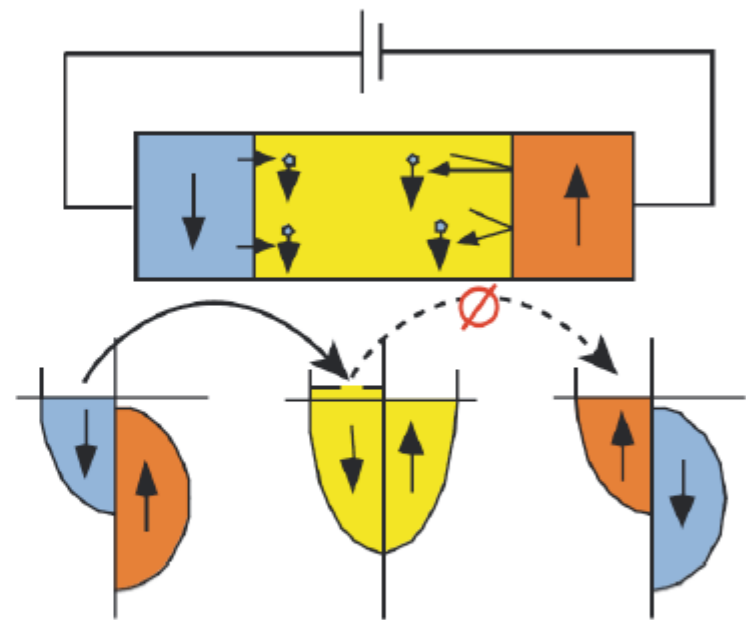
- imbalance of spin population at Fermi level leads naturally to spin-polarized transport
- commonly occurs in ferromagnetic metals (or alloys) with  $P$  up to 50 %

Magnetic materials  
are involved.

# Spin valve

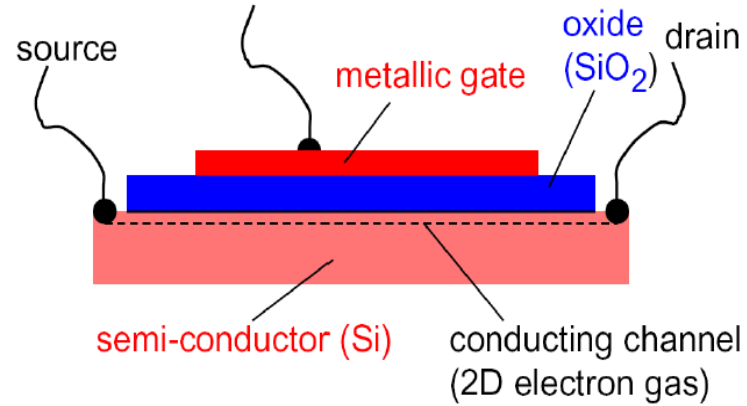


low resistance

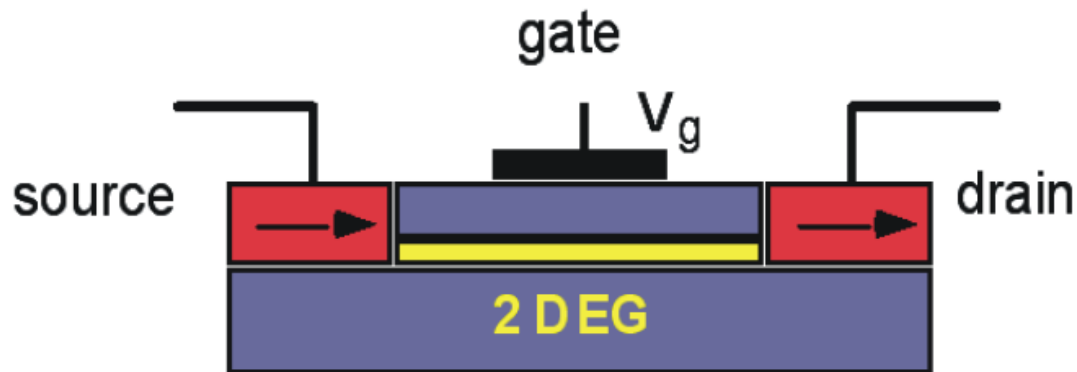


high resistance

## “Normal” transistor (MOSFET)



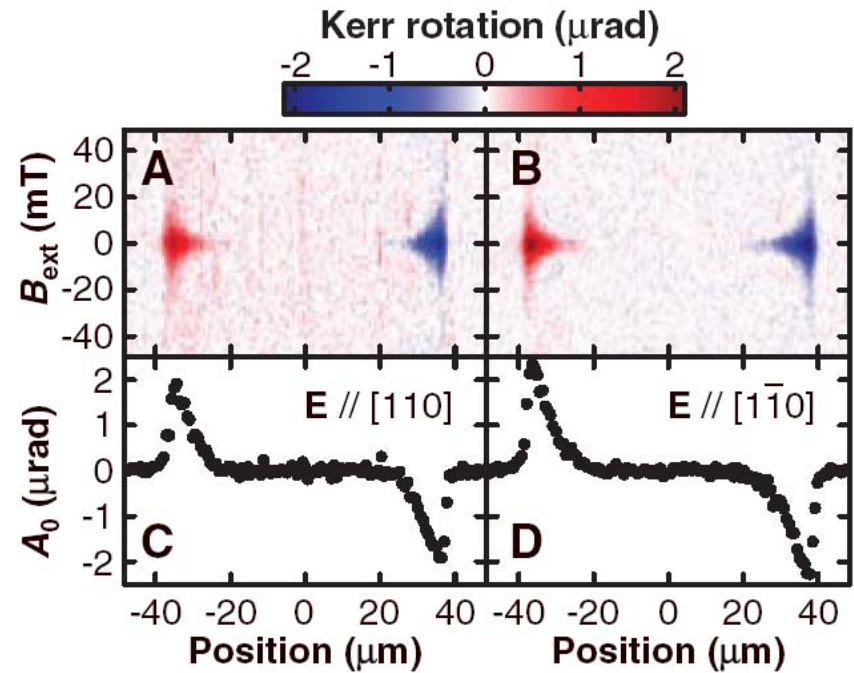
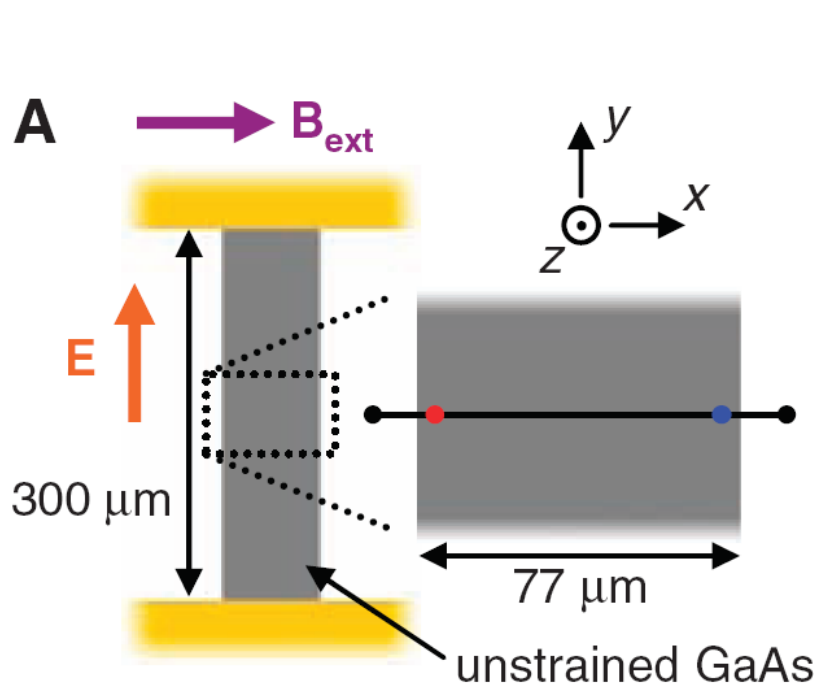
## Spin transistor



Datta and Das

## Why spintronics in semiconductors ?

- compatible with the semiconductor industries
- highly tunable
- spin-orbit interaction (SOI) is much larger than in vacuum
- zero magnetic field spin splitting in samples that has bulk inversion asymmetry (BIA) or structure inversion asymmetry (SIA).



$S_z$  fits well to a Lorentzian function

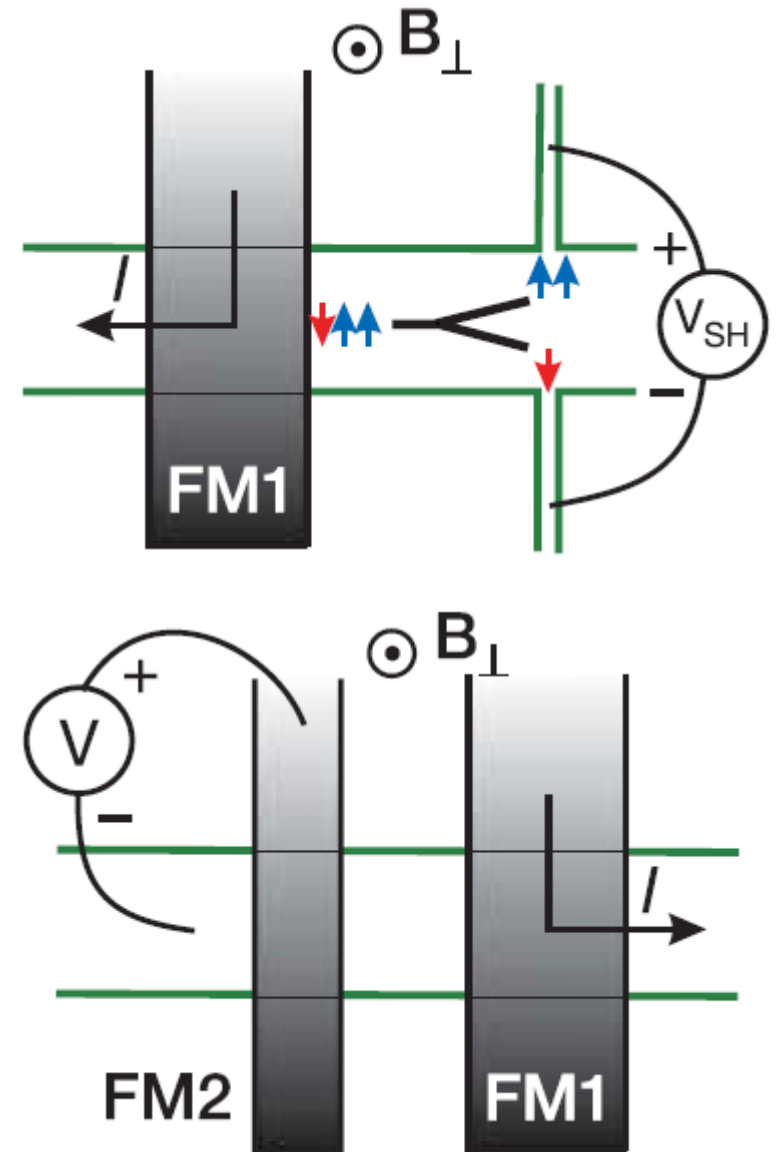
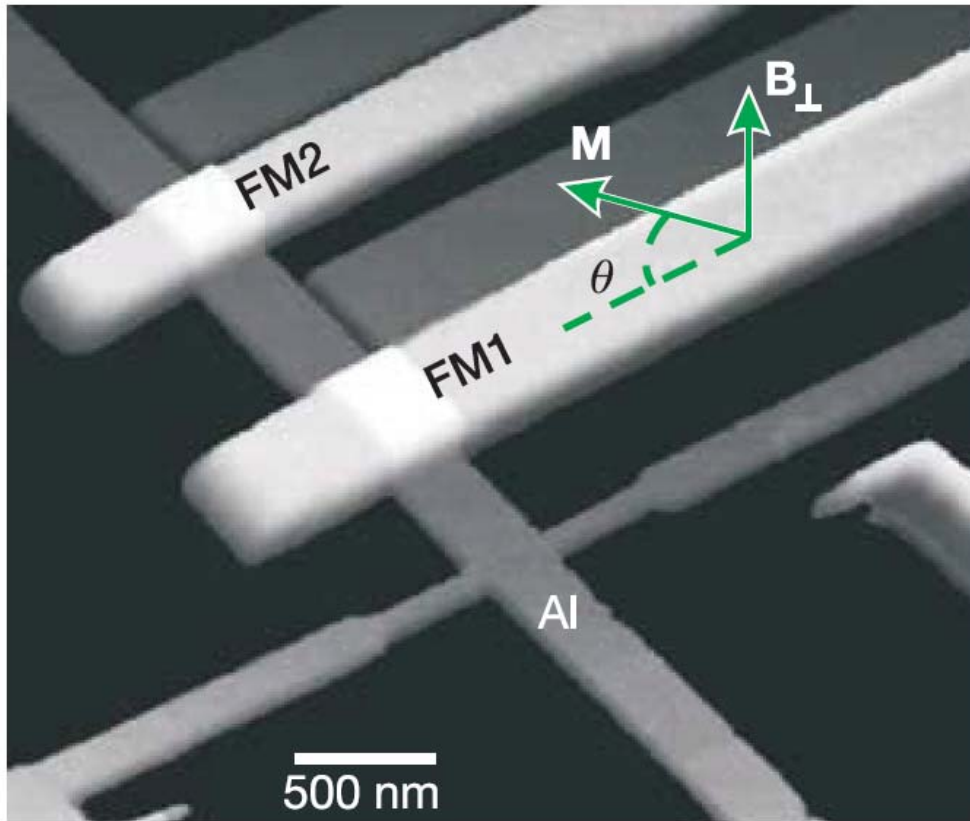
**Experimental observation of extrinsic spin Hall Effect in thin 3D layers (weak dependence on crystal orientation)**

**Y.K. Kato, R.C. Myers, A.C. Gossard, D.D. Awschalom, Science 306, 1910 (2004)**

$$\frac{A_0}{\left[1 + (\omega_L \tau_s)^2\right]}$$

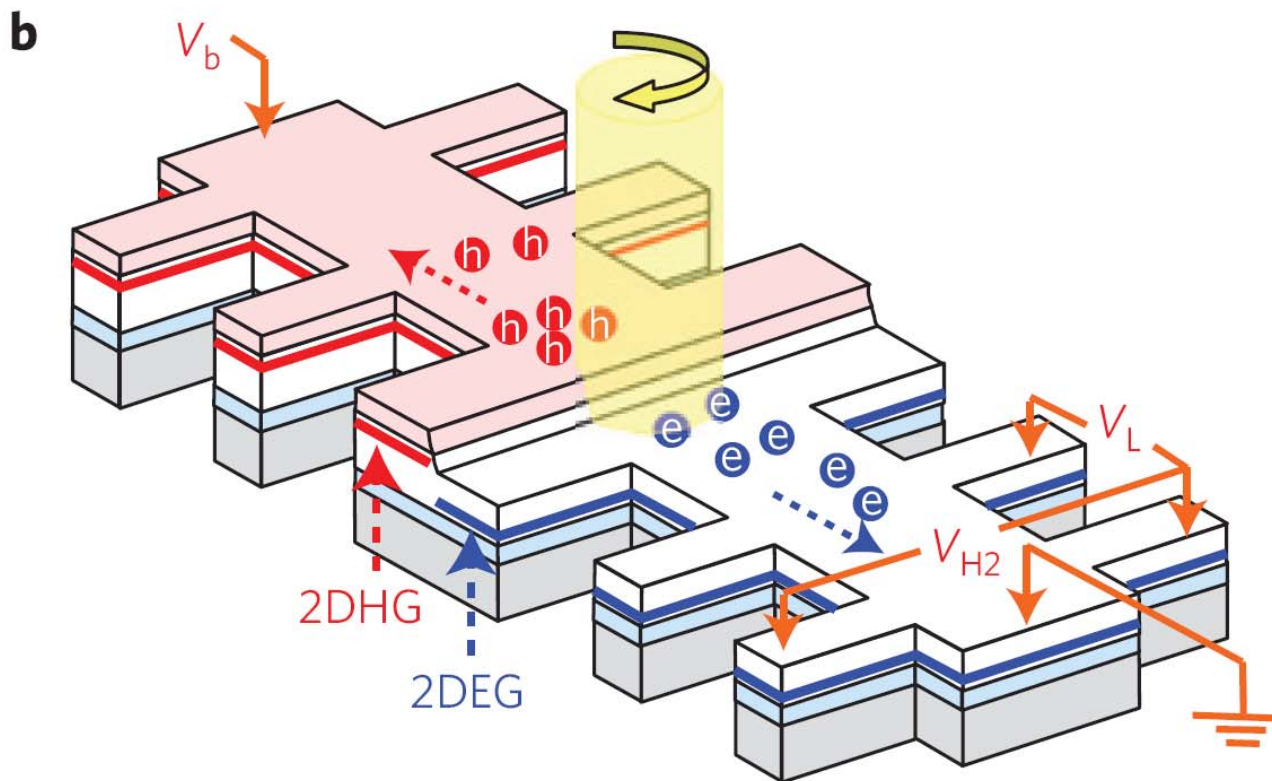
# Direct electronic measurement of the spin Hall effect

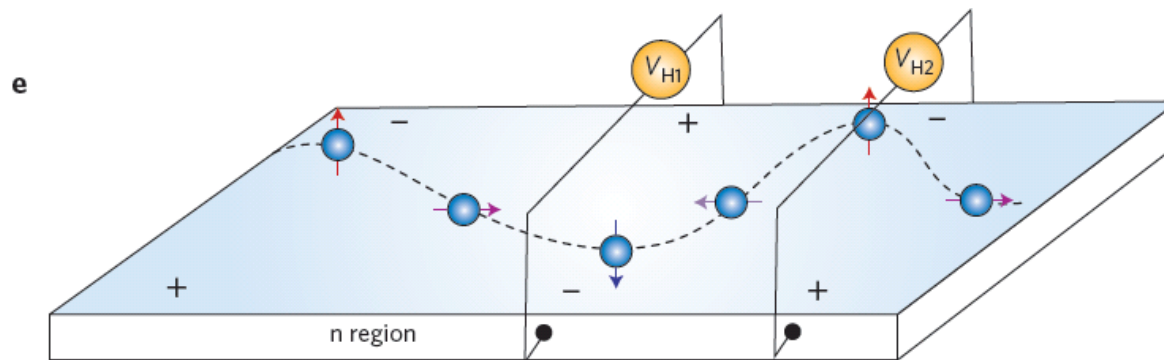
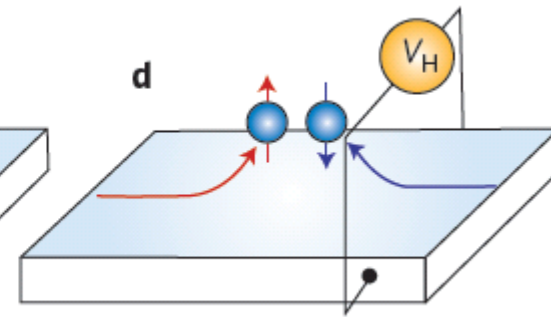
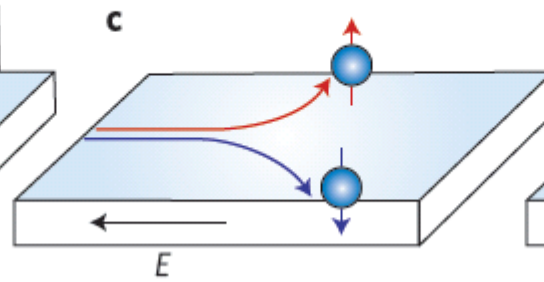
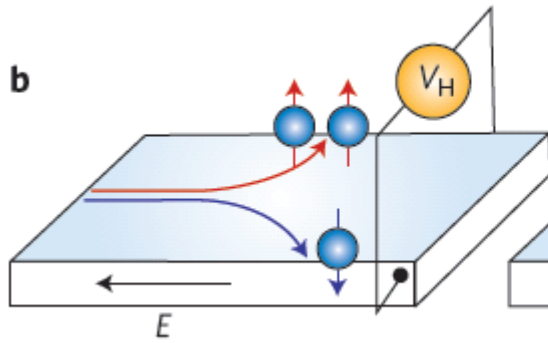
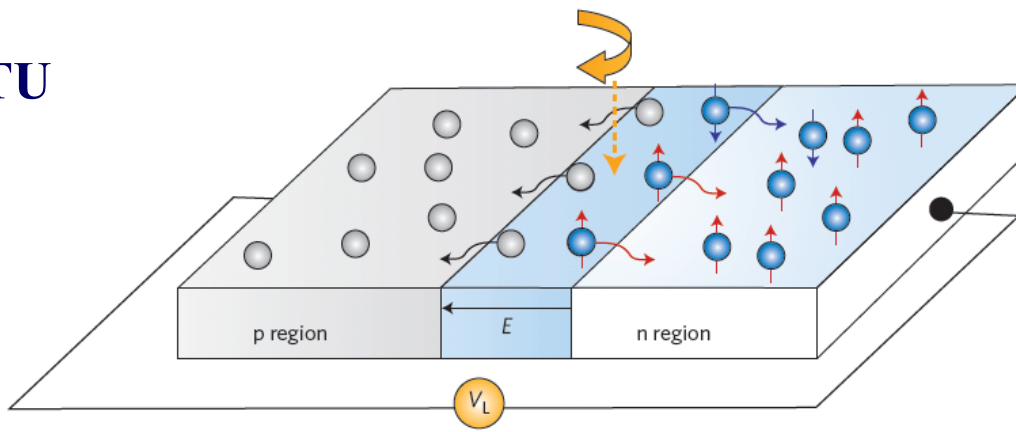
S. O. Valenzuela<sup>1†</sup> & M. Tinkham<sup>1</sup>



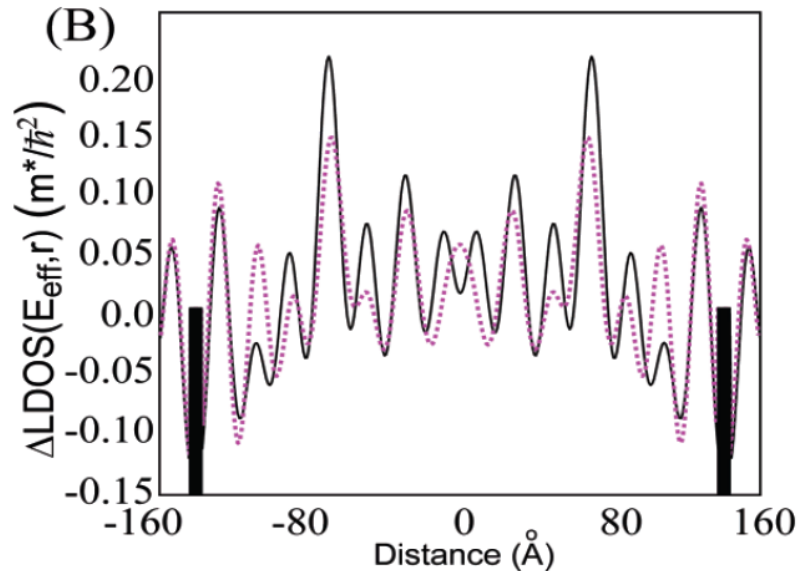
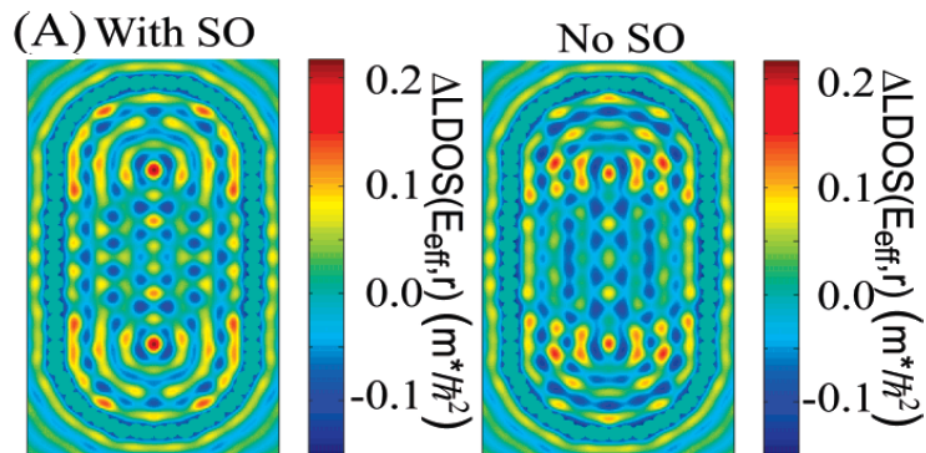


# Spin-injection Hall effect in a planar photovoltaic cell





# Electrical means of probing spin or spin-orbit effects ?



## Spin–Orbit Coupling Induced Interference in Quantum Corrals

Jamie D. Walls<sup>\*,‡</sup> and Eric J. Heller<sup>†,‡,§</sup>

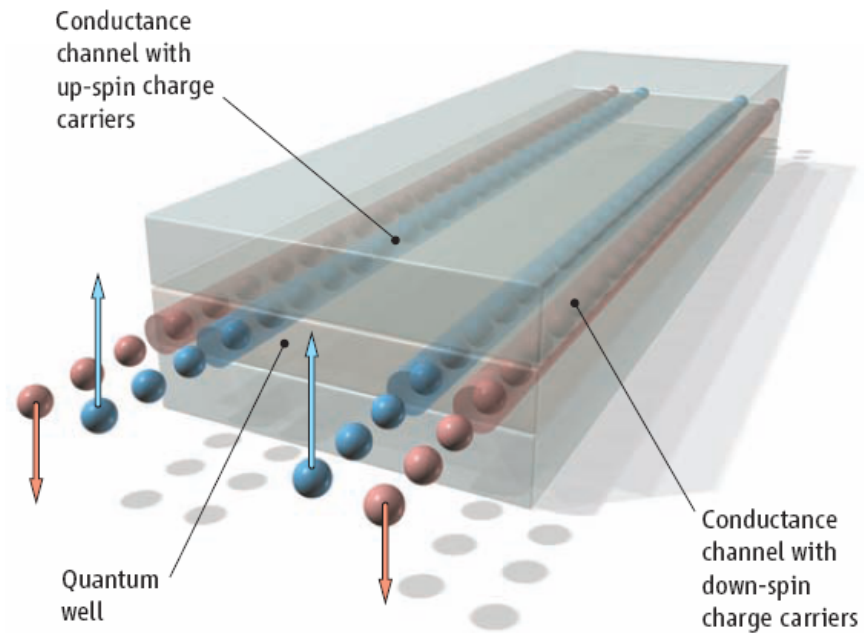
*Department of Chemistry and Chemical Biology, Harvard University, Cambridge, Massachusetts 02138, and Department of Physics, Harvard University, Cambridge, Massachusetts 02138*

*Received July 15, 2007; Revised Manuscript Received August 7, 2007*

NANO  
LETTERS

2007  
Vol. 7, No. 11  
3377–3382

## Spin physics at the edges !?



Schematic of the spin-polarized edge channels in a quantum spin Hall insulator.

## Quantum Spin Hall Insulator State in HgTe Quantum Wells

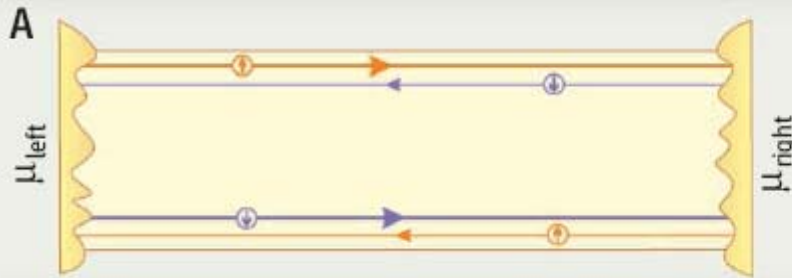
Markus König,<sup>1</sup> Steffen Wiedmann,<sup>1</sup> Christoph Brüne,<sup>1</sup> Andreas Roth,<sup>1</sup> Hartmut Buhmann,<sup>1</sup> Laurens W. Molenkamp,<sup>1\*</sup> Xiao-Liang Qi,<sup>2</sup> Shou-Cheng Zhang<sup>2</sup>

2 NOVEMBER 2007 VOL 318 SCIENCE [www.sciencemag.org](http://www.sciencemag.org)

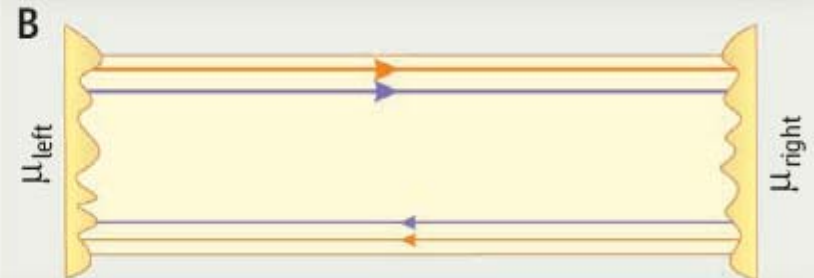
# Edge-State Physics Without Magnetic Fields

Markus Büttiker

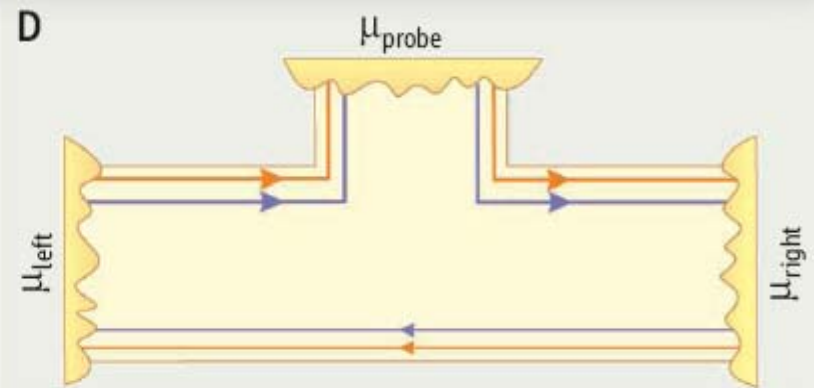
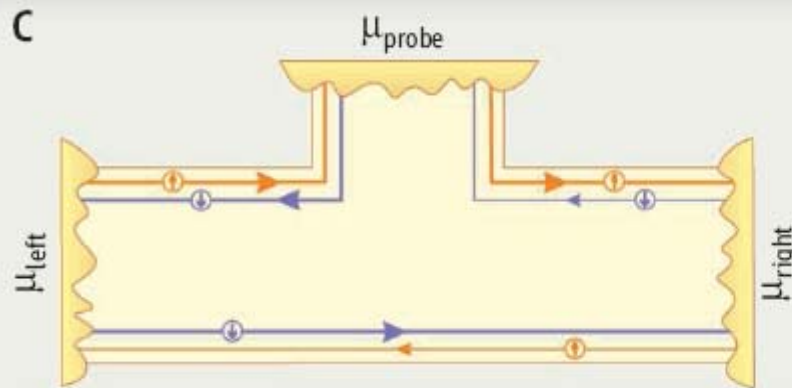
TOPOLOGICAL INSULATOR



QUANTUM HALL CONDUCTOR



Two-terminal geometry

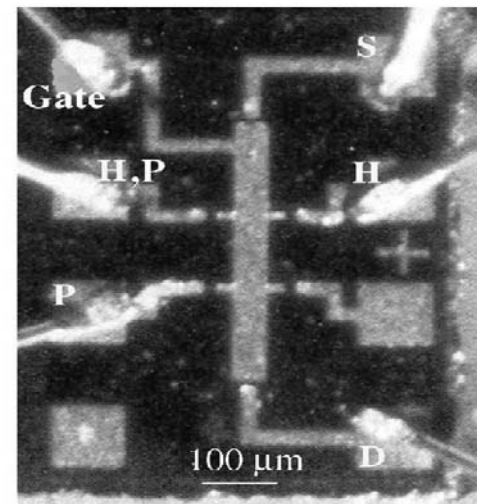


Three-terminal geometry

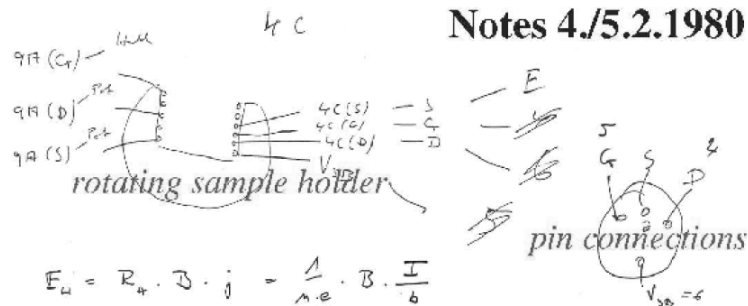


# Klaus von Klitzing

The birthday of the quantum Hall effect (QHE) can be fixed very accurately. It was the night of the 4th to the 5th of February 1980 at around 2 a.m. during an experiment at the High Magnetic Field Laboratory in Grenoble. The research



## Notes 4/5.2.1980



$$E_H = R_H \cdot D \cdot j = \frac{1}{n \cdot e} \cdot B \cdot \frac{I}{b}$$

$$U_H = \frac{B}{n \cdot e} \cdot I$$

$$U_H = \frac{B \cdot I}{e \cdot n \cdot b}$$

$$N = \frac{eB}{2\pi k} \quad (g_s \cdot g_v = 1)$$

$$U_H = \frac{h}{e^2} \cdot \frac{I}{N}$$

Josephson

$$\frac{h}{e^2} = \frac{h}{4\pi^2 m_e v_F}$$

$$\rho_{xy} = \frac{h}{2} \cdot \frac{1}{\epsilon_0} \Rightarrow 25813 \, \Omega$$

notes of the phone call to PTB

PTB 531/5920 (5.2.1980)

Prof. V. Kose

2240

$$\mu_0 = 4\pi \cdot 10^{-7} \frac{Vs}{A \cdot m}$$

$$\xi_0 = 0.8854 \cdot 10^{-13} \frac{Vs}{V_{cm}}$$

10<sup>-6</sup>

10<sup>-6</sup>

12945

$$\sqrt{\frac{\epsilon_0}{\mu_0}} = 2.65 \cdot 10^{-3} \, \Omega^{-1}$$

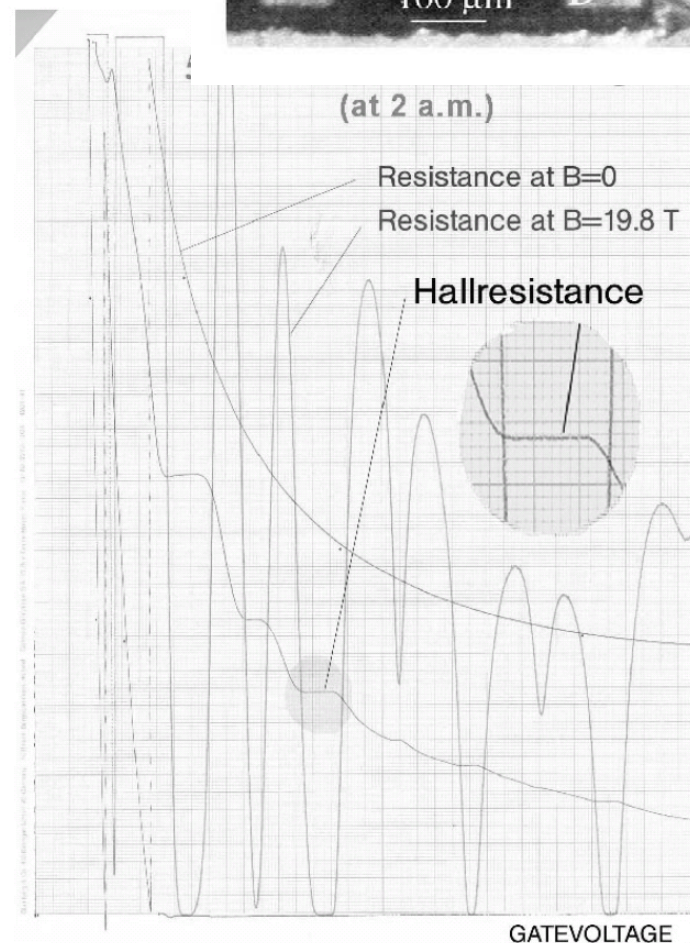
6 · 10<sup>-2</sup>

10<sup>-5</sup> 12907

$$\sqrt{\frac{h}{e^2}} = 376.7 \, \Omega$$

25813 Ω : N } 25813 → 25163.46  
114 Ω parallel 12906.5 12742.04

quantized resistances  
with and without the  
input resistance of the x-y recorder



## Why spintronics in semiconductors ?

- compatible with the semiconductor industries
- highly tunable
- spin-orbit interaction (SOI) is much larger than in vacuum
- zero magnetic field spin splitting in samples that has bulk inversion asymmetry (BIA) or structure inversion asymmetry (SIA).

## Amazing Spin-Orbit interaction in semiconductor:

In vacuum:

$$\begin{aligned} & \frac{\hbar}{4m_0^2c^2} \vec{\sigma} \cdot [\vec{\nabla} V \times \vec{p}] \\ & - \frac{\hbar^2}{4m_0^2c^2} \vec{\sigma} \cdot [\vec{k} \times \vec{\nabla} V] \\ & \lambda \vec{\sigma} \cdot (\vec{k} \times \vec{\nabla} V) \end{aligned}$$

In vacuum:  $\lambda = -3.7 \times 10^{-6} \text{ \AA}^2$

In semiconductor such as GaAs:  $\lambda = 5.3 \text{ \AA}^2$

In semiconductor such as InAs:  $\lambda = 120 \text{ \AA}^2$



Compound	$\Delta_0^{\text{exp}}$ (eV)	$\Delta_0^{\text{theo}}$ (eV)	$f_i$
C	0.006	0.006	0
Si	0.044	0.044	0
Ge	0.29	0.29	0
$\alpha$ -Sn		0.80	0
AlN		0.012	0.449
AlP		0.060	0.307
AlAs		0.29	0.274
AlSb	0.75	0.80	0.250
GaN	0.011	0.095	0.500
GaP	0.127	0.11	0.327
GaAs	0.34	0.34	0.310
GaSb	0.80	0.98	0.261
InN		0.08	0.578
InP	0.11	0.16	0.421
InAs	0.38	0.40	0.357
InSb	0.82	0.80	0.321
ZnO	-0.005	0.03	0.616
ZnS	0.07	0.09	0.623
ZnSe	0.43	0.42	0.630
ZnTe	0.93	0.86	0.609
CdS	0.066	0.09	0.685
CdSe		0.42	0.699
CdTe	0.92	0.94	0.717
HgS		0.13	0.79
HgSe		0.48	0.68
HgTe		0.99	0.65

Strength of  
spin-orbit  
goes as  $Z^4$ .

It is larger  
for heavier  
atoms.

## **Physical origin of this large enhancement in the SOI coupling constant:**

- **a brief review of how SOI comes about,  
starting from the Dirac equation.**
- **how does the SOI coupling constant gets  
enhanced in semiconductors:  
a  $k \cdot p$  approach.**

How does spin-orbit interaction arises from Dirac equation, when relativity is fully taken into account ?

$$(c \boldsymbol{\alpha} \cdot \mathbf{p} + \beta m_0 c^2 + V) \psi = E \psi$$

$$\boldsymbol{\alpha} = \begin{pmatrix} 0 & \boldsymbol{\sigma} \\ \boldsymbol{\sigma} & 0 \end{pmatrix} \quad \beta = \begin{pmatrix} \mathbf{1}_{2 \times 2} & 0 \\ 0 & -\mathbf{1}_{2 \times 2} \end{pmatrix}$$

$$\psi = \begin{bmatrix} \psi_A \\ \psi_B \end{bmatrix}$$

$$\boldsymbol{\sigma} \cdot \mathbf{p} \psi_B = \frac{1}{c} (\tilde{E} - V) \psi_A ,$$

$$\boldsymbol{\sigma} \cdot \mathbf{p} \psi_A = \frac{1}{c} (\tilde{E} - V + 2m_0c^2) \psi_B$$

$$\tilde{E} = E - m_0c^2 \quad \text{and}$$

normalization of  $\psi$  gives

$$\int d\vec{r} \psi^\dagger \psi = \int d\vec{r} [\psi_A^\dagger \psi_A + \psi_B^\dagger \psi_B] = 1$$

$$\boldsymbol{\sigma} \cdot \mathbf{p} \left[ \frac{c^2}{\tilde{E} - V + 2m_0c^2} \right] \boldsymbol{\sigma} \cdot \mathbf{p} \psi_A = (\tilde{E} - V) \psi_A$$

We focus upon the large component, when  $E > m_0c^2$  .

$$\boldsymbol{\sigma} \cdot \mathbf{p} \left[ \frac{c^2}{\tilde{E} - V + 2m_0c^2} \right] \boldsymbol{\sigma} \cdot \mathbf{p} \psi_A = (\tilde{E} - V) \psi_A$$

Note that this equation cannot replace the original Dirac equation, when large and small components are coupled. This is because  $\psi_A$  alone is not normalized. From

$$\psi_B = \left[ 2m_0c^2 + \tilde{E} - V \right]^{-1} c \vec{\sigma} \cdot \vec{\pi} \psi_A \quad \text{we have}$$

$$\begin{aligned} \psi_B^\dagger \psi_B &= \psi_A^\dagger (c \vec{\sigma} \cdot \vec{\pi}) \left[ 2m_0c^2 + \tilde{E} - V \right]^{-2} (c \vec{\sigma} \cdot \vec{\pi}) \psi_A \\ &\approx \frac{1}{4m_0^2c^2} \psi_A^\dagger \left( \vec{\pi}^2 + e\hbar \vec{\sigma} \cdot \vec{B} \right) \psi_A \end{aligned}$$

$$\vec{\pi} = \vec{p} + e\vec{A} \quad \text{where } e > 0$$

$$\tilde{\psi} = \left( 1 + \frac{\vec{\pi}^2 + e\hbar \vec{\sigma} \cdot \vec{B}}{8m_0^2 c^2} \right) \psi_A$$

$$\psi_A = \left( 1 - \frac{\vec{\pi}^2 + e\hbar \vec{\sigma} \cdot \vec{B}}{8m_0^2 c^2} \right) \tilde{\psi}$$

$$\begin{aligned} (\vec{\sigma} \cdot \vec{\pi}) \left[ \frac{c^2}{2m_0 c^2 + \tilde{E} - V} \right] (\vec{\sigma} \cdot \vec{\pi}) \left( 1 - \frac{\vec{\pi}^2 + e\hbar \vec{\sigma} \cdot \vec{B}}{8m_0^2 c^2} \right) \tilde{\psi} \\ = (\tilde{E} - V) \left( 1 - \frac{\vec{\pi}^2 + e\hbar \vec{\sigma} \cdot \vec{B}}{8m_0^2 c^2} \right) \tilde{\psi} \end{aligned}$$

$$\frac{c^2}{2m_0 c^2 + \tilde{E} - V} \approx \frac{1}{2m_0} \left( 1 - \frac{\tilde{E} - V}{2m_0 c^2} \right) \quad \text{up to order } (v/c)^2$$



$$\begin{aligned}
 & \frac{1}{2m_0} (\vec{\sigma} \cdot \vec{\pi}) \left[ 1 - \frac{\tilde{E} - V}{2m_0 c^2} \right] (\vec{\sigma} \cdot \vec{\pi}) \left( 1 - \frac{\vec{\pi}^2 + e\hbar \vec{\sigma} \cdot \vec{B}}{8m_0^2 c^2} \right) \tilde{\psi} \\
 & = (\tilde{E} - V) \left( 1 - \frac{\vec{\pi}^2 + e\hbar \vec{\sigma} \cdot \vec{B}}{8m_0^2 c^2} \right) \tilde{\psi}
 \end{aligned}$$

$$\begin{aligned}
 & \left( \frac{\vec{\pi}^2 + e\hbar \vec{\sigma} \cdot \vec{B}}{2m_0} \right) \left( 1 - \frac{\vec{\pi}^2 + e\hbar \vec{\sigma} \cdot \vec{B}}{8m_0^2 c^2} \right) \tilde{\psi} + \frac{1}{4m_0^2 c^2} (\vec{\sigma} \cdot \vec{\pi}) V (\vec{\sigma} \cdot \vec{\pi}) \tilde{\psi} \\
 & - \frac{\tilde{E}}{4m_0^2 c^2} (\vec{\pi}^2 + e\hbar \vec{\sigma} \cdot \vec{B}) \tilde{\psi} \\
 & = (\tilde{E} - V) \left( 1 - \frac{\vec{\pi}^2 + e\hbar \vec{\sigma} \cdot \vec{B}}{8m_0^2 c^2} \right) \tilde{\psi}
 \end{aligned}$$



$$\begin{aligned}
& \left( \frac{\vec{\pi}^2 + e\hbar \vec{\sigma} \cdot \vec{B}}{2m_o} \right) \left( 1 - \frac{\vec{\pi}^2 + e\hbar \vec{\sigma} \cdot \vec{B}}{8m_o^2 c^2} \right) \tilde{\psi} + \frac{1}{4m_o^2 c^2} (\vec{\sigma} \cdot \vec{\pi}) V (\vec{\sigma} \cdot \vec{\pi}) \tilde{\psi} \\
& + V \left( 1 - \frac{\vec{\pi}^2 + e\hbar \vec{\sigma} \cdot \vec{B}}{8m_o^2 c^2} \right) \tilde{\psi} \\
& = \tilde{E} \left( 1 + \frac{\vec{\pi}^2 + e\hbar \vec{\sigma} \cdot \vec{B}}{8m_o^2 c^2} \right) \tilde{\psi}
\end{aligned}$$

$$\begin{aligned}
& \left( 1 - \frac{\vec{\pi}^2 + e\hbar \vec{\sigma} \cdot \vec{B}}{8m_o^2 c^2} \right) \left( \frac{\vec{\pi}^2 + e\hbar \vec{\sigma} \cdot \vec{B}}{2m_o} \right) \left( 1 - \frac{\vec{\pi}^2 + e\hbar \vec{\sigma} \cdot \vec{B}}{8m_o^2 c^2} \right) \tilde{\psi} \\
& + \left( 1 - \frac{\vec{\pi}^2 + e\hbar \vec{\sigma} \cdot \vec{B}}{8m_o^2 c^2} \right) \frac{1}{4m_o^2 c^2} (\vec{\sigma} \cdot \vec{\pi}) V (\vec{\sigma} \cdot \vec{\pi}) \tilde{\psi} \\
& + \left( 1 - \frac{\vec{\pi}^2 + e\hbar \vec{\sigma} \cdot \vec{B}}{8m_o^2 c^2} \right) V \left( 1 - \frac{\vec{\pi}^2 + e\hbar \vec{\sigma} \cdot \vec{B}}{8m_o^2 c^2} \right) \tilde{\psi} \\
& = \tilde{E} \tilde{\psi}
\end{aligned}$$



$$\begin{aligned}
 & (\vec{\sigma} \cdot \vec{\pi}) V (\vec{\sigma} \cdot \vec{\pi}) \\
 &= -i\hbar \vec{\nabla} V \cdot \vec{\pi} + \hbar (\vec{\nabla} V \times \vec{\pi}) \cdot \vec{\sigma} + V(\vec{\pi}^2 + e\hbar \vec{\sigma} \cdot \vec{B})
 \end{aligned}$$

$$\begin{aligned}
 & \left[ \frac{\pi^2}{2m_0} + V + \frac{e\hbar}{2m_0} \vec{\sigma} \cdot \vec{B} - \frac{e\hbar}{4m_0^2 c^2} \vec{\sigma} \cdot (\vec{\pi} \times \vec{\varepsilon}) + \frac{e\hbar^2}{8m_0^2 c^2} \vec{\nabla} \cdot \vec{\varepsilon} \right. \\
 & \quad \left. - \frac{(\vec{\pi}^2)^2}{8m_0^3 c^2} - \frac{e\hbar \vec{\pi}^2}{4m_0^3 c^2} \vec{\sigma} \cdot \vec{B} - \frac{(e\hbar B)^2}{8m_0^3 c^2} \right] \tilde{\psi} \\
 &= \tilde{E} \tilde{\psi}
 \end{aligned}$$

The spin orbit interaction term comes from the action of gradient  $V$  onto the small component wavefunction.

$$\vec{\varepsilon} = \frac{1}{e} \vec{\nabla} V$$

We know now how the spin-orbit interaction comes from the relativistic effect. The Thomas precession has also been taken into account in our taking of the nonrelativistic limit.

Can we then understand the amazing enlargement of the spin-orbit coupling parameter  $\lambda$  in semiconductor ?

## Amazing Spin-Orbit interaction in semiconductor: To refresh our memory

In vacuum:

$$\begin{aligned} & \frac{\hbar}{4m_0^2c^2} \vec{\sigma} \cdot [\vec{\nabla} V \times \vec{p}] \\ & - \frac{\hbar^2}{4m_0^2c^2} \vec{\sigma} \cdot [\vec{k} \times \vec{\nabla} V] \\ & \lambda \vec{\sigma} \cdot (\vec{k} \times \vec{\nabla} V) \end{aligned}$$

In vacuum:  $\lambda = -3.7 \times 10^{-6} \text{ \AA}^2$

In semiconductor such as GaAs:  $\lambda = 5.3 \text{ \AA}^2$

In semiconductor such as InAs:  $\lambda = 120 \text{ \AA}^2$

## $\mathbf{k} \cdot \mathbf{p}$ Method for an electron in a periodic potential $V_0(\mathbf{r})$

The derivation of the  $\mathbf{k} \cdot \mathbf{p}$  method is based on the Schrödinger equation for the Bloch functions  $e^{i\mathbf{k} \cdot \mathbf{r}} u_{\nu\mathbf{k}}(\mathbf{r}) \equiv e^{i\mathbf{k} \cdot \mathbf{r}} \langle \mathbf{r} | \nu \mathbf{k} \rangle$  in the microscopic lattice-periodic crystal potential  $V_0(\mathbf{r})$

$$\left[ \frac{p^2}{2m_0} + V_0(\mathbf{r}) \right] e^{i\mathbf{k} \cdot \mathbf{r}} u_{\nu\mathbf{k}}(\mathbf{r}) = E_{\nu}(\mathbf{k}) e^{i\mathbf{k} \cdot \mathbf{r}} u_{\nu\mathbf{k}}(\mathbf{r}) .$$

$$\left[ \frac{p^2}{2m_0} + V_0 + \frac{\hbar^2 k^2}{2m_0} + \frac{\hbar}{m_0} \mathbf{k} \cdot \mathbf{p} \right] |\nu \mathbf{k}\rangle = E_{\nu}(\mathbf{k}) |\nu \mathbf{k}\rangle .$$

If we include the spin-orbit interaction, given by


$$\frac{\hbar}{4m_0^2c^2} \vec{\sigma} \cdot [\vec{\nabla} V \times \vec{p}]$$

we get

$$\left[ \frac{p^2}{2m_0} + V_0 + \frac{\hbar^2 k^2}{2m_0} + \frac{\hbar}{m_0} \mathbf{k} \cdot \boldsymbol{\pi} + \frac{\hbar}{4m_0^2c^2} \mathbf{p} \cdot \boldsymbol{\sigma} \times (\nabla V_0) \right] |n\mathbf{k}\rangle = E_n(\mathbf{k}) |n\mathbf{k}\rangle$$

where

$$\boldsymbol{\pi} := \mathbf{p} + \frac{\hbar}{4m_0c^2} \boldsymbol{\sigma} \times \nabla V_0$$



Two component  
spinors

For a fixed wave vector  $\mathbf{k}_0$  the sets of lattice periodic functions  $\{|\mathbf{n}\mathbf{k}_0\rangle\}$  provide a complete and orthonormal basis. Therefore, we can expand the kets  $\{|\mathbf{n}\mathbf{k}\rangle\}$  in terms of band edge Bloch functions  $\{|\mathbf{v}\mathbf{0}\rangle\}$  times spin eigenstates  $|\sigma\rangle$

$$|\mathbf{n}\mathbf{k}\rangle = \sum_{\substack{\nu' \\ \sigma'=\uparrow,\downarrow}} c_{n\nu'\sigma'}(\mathbf{k}) |\nu'\sigma'\rangle ,$$

where

$$|\nu'\sigma'\rangle := |\nu'\mathbf{0}\rangle \otimes |\sigma'\rangle .$$

$$\sum_{\nu', \sigma'} \left\{ \left[ E_{\nu'}(\mathbf{0}) + \frac{\hbar^2 k^2}{2m_0} \right] \delta_{\nu\nu'} \delta_{\sigma\sigma'} + \frac{\hbar}{m_0} \mathbf{k} \cdot \mathbf{P}_{\sigma\sigma'}^{\nu\nu'} + \Delta_{\sigma\sigma'}^{\nu\nu'} \right\} c_{n\nu'\sigma'}(\mathbf{k})$$

$$= E_n(\mathbf{k}) c_{n\nu\sigma}(\mathbf{k}) ,$$

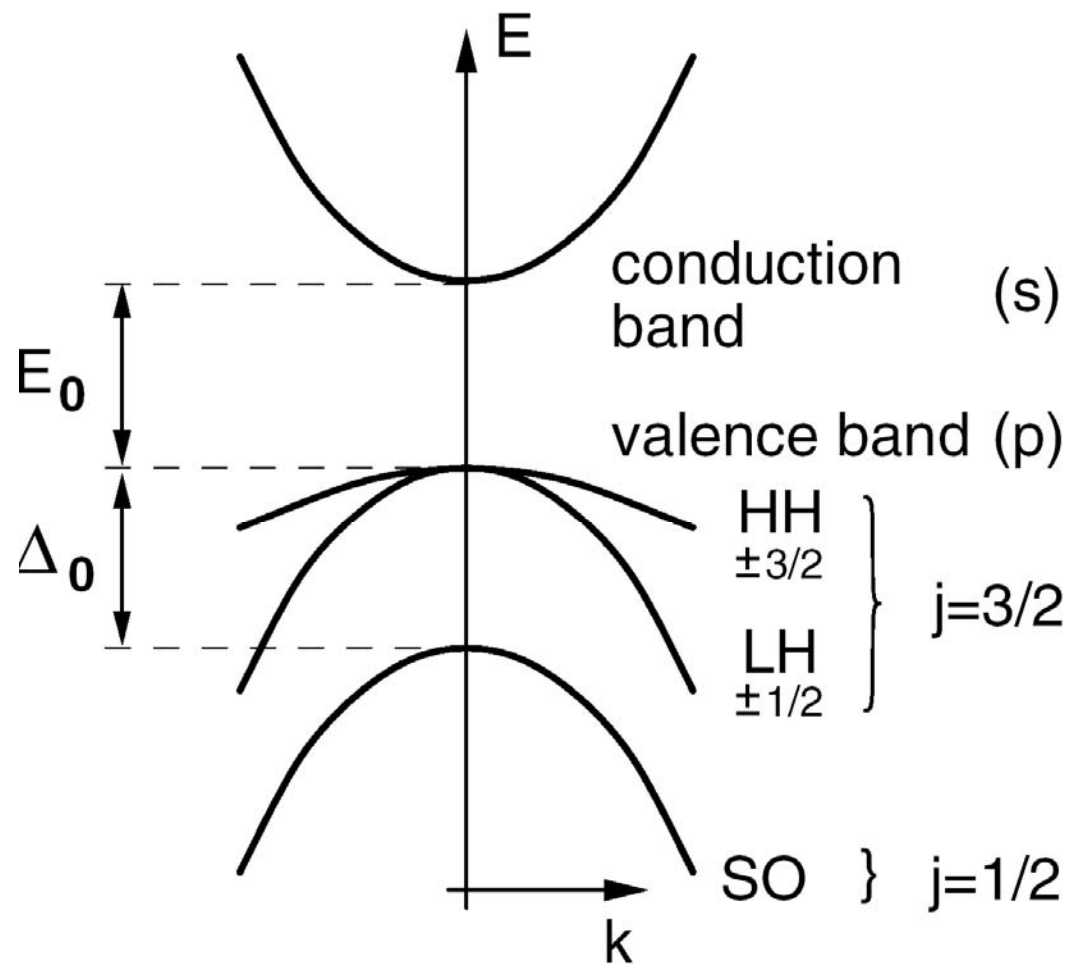
where

$$\mathbf{P}_{\sigma\sigma'}^{\nu\nu'} := \langle \nu\sigma | \boldsymbol{\pi} | \nu'\sigma' \rangle ,$$

$$\Delta_{\sigma\sigma'}^{\nu\nu'} := \frac{\hbar}{4m_0^2 c^2} \langle \nu\sigma | [\mathbf{p} \cdot \boldsymbol{\sigma} \times (\nabla V_0)] | \nu'\sigma' \rangle .$$

**We choose the  $S$  and  $P$  orbitals for states  $|\nu'\sigma'\rangle$  .**

$$\boldsymbol{\pi} := \mathbf{p} + \frac{\hbar}{4m_0 c^2} \boldsymbol{\sigma} \times \nabla V_0$$





$ J, m_j\rangle$	$\psi_{jm}$	$E(k=0)$	
$ \frac{3}{2}, \frac{3}{2}\rangle$	$-\frac{1}{\sqrt{2}} X+iY\rangle \uparrow\rangle$	$E_v$	$\Gamma_8^v$
$ \frac{3}{2}, \frac{1}{2}\rangle$	$\sqrt{\frac{2}{3}} Z\rangle \uparrow\rangle - \frac{1}{\sqrt{6}} X+iY\rangle \downarrow\rangle$	$E_v$	
$ \frac{3}{2}, \frac{-1}{2}\rangle$	$\sqrt{\frac{2}{3}} Z\rangle \downarrow\rangle + \frac{1}{\sqrt{6}} X-iY\rangle \uparrow\rangle$	$E_v$	
$ \frac{3}{2}, \frac{-3}{2}\rangle$	$\frac{1}{\sqrt{2}} X-iY\rangle \downarrow\rangle$	$E_v$	
$ \frac{1}{2}, \frac{1}{2}\rangle$	$-\sqrt{\frac{1}{3}} Z\rangle \uparrow\rangle - \frac{1}{\sqrt{3}} X+iY\rangle \downarrow\rangle$	$E_v - \Delta_0$	$\Gamma_7^v$
$ \frac{1}{2}, \frac{-1}{2}\rangle$	$\sqrt{\frac{1}{3}} Z\rangle \downarrow\rangle - \frac{1}{\sqrt{3}} X-iY\rangle \uparrow\rangle$	$E_v - \Delta_0$	

$\left \frac{1}{2}, \frac{1}{2}\right\rangle$	$ S\rangle \uparrow\rangle$	$E_c$	$\Gamma_6^c$
$\left \frac{1}{2}, \frac{-1}{2}\right\rangle$	$ S\rangle \downarrow\rangle$	$E_c$	
$\left \frac{3}{2}, \frac{3}{2}\right\rangle$	$-\frac{1}{\sqrt{2}} X+iY\rangle \uparrow\rangle$	$E_v$	$\Gamma_8^v$
$\left \frac{3}{2}, \frac{1}{2}\right\rangle$	$\sqrt{\frac{2}{3}} Z\rangle \uparrow\rangle - \frac{1}{\sqrt{6}} X+iY\rangle \downarrow\rangle$	$E_v$	
$\left \frac{3}{2}, \frac{-1}{2}\right\rangle$	$\sqrt{\frac{2}{3}} Z\rangle \downarrow\rangle + \frac{1}{\sqrt{6}} X-iY\rangle \uparrow\rangle$	$E_v$	
$\left \frac{3}{2}, \frac{-3}{2}\right\rangle$	$\frac{1}{\sqrt{2}} X-iY\rangle \downarrow\rangle$	$E_v$	
$\left \frac{1}{2}, \frac{1}{2}\right\rangle$	$-\sqrt{\frac{1}{3}} Z\rangle \uparrow\rangle - \frac{1}{\sqrt{3}} X+iY\rangle \downarrow\rangle$	$E_v - \Delta_0$	$\Gamma_7^v$
$\left \frac{1}{2}, \frac{-1}{2}\right\rangle$	$\sqrt{\frac{1}{3}} Z\rangle \downarrow\rangle - \frac{1}{\sqrt{3}} X-iY\rangle \uparrow\rangle$	$E_v - \Delta_0$	

**Table C.1.** Basis functions  $|jm\rangle$  of the extended Kane model. The quantization axis of angular momentum is the crystallographic direction  $[001]$ . In accordance with time reversal symmetry, we have choosen the phase convention that  $|X\rangle$ ,  $|Y\rangle$ , and  $|Z\rangle$  are real and  $|S\rangle$ ,  $|X'\rangle$ ,  $|Y'\rangle$ , and  $|Z'\rangle$  are purely imaginary. Note that our definition of the basis functions  $|jm\rangle$  agrees with common definitions of angular-momentum eigenfunctions (see e.g. [1])

$\Gamma_8^c$	$\left  \frac{3}{2} \quad \frac{3}{2} \right\rangle_{c'} = -\frac{1}{\sqrt{2}} \begin{vmatrix} X' + iY' \\ 0 \end{vmatrix}$	$\left  \frac{3}{2} \quad \frac{1}{2} \right\rangle_{c'} = \frac{1}{\sqrt{6}} \begin{vmatrix} 2Z' \\ -X' - iY' \end{vmatrix}$
	$\left  \frac{3}{2} \quad -\frac{1}{2} \right\rangle_{c'} = \frac{1}{\sqrt{6}} \begin{vmatrix} X' - iY' \\ 2Z' \end{vmatrix}$	$\left  \frac{3}{2} \quad -\frac{3}{2} \right\rangle_{c'} = \frac{1}{\sqrt{2}} \begin{vmatrix} 0 \\ X' - iY' \end{vmatrix}$
$\Gamma_7^c$	$\left  \frac{1}{2} \quad \frac{1}{2} \right\rangle_{c'} = -\frac{1}{\sqrt{3}} \begin{vmatrix} Z' \\ X' + iY' \end{vmatrix}$	$\left  \frac{1}{2} \quad -\frac{1}{2} \right\rangle_{c'} = -\frac{1}{\sqrt{3}} \begin{vmatrix} X' - iY' \\ -Z' \end{vmatrix}$
	$\left  \frac{1}{2} \quad \frac{1}{2} \right\rangle_c = \begin{vmatrix} S \\ 0 \end{vmatrix}$	$\left  \frac{1}{2} \quad -\frac{1}{2} \right\rangle_c = \begin{vmatrix} 0 \\ S \end{vmatrix}$
$\Gamma_8^v$	$\left  \frac{3}{2} \quad \frac{3}{2} \right\rangle_v = -\frac{1}{\sqrt{2}} \begin{vmatrix} X + iY \\ 0 \end{vmatrix}$	$\left  \frac{3}{2} \quad \frac{1}{2} \right\rangle_v = \frac{1}{\sqrt{6}} \begin{vmatrix} 2Z \\ -X - iY \end{vmatrix}$
	$\left  \frac{3}{2} \quad -\frac{1}{2} \right\rangle_v = \frac{1}{\sqrt{6}} \begin{vmatrix} X - iY \\ 2Z \end{vmatrix}$	$\left  \frac{3}{2} \quad -\frac{3}{2} \right\rangle_v = \frac{1}{\sqrt{2}} \begin{vmatrix} 0 \\ X - iY \end{vmatrix}$
$\Gamma_7^v$	$\left  \frac{1}{2} \quad \frac{1}{2} \right\rangle_v = -\frac{1}{\sqrt{3}} \begin{vmatrix} Z \\ X + iY \end{vmatrix}$	$\left  \frac{1}{2} \quad -\frac{1}{2} \right\rangle_v = -\frac{1}{\sqrt{3}} \begin{vmatrix} X - iY \\ -Z \end{vmatrix}$

$$\mathcal{H}_{8 \times 8} = \begin{pmatrix} (E_c + V) \mathbf{1}_{2 \times 2} & \sqrt{3} P \mathbf{T} \cdot \mathbf{k} & -\frac{1}{\sqrt{3}} P \boldsymbol{\sigma} \cdot \mathbf{k} \\ \sqrt{3} P \mathbf{T}^\dagger \cdot \mathbf{k} & (E_v + V) \mathbf{1}_{4 \times 4} & 0 \\ -\frac{1}{\sqrt{3}} P \boldsymbol{\sigma} \cdot \mathbf{k} & 0 & (E_v - \Delta_0 + V) \mathbf{1}_{2 \times 2} \end{pmatrix}$$

$$= \begin{pmatrix} E_c + V & 0 & \frac{-1}{\sqrt{2}} P k_+ & \sqrt{\frac{2}{3}} P k_z & \frac{1}{\sqrt{6}} P k_- & 0 & \frac{-1}{\sqrt{3}} P k_z & \frac{-1}{\sqrt{3}} P k_- \\ 0 & E_c + V & 0 & \frac{-1}{\sqrt{6}} P k_+ & \sqrt{\frac{2}{3}} P k_z & \frac{1}{\sqrt{2}} P k_- & \frac{-1}{\sqrt{3}} P k_+ & \frac{1}{\sqrt{3}} P k_z \\ \frac{-1}{\sqrt{2}} P k_- & 0 & E_v + V & 0 & 0 & 0 & 0 & 0 \\ \sqrt{\frac{2}{3}} P k_z & \frac{-1}{\sqrt{6}} P k_- & 0 & E_v + V & 0 & 0 & 0 & 0 \\ \frac{1}{\sqrt{6}} P k_+ & \sqrt{\frac{2}{3}} P k_z & 0 & 0 & E_v + V & 0 & 0 & 0 \\ 0 & \frac{1}{\sqrt{2}} P k_+ & 0 & 0 & 0 & E_v + V & 0 & 0 \\ \frac{-1}{\sqrt{3}} P k_z & \frac{-1}{\sqrt{3}} P k_- & 0 & 0 & 0 & 0 & E_v - \Delta_0 + V & 0 \\ \frac{-1}{\sqrt{3}} P k_+ & \frac{1}{\sqrt{3}} P k_z & 0 & 0 & 0 & 0 & 0 & E_v - \Delta_0 + V \end{pmatrix}.$$

$$P = \frac{\hbar}{m_0} \langle S | p_x | X \rangle$$

$$\Delta_0 = - \frac{3i\hbar}{4m_0^2 c^2} \langle X | [(\nabla V_0) \times \mathbf{p}]_y | Z \rangle$$

$$\begin{bmatrix} (E_c + V)1_{2 \times 2} & \sqrt{3}PT \cdot \vec{k} & -\frac{1}{\sqrt{3}}P\vec{\sigma} \cdot \vec{k} \\ \sqrt{3}PT^+ \cdot \vec{k} & (E_v + V)1_{4 \times 4} & 0 \\ -\frac{1}{\sqrt{3}}P\vec{\sigma} \cdot \vec{k} & 0 & (E_v - \Delta_0 + V)1_{2 \times 2} \end{bmatrix} \begin{bmatrix} \psi_c \\ \psi_{v+} \\ \psi_{v-} \end{bmatrix} = E \begin{bmatrix} \psi_c \\ \psi_{v+} \\ \psi_{v-} \end{bmatrix}$$

$$\sqrt{3}PT^+ \cdot \vec{k} \psi_c = (\tilde{E} + E_0 - V) \psi_{v+}$$

or

$$\psi_{v+} = \frac{\sqrt{3}P}{\tilde{E} + E_0 - V} T^+ \cdot \vec{k} \psi_c$$

$$-\frac{P}{\sqrt{3}}\vec{\sigma} \cdot \vec{k} \psi_c = (E - E_v + \Delta_0 - V) \psi_{v-}$$

or

$$\psi_{v-} = -\frac{P}{\sqrt{3}(\tilde{E} + E_0 + \Delta_0 - V)} \vec{\sigma} \cdot \vec{k} \psi_c$$

$$\left[ \mathbf{T} \cdot \mathbf{k} \frac{3P^2}{\tilde{E} - V + E_0} \mathbf{T}^\dagger \cdot \mathbf{k} + \boldsymbol{\sigma} \cdot \mathbf{k} \frac{P^2/3}{\tilde{E} - V + E_0 + \Delta_0} \boldsymbol{\sigma} \cdot \mathbf{k} \right] \psi_c$$

$$= (\tilde{E} - V) \psi_c,$$

From normalization consideration

$$\psi_c^+ \psi_c + \psi_{v+}^+ \psi_{v+} + \psi_{v-}^+ \psi_{v-}$$

$$= \psi_c^+ \left[ 1 + \mathbf{T} \cdot \vec{k} \frac{3P^2}{(E_0 + \tilde{E} - V)^2} \mathbf{T}^+ \cdot \vec{k} + \vec{\sigma} \cdot \vec{k} \frac{P^2}{3(E_0 + \tilde{E} + \Delta_0 - V)^2} \vec{\sigma} \cdot \vec{k} \right] \psi_c$$

$$= \psi_c^+ \left[ 1 + 3P^2 \frac{(\mathbf{T} \cdot \vec{\pi})(\mathbf{T}^+ \cdot \vec{\pi})}{\hbar^2 E_0^2} + \frac{P^2}{3} \frac{(\vec{\sigma} \cdot \vec{\pi})(\vec{\sigma} \cdot \vec{\pi})}{\hbar^2 (E_0 + \Delta_0)^2} \right] \psi_c$$

$$(\mathbf{T} \cdot \vec{\pi})(\mathbf{T}^+ \cdot \vec{\pi}) = \frac{(2\vec{\pi}^2 - e\hbar \vec{\sigma} \cdot \vec{B})}{9}$$

Physical meaning of  $P^2$  :

$$\left[ \mathbf{T} \cdot \mathbf{k} \frac{3P^2}{\tilde{E} - V + E_0} \mathbf{T}^\dagger \cdot \mathbf{k} + \boldsymbol{\sigma} \cdot \mathbf{k} \frac{P^2/3}{\tilde{E} - V + E_0 + \Delta_0} \boldsymbol{\sigma} \cdot \mathbf{k} \right] \psi_c$$

$$= (\tilde{E} - V) \psi_c ,$$

Taking the  $E_0 \gg \Delta_0$  :

$$\frac{3P^2}{E_0} \frac{(2\vec{\pi}^2 - e\hbar \vec{\sigma} \cdot \vec{B})}{9\hbar^2} \psi_c + \frac{P^2}{3E_0} \frac{(\vec{\pi}^2 + e\hbar \vec{\sigma} \cdot \vec{B})}{\hbar^2} \psi_c$$

$$= (\tilde{E} - V) \psi_c$$

$$\frac{P^2}{3E_0} \frac{3\vec{\pi}^2}{\hbar^2} \psi_c = (\tilde{E} - V) \psi_c$$

$$\boxed{\frac{1}{2m^*} = \frac{P^2}{\hbar^2 E_0}}$$

$P^2$  and  $E_0$  combined to give the effective mass of the electron

Define a normalized wavefunction

$$\tilde{\psi}_c = \left[ 1 + \frac{P^2}{6\hbar^2} \left( \frac{2\vec{\pi}^2 - e\hbar \vec{\sigma} \cdot \vec{B}}{E_0^2} + \frac{\vec{\pi}^2 + e\hbar \vec{\sigma} \cdot \vec{B}}{(E_0 + \Delta_0)^2} \right) \right] \psi_c$$

$$\left[ \mathbf{T} \cdot \mathbf{k} \frac{3P^2}{\tilde{E} - V + E_0} \mathbf{T}^\dagger \cdot \mathbf{k} + \boldsymbol{\sigma} \cdot \mathbf{k} \frac{P^2/3}{\tilde{E} - V + E_0 + \Delta_0} \boldsymbol{\sigma} \cdot \mathbf{k} \right] \psi_c$$

$$= (\tilde{E} - V) \psi_c,$$





$$\begin{aligned}
& \left[ 1 - \frac{P^2}{6\hbar^2} \left( \frac{2\vec{\pi}^2 - e\hbar \vec{\sigma} \cdot \vec{B}}{E_0^2} + \frac{\vec{\pi}^2 + e\hbar \vec{\sigma} \cdot \vec{B}}{(E_0 + \Delta_0)^2} \right) \right] \frac{P^2}{3\hbar^2 E_0} (2\vec{\pi}^2 - e\hbar \vec{\sigma} \cdot \vec{B}) \left[ 1 - \frac{P^2}{6\hbar^2} \left( \frac{2\vec{\pi}^2 - e\hbar \vec{\sigma} \cdot \vec{B}}{E_0^2} + \frac{\vec{\pi}^2 + e\hbar \vec{\sigma} \cdot \vec{B}}{(E_0 + \Delta_0)^2} \right) \right] \tilde{\psi}_c \\
& + \frac{3P^2}{\hbar^2 E_0^2} (T \cdot \vec{\pi}) V (T^+ \cdot \vec{\pi}) \tilde{\psi}_c \\
& + \frac{P^2}{3\hbar^2 (E_0 + \Delta_0)^2} \left[ 1 - \frac{P^2}{6\hbar^2} \left( \frac{2\vec{\pi}^2 - e\hbar \vec{\sigma} \cdot \vec{B}}{E_0^2} + \frac{\vec{\pi}^2 + e\hbar \vec{\sigma} \cdot \vec{B}}{(E_0 + \Delta_0)^2} \right) \right] (\vec{\pi}^2 + e\hbar \vec{\sigma} \cdot \vec{B}) \left[ 1 - \frac{P^2}{6\hbar^2} \left( \frac{2\vec{\pi}^2 - e\hbar \vec{\sigma} \cdot \vec{B}}{E_0^2} + \frac{\vec{\pi}^2 + e\hbar \vec{\sigma} \cdot \vec{B}}{(E_0 + \Delta_0)^2} \right) \right] \tilde{\psi}_c \\
& + \frac{P^2}{3\hbar^2 (E_0 + \Delta_0)^2} (\vec{\sigma} \cdot \vec{\pi}) V (\vec{\sigma} \cdot \vec{\pi}) \tilde{\psi}_c \\
& + \left[ 1 - \frac{P^2}{6\hbar^2} \left( \frac{2\vec{\pi}^2 - e\hbar \vec{\sigma} \cdot \vec{B}}{E_0^2} + \frac{\vec{\pi}^2 + e\hbar \vec{\sigma} \cdot \vec{B}}{(E_0 + \Delta_0)^2} \right) \right] V \left[ 1 - \frac{P^2}{6\hbar^2} \left( \frac{2\vec{\pi}^2 - e\hbar \vec{\sigma} \cdot \vec{B}}{E_0^2} + \frac{\vec{\pi}^2 + e\hbar \vec{\sigma} \cdot \vec{B}}{(E_0 + \Delta_0)^2} \right) \right] \tilde{\psi}_c \\
& = \tilde{E} \tilde{\psi}_c
\end{aligned}$$



$$\begin{aligned} & \left\{ \frac{P^2}{3} \left[ \frac{2}{E_0} + \frac{1}{E_0 + \Delta_0} \right] \left( \frac{\vec{\pi}^2}{\hbar^2} \right) + V \right. \\ & \quad - \frac{P^2}{3} \left[ \frac{1}{E_0} - \frac{1}{E_0 + \Delta_0} \right] \frac{e}{\hbar} \vec{\sigma} \cdot \vec{B} \\ & \quad - \frac{eP^2}{3\hbar} \left[ \frac{1}{E_0^2} - \frac{1}{(E_0 + \Delta_0)^2} \right] \vec{\sigma} \cdot (\vec{\varepsilon} \times \vec{\pi}) \\ & \quad \left. + \frac{eP^2}{6} \left( \frac{2}{E_0^2} + \frac{1}{(E_0 + \Delta_0)^2} \right) \vec{\nabla} \cdot \vec{\varepsilon} \right\} \tilde{\psi}_c \\ & = \tilde{E} \tilde{\psi}_c \end{aligned}$$

$$\lambda \vec{\sigma} \cdot (\vec{k} \times \vec{\nabla} V)$$

$$\frac{1}{2m^*} = \frac{P^2}{\hbar^2 E_0}$$

In semiconductor :

$$\begin{aligned} \lambda &= \frac{P^2}{3} \left[ \frac{1}{E_0^2} - \frac{1}{(E_0 + \Delta_0)^2} \right] \\ &= \frac{\hbar^2}{3} \frac{P^2}{\hbar^2 E_0} \left[ \frac{1}{E_0} - \frac{E_0}{(E_0 + \Delta_0)^2} \right] \\ &= \frac{\hbar^2}{6m^* E_0} \left[ 1 - \frac{E_0^2}{(E_0 + \Delta_0)^2} \right] \end{aligned}$$

In vacuum :

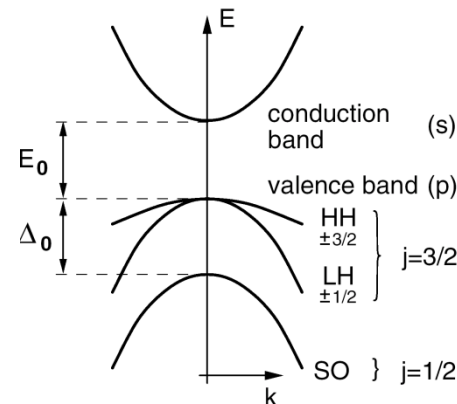
$$\lambda_{\text{vac}} = -\frac{\hbar^2}{4m_0^2 c^2} = -\frac{\hbar^2}{4m_0(m_0 c^2)}$$

The enhancement factor for InAs:

$$\begin{aligned} \left| \frac{\lambda}{\lambda_{\text{vac}}} \right| &\approx \frac{m_0 c^2}{E_0} \times \frac{m_0}{m^*} \times \frac{2}{3} \\ &= \frac{0.5 \text{ MeV}}{0.418 \text{ eV}} \times \frac{1}{0.023} \times \frac{2}{3} = 34.7 \times 10^6 \end{aligned}$$

Compare with the actual values :

$$\left| \frac{\lambda}{\lambda_{\text{vac}}} \right| = \frac{120 \text{ A}^2}{3.73 \times 10^{-6} \text{ A}^2} = 32 \times 10^6$$



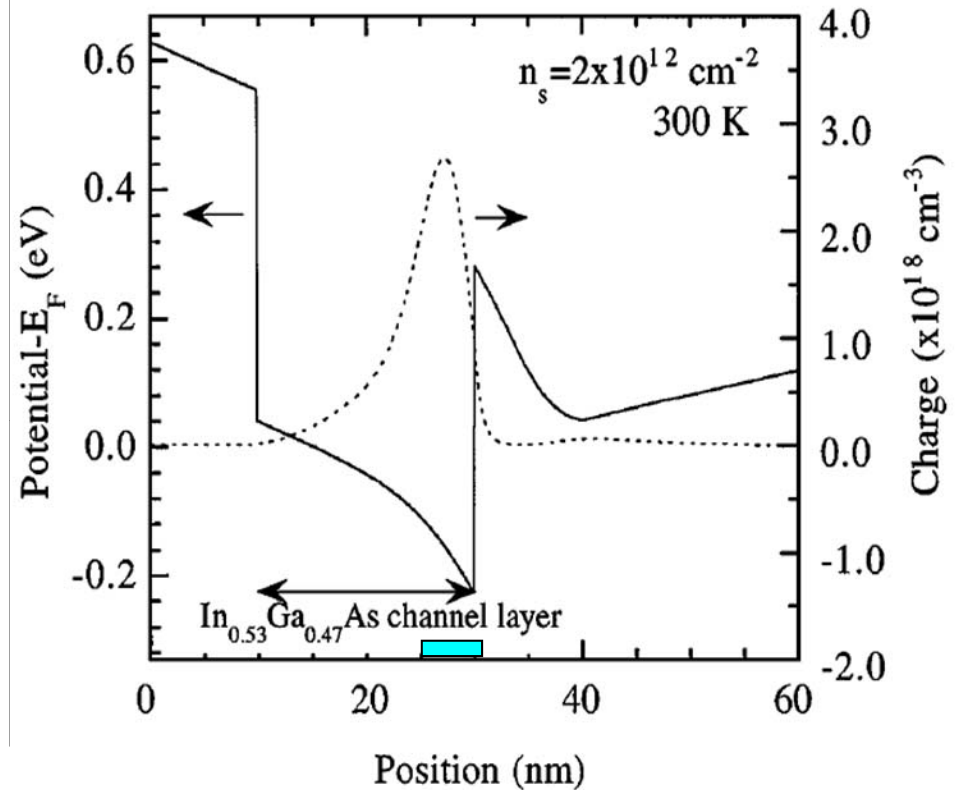


# SOI due to Structure Inversion Asymmetry

## Rashba SOI

ud-In <sub>0.52</sub> Al <sub>0.48</sub> As gate Schottky layer ( 20 nm )
ud-In <sub>0.53</sub> Ga <sub>0.47</sub> As channel layer ( 20 nm )
ud-In <sub>0.52</sub> Al <sub>0.48</sub> As spacer layer ( 6 nm )
n <sup>+</sup> -In <sub>0.52</sub> Al <sub>0.48</sub> As carrier-supply layer ( 7 nm , n=4 × 10 <sup>18</sup> cm <sup>-3</sup> )
ud-In <sub>0.52</sub> Al <sub>0.48</sub> As buffer layer
S. I.-InP substrate

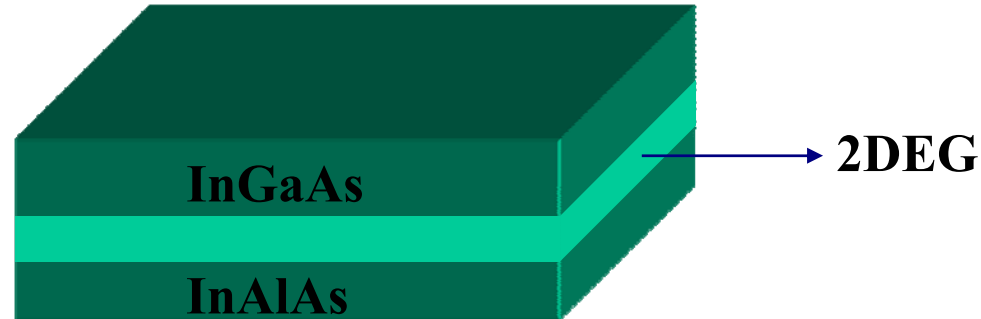
Schematic layer structure of an inverted In<sub>0.53</sub>Ga<sub>0.47</sub>As / In<sub>0.52</sub>Al<sub>0.48</sub>As heterostructure.  
(Nitta *et al.* Phys. Rev. Lett.**78**, 1355(1997))



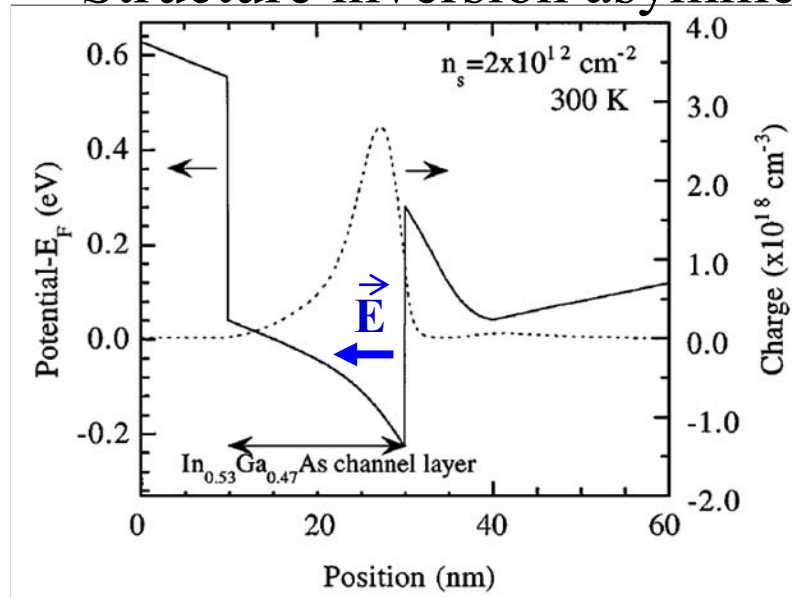
Calculated conduction band diagram (solid line) and electron distribution (dash line).  
(Nitta *et al.* Physica E, **2**, 527(1998))

# Rashba effect (spin-orbit interaction)

Asymmetric Heterostructure:

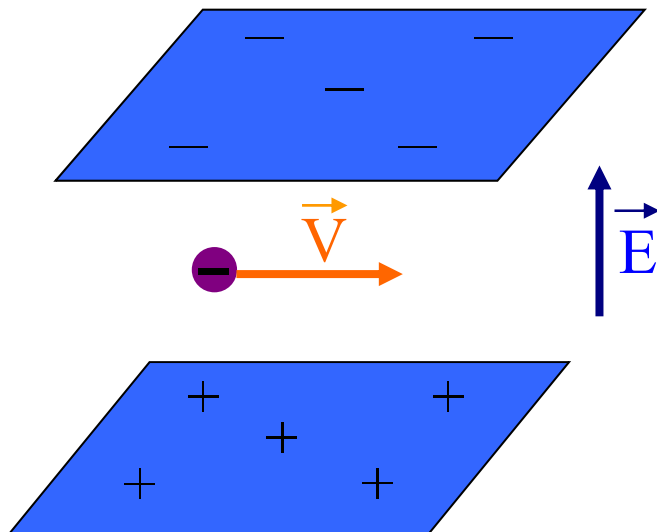


Structure inversion asymmetry:





**An electron moves between two charged plane**



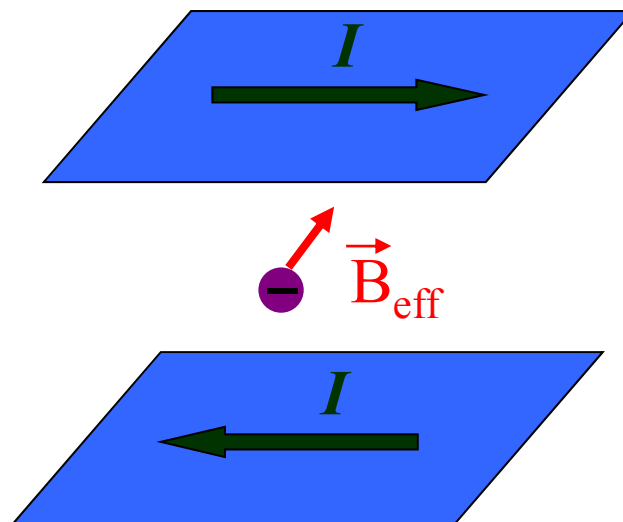
**In Lab. frame**

The SOI hamiltonian is given by

$$H = -\vec{\mu} \cdot \vec{B}_{eff} \propto \vec{\sigma} \cdot (-\vec{V} \times \vec{E})$$

$$H_{\text{Rashba}} \equiv \alpha_0 (\vec{p} \times \hat{z}) \cdot \vec{\sigma}$$

**Effective magnetic field induced by the effective current  $I$ .**



**In the rest frame of an electron**

where  $\alpha_0$  is called the Rashba constant.



# Rashba spin-orbit interaction (SOI)

- SOI is significant in **narrow gap semiconductor heterostructures**.
- Large variation (up to 50%) of the SOI coupling constant  $\alpha$ , tuned by metal gates, has been observed experimentally.

[ Nitta *et. al.* PRL **78** (1997)

Engels *et. al.* PRB **55** (1997)

Grundler, PRL **84** (2000) ]

- Static gate control of  $\alpha$  has been the focus of previous proposals on spin polarized transistors.

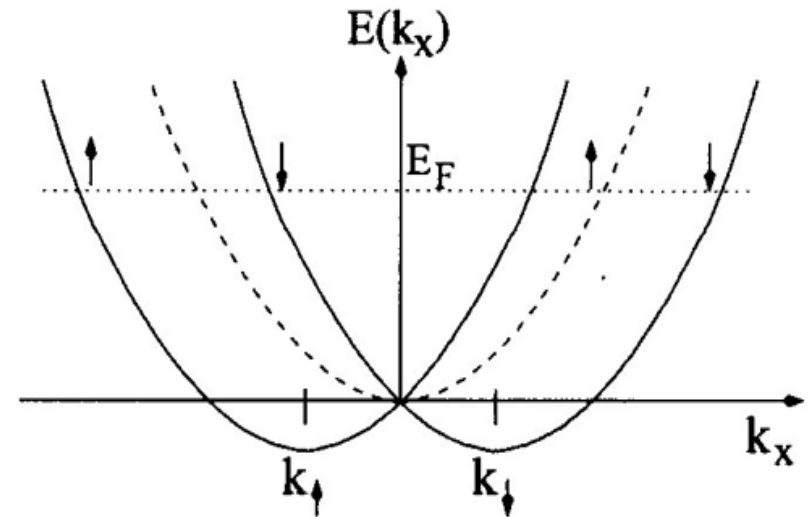
[ Datta *et. al.* APL **56** (1990), ..... ]

Rashba term:

$$H_{\text{so}} = \alpha (\vec{p} \times \hat{v}) \cdot \vec{\sigma}$$

$\hat{v}$  : normal to interface

$\vec{\sigma}$  : the Pauli spin operator





$$E_{2D} = k_x^2 + k_y^2 \pm \alpha_0 \sqrt{k_x^2 + k_y^2}$$

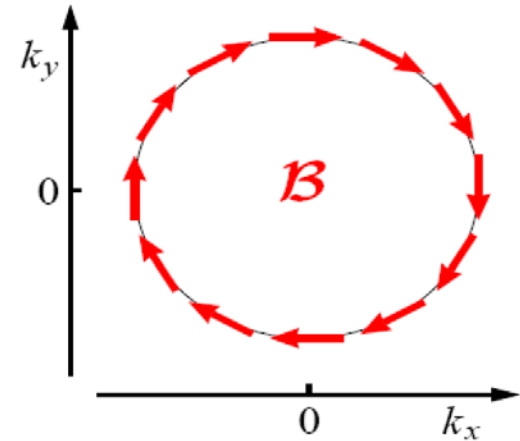
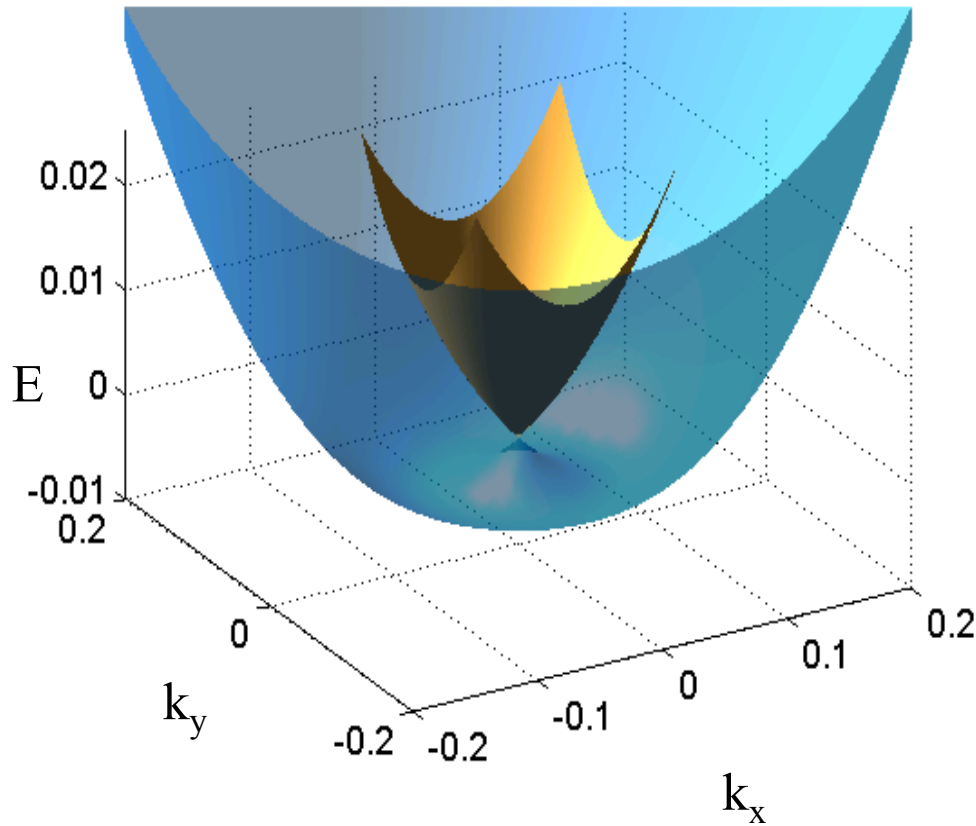


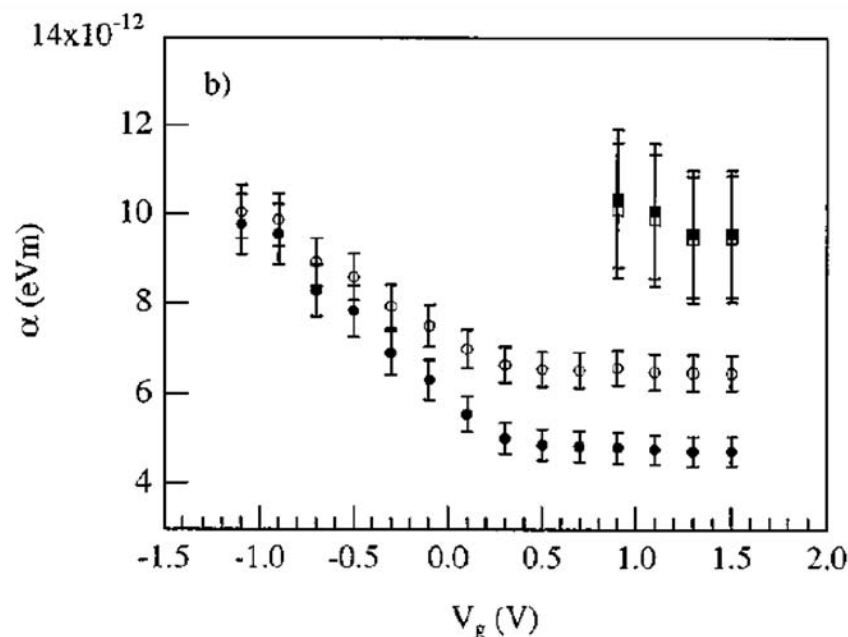
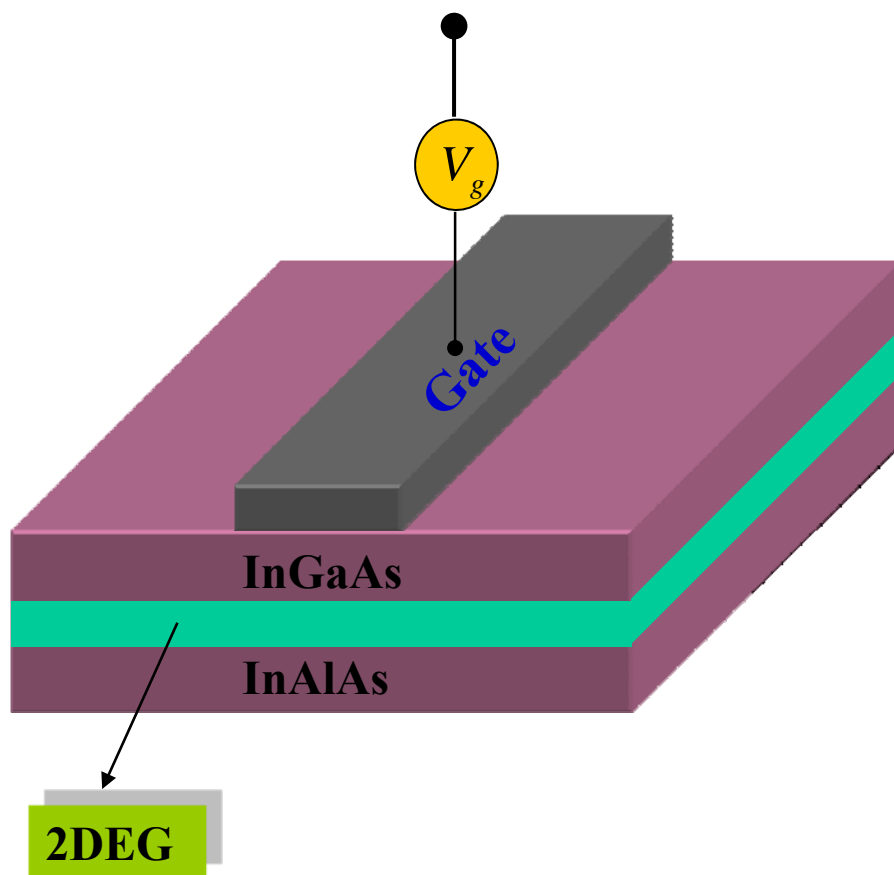
Figure 13: SIA (001) effective field.

Fig.3. Dispersion relation for a 2D Rashba-type system and the Rashba constant  $\alpha_0 = 0.13$ .





# Tuning of the coupling constant $\alpha_0$ by a metal gate



Spin-orbit coupling parameter  $\alpha$  of the first (circle) and second (square) subband as a function of the gate voltage: including (solid) and not including (open) band nonparabolicity correlation.

(Nitta. *et al.* Phys.Rev.B **60**,7736(1999))

# SOI due to Bulk Inversion Asymmetry

## Dresselhaus SOI

Examples: Zincblende structures GaAs, InAs

$$H_{\text{SOI}} = \vec{h}_{\vec{p}} \cdot \vec{\sigma}$$

$$h_k^x = \beta k_x (k_y^2 - \kappa^2);$$

$$h_k^y = -\beta k_y (k_x^2 - \kappa^2)$$

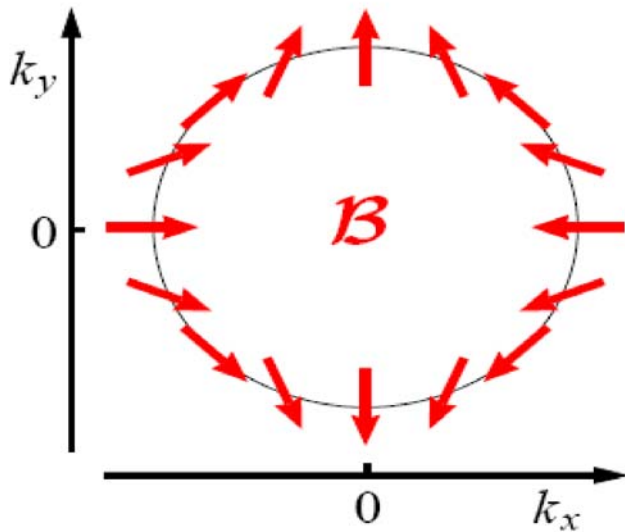


Figure 11: BIA (001) effective field.

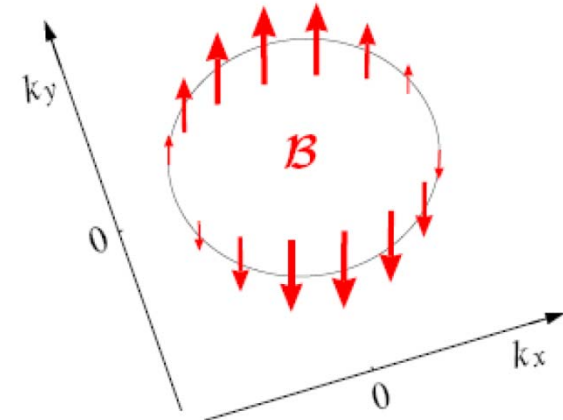


Figure 12: BIA (110) effective field.

## Summary: Physical origin of SOI

**Extrinsic origin:**  
SOI impurity

$$\lambda \vec{\sigma} \cdot (\vec{k} \times \vec{\nabla} V)$$

**Intrinsic origin:**  
Structural effect

$$H_{\text{SOI}} = \vec{h}_{\vec{p}} \cdot \vec{\sigma}$$

**Dresselhaus SOI:**  
Bulk Inversion asymmetry

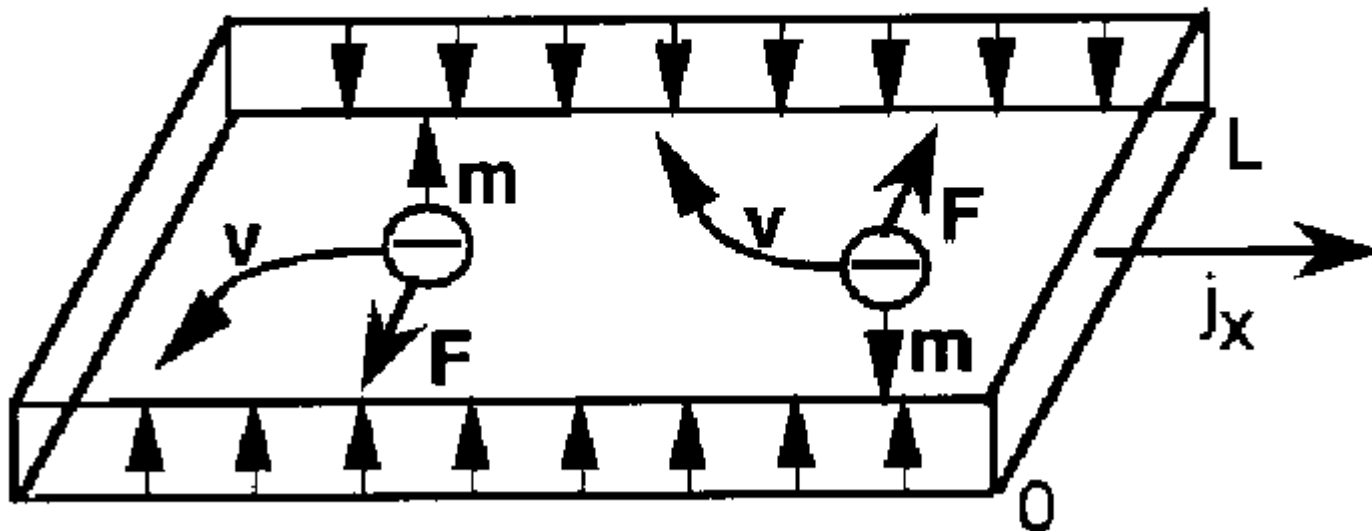
$$\begin{aligned} h_k^x &= \beta k_x (k_y^2 - \kappa^2); \\ h_k^y &= -\beta k_y (k_x^2 - \kappa^2) \end{aligned}$$

**Rashba SOI:**  
Structure inversion  
asymmetry

$$\vec{h}_{\vec{k}} = \alpha (\vec{k} \times \hat{z})$$

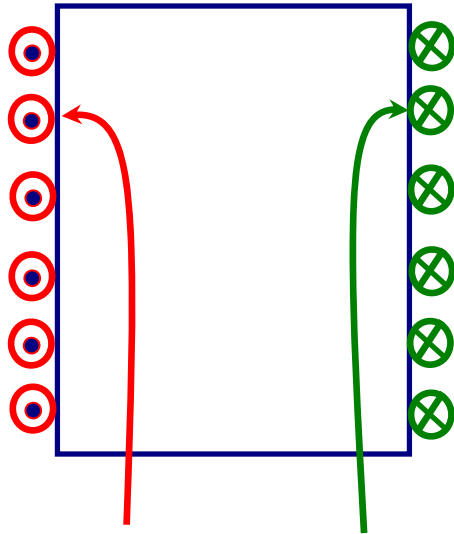
## A simple picture for the extrinsic spin Hall effect

### Spin Hall effect



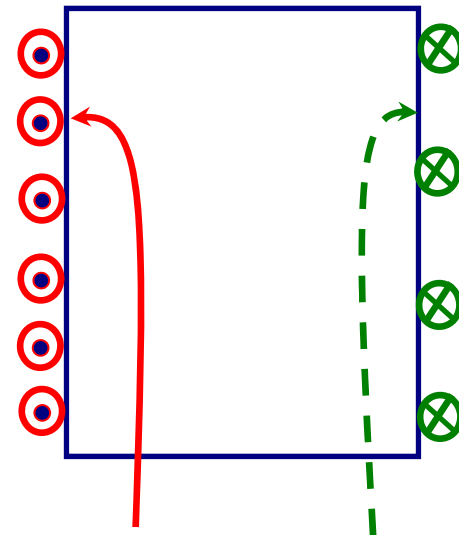
J.E. Hirsch, PRL 83, 1834 (1999)

## Spin accumulation & Spin Hall Effect: Spin-dependent deflection of injected carriers produces spin accumulation at lateral edges



**Injection of  
unpolarized current:**

**Spin accumulation  
without charge  
accumulation**



**Injection of partially  
polarized current:**

**Spin accumulation is  
accompanied by charge  
accumulation**

## Earliest proposal:

An electrical current passes through a sample with spin-orbit interaction induces a *spin polarization near the lateral edges*, with opposite polarization at opposing edges (M.I. D'yakonov and V.I. Perel', *JEPT Lett.*, 13, 467 (1971)).

This effect does not require an external magnetic field or magnetic order in the equilibrium state before the current is applied.

The M.I. D'yakonov and V.I. Perel' (1971) paper was titled: “*Possibility of orienting electron spins with current*” in which an *extrinsic mechanism* was proposed for the spin Hall effect.

V.M. Edelstein, *Solid State Commun.* 73, 233 (1990)  
“Spin polarization of conduction electrons induced  
by electric current in two-dimensional asymmetric  
electron systems”

S. Murakami, N. Nagaosa, S.C. Zhang,  
*Science* 301, 1348 (2003)

$$\mathbf{j}_j^i = \sigma_s \epsilon^{ijk} E_k$$

“Dissipationless quantum spin current at room  
temperature”

J. Sinova, D. Culcer, Q. Niu, N.A. Sinitsyn, T.  
Jungwirth, and A.H. MacDonald,  
*Physical Review Letters* 92, 126603 (2004)

“Universal Intrinsic Spin Hall Effect”

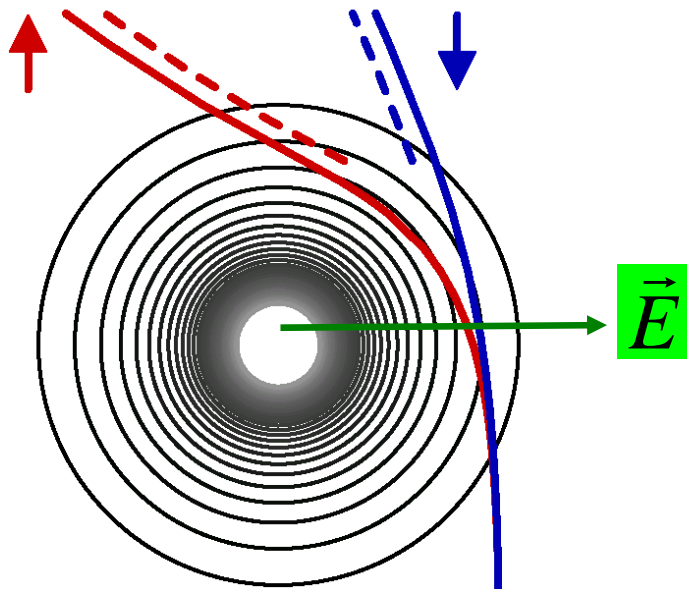
## A simple picture for the extrinsic SOI effect

$$H = \frac{p^2}{2m} + V(\vec{r}) + \lambda e \vec{\sigma} \cdot (\vec{p} \times \vec{E})$$

$$m\ddot{\vec{r}} = -\vec{\nabla}V + \lambda me \frac{d}{dt}(\vec{E} \times \vec{\sigma}) - \lambda e \vec{\nabla}[\vec{\sigma} \cdot (\vec{p} \times \vec{E})]$$

$$m\ddot{\vec{r}} = -\vec{\nabla}V + \lambda me \sigma (\vec{v} \times \hat{z})[dE/dr + E/r]$$

$e > 0$ ;  $\vec{\sigma}$  along  $\hat{z}$ , and linear in  $\lambda$ .



For an attractive scatterer with  $E \sim r^{-n}$  ( $n > 1$ ), **spin up electron** is deflected more to the **left** and **spin down electron** is deflected more to the **right**.

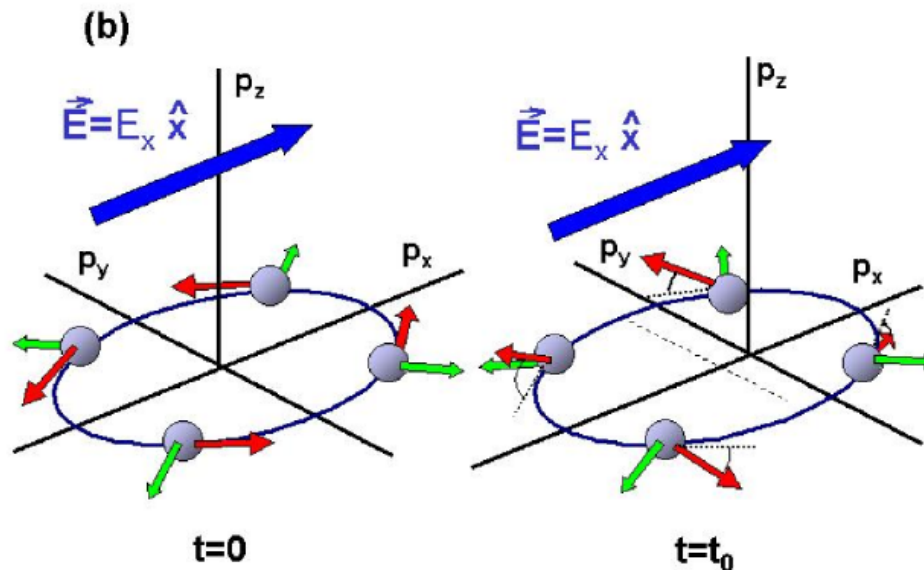


In the presence of an electric field the Fermi surface (circle) is displaced an amount  $|eE_x t_0 / \hbar|$  at time  $t_0$  (shorter than typical scattering times). While moving in momentum space, electrons experience an effective torque which tilts the spins up for  $p_y > 0$  and down for  $p_y < 0$ , creating a spin current in the  $y$  direction.

**J. Sinova, *et al* PRL 92, 126603 (2004)**

Green arrows:  
wavevector

Green arrows:  
Effective  
magnetic field  
direction



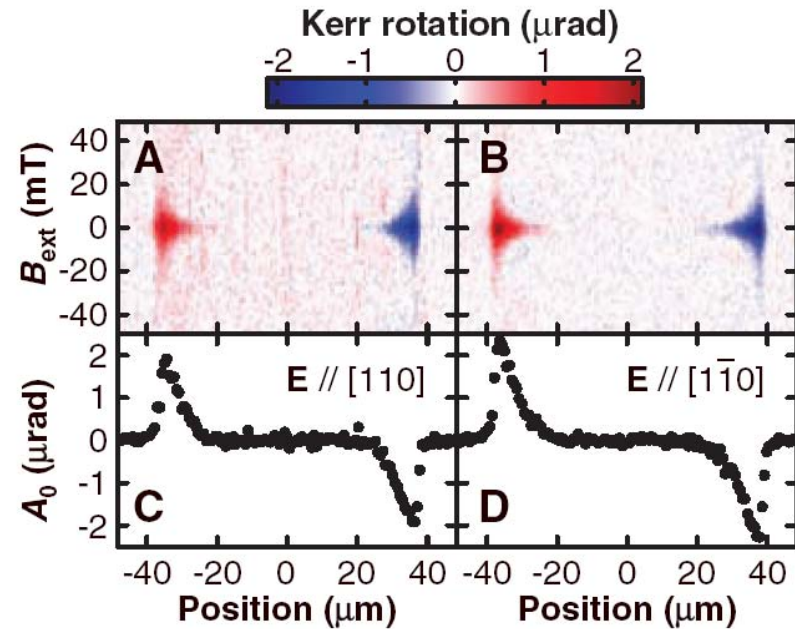
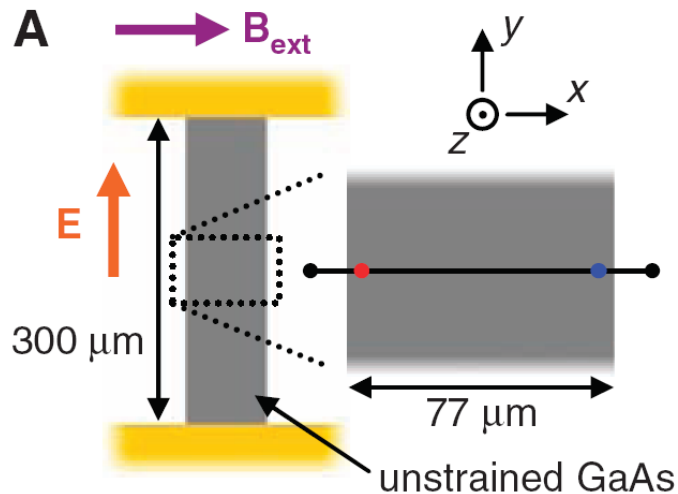
**This picture is not correct because it has not taken into account 2 features:**

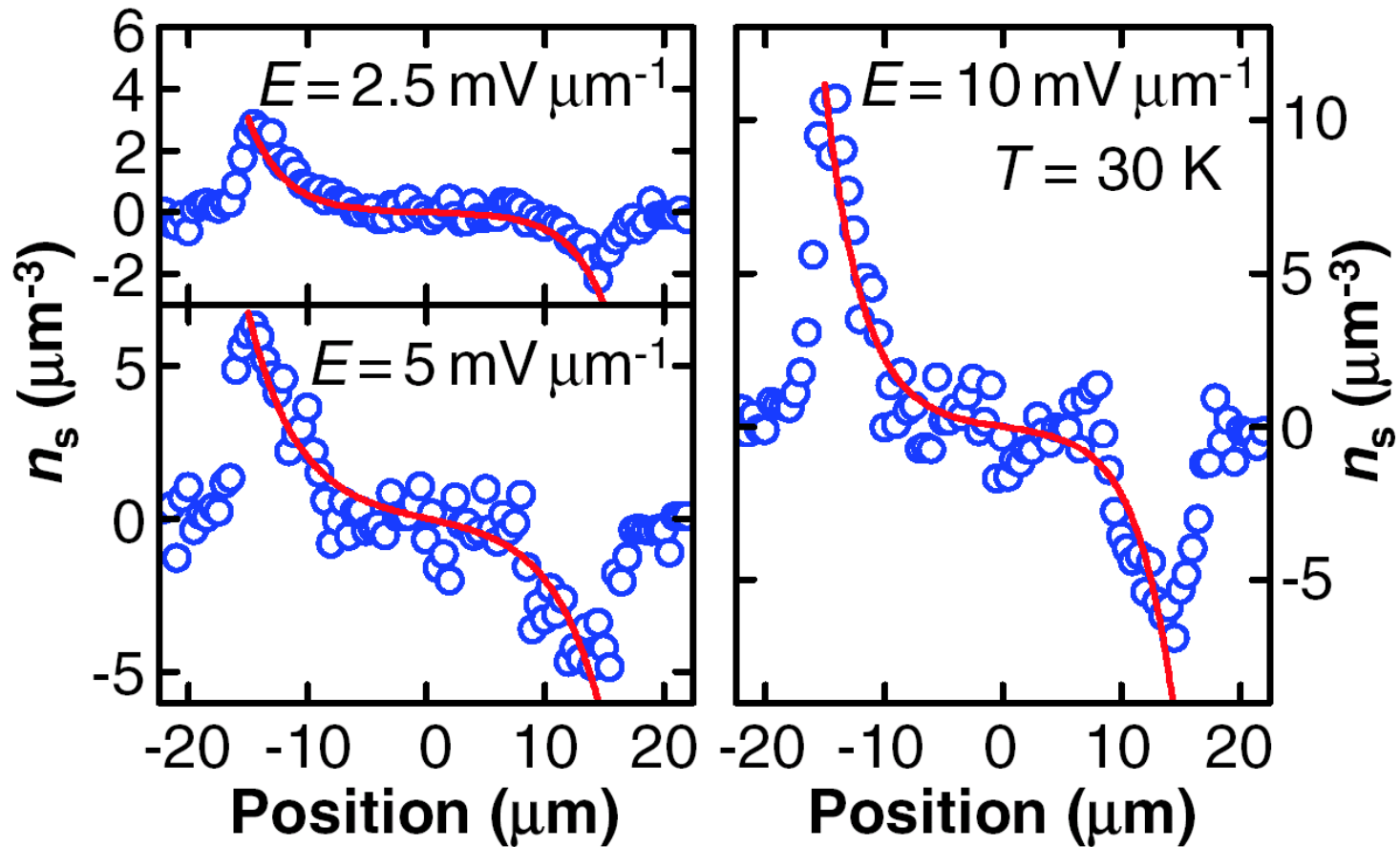
- 1. the effect of background impurities;**
- 2. the form of SOI: linear or non-linear in  $k$  ?**

**J. Sinova, *et al* PRL 92, 126603 (2004)**

# Experimental observation of **extrinsic** spin Hall Effect in thin 3D layers (weak dependence on crystal orientation)

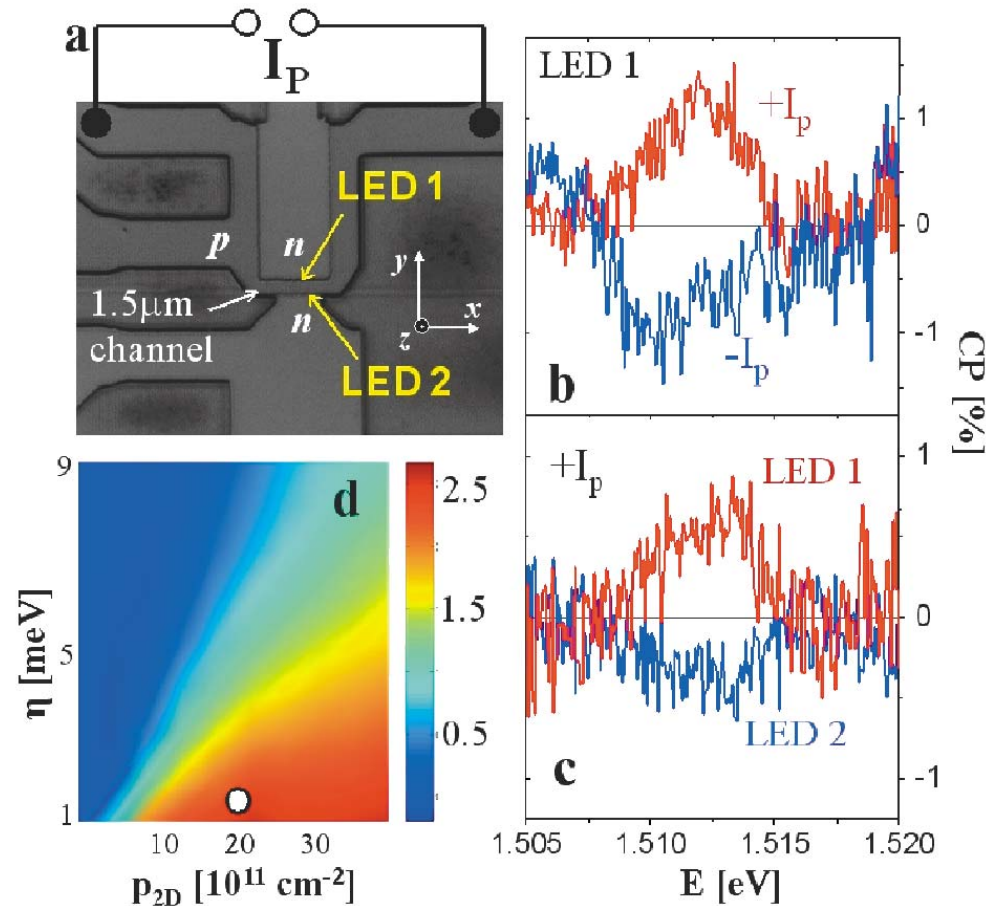
Y.K. Kato, R.C. Myers, A.C. Gossard, D.D. Awschalom, Science 306, 1910 (2004)



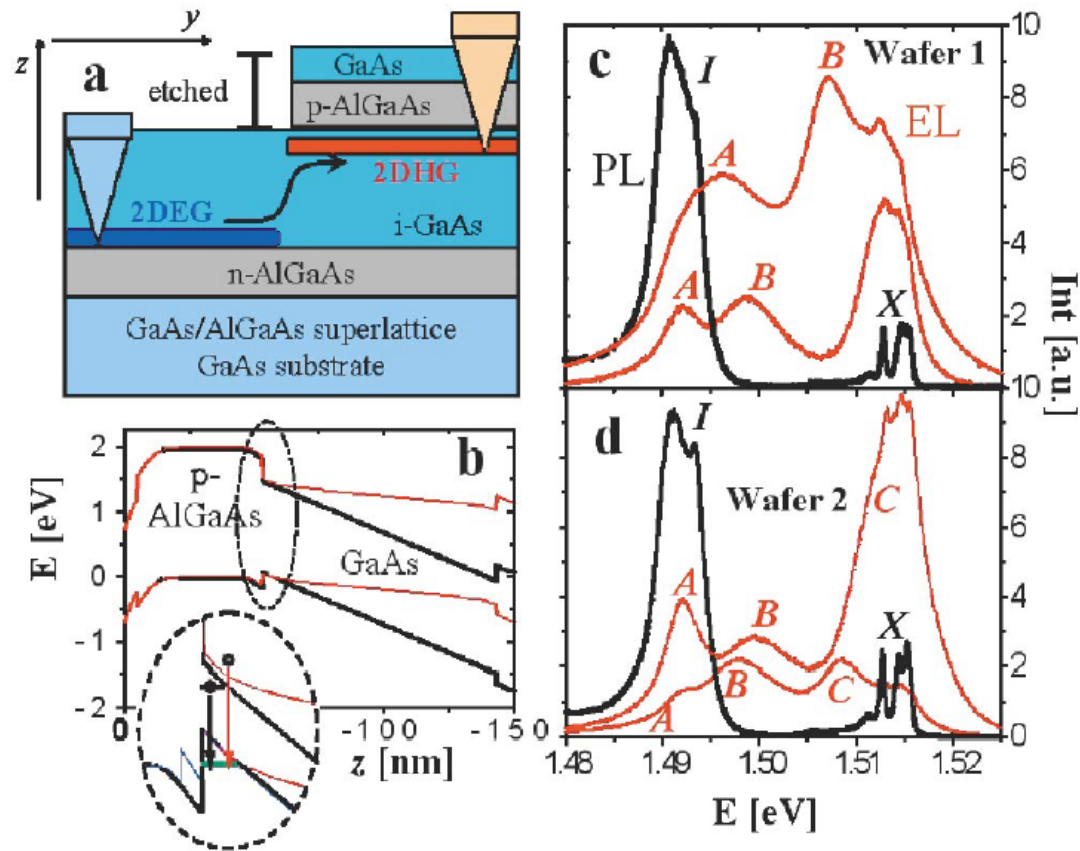


# Experimental confirmation of spin Hall Effect in a 2D hole gas (intrinsic SHE)

J. Wunderlich, B. Kaestner, J. Sinova, and T. Jungwirth, Phys. Rev. Lett. 94, 047204 (2005)



J. Wunderlich, B. Kaestner, J. Sinova, and T. Jungwirth, Phys. Rev. Lett. 94, 047204 (2005)



# Nonequilibrium Spin Polarization in the bulk Case of Rashba SOI

$$H_{\text{SOI}} = \vec{h}_{\vec{k}} \cdot \vec{\sigma}$$

$$\vec{h}_{\vec{k}} = \alpha \vec{k} \times \hat{z}$$

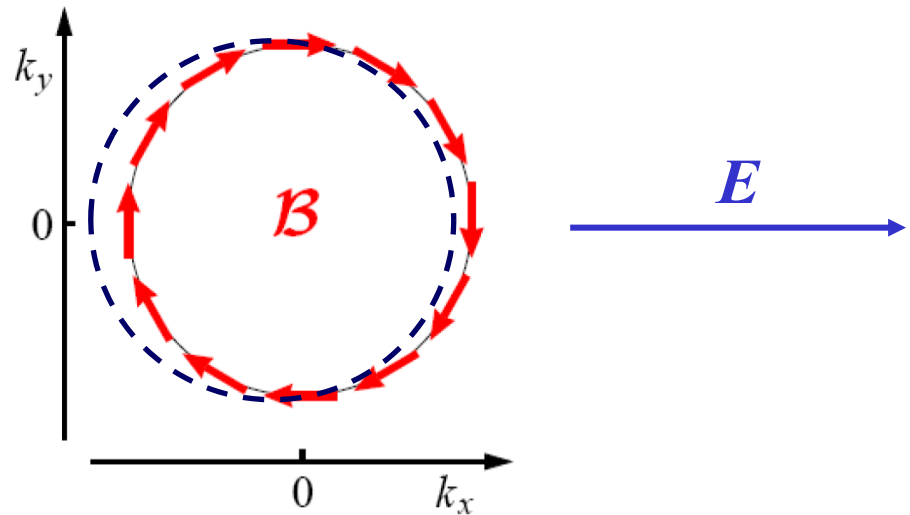


Fig. 13: SIA (001) effective field.

**Spin polarization is normal to the driving  $E$  field**

V.M. Edelstein, Solid State Commun. 73, 233 (1990)

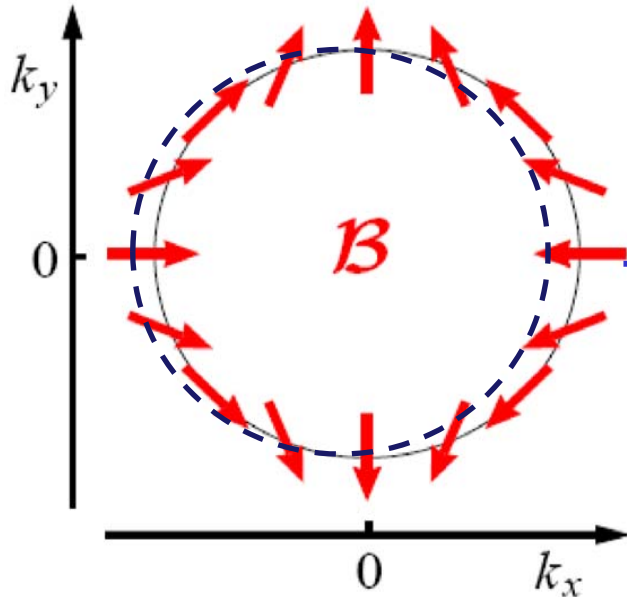


# Nonequilibrium Spin Polarization in the bulk

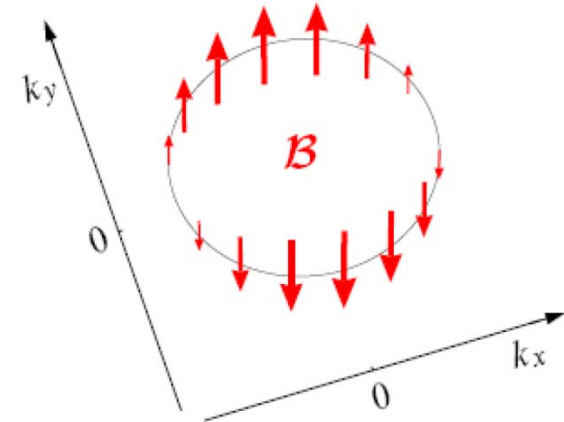
## Case of Dresselhaus SOI

$$H_{\text{SOI}} = \vec{h}_{\vec{p}} \cdot \vec{\sigma}$$

$$h_k^x = \beta k_x (k_y^2 - \kappa^2);$$
$$h_k^y = -\beta k_y (k_x^2 - \kappa^2)$$



BIA (001) effective field.



BIA (110) effective field.

**Spin polarization is in the direction of the driving  $E$  field**

# Nonequilibrium Spin Polarization in the bulk

## Case of Extrinsic SOI

PRL **95**, 166605 (2005)

PHYSICAL REVIEW LETTERS

week ending  
14 OCTOBER 2005

### Theory of Spin Hall Conductivity in *n*-Doped GaAs

Hans-Andreas Engel, Bertrand I. Halperin, and Emmanuel I. Rashba

*Department of Physics, Harvard University, Cambridge, Massachusetts 02138, USA*

(Received 21 May 2005; published 13 October 2005)

We develop a theory of extrinsic spin currents in semiconductors, resulting from spin-orbit coupling at charged scatterers, which leads to skew-scattering and side-jump contributions to the spin-Hall conductivity. Applying the theory to bulk *n*-GaAs, without any free parameters, we find spin currents that are in reasonable agreement with experiments by Kato *et al.* [Science **306**, 1910 (2004)].

$$H_{\text{SOI}} = \lambda \vec{\sigma} \cdot (\vec{k} \times \vec{\nabla} V)$$

$$C_k = -(e\hbar\tau/m^*) \frac{\partial f_0}{\partial \epsilon}$$

$$\hat{f}(\mathbf{k}) = f_0(k) + \mathbf{k} \cdot \left[ \mathbf{E} + \frac{\gamma_k}{2} (\boldsymbol{\sigma} \times \mathbf{E}) \right] C_k$$

**Spin polarization is zero**



**Spin is not conserved:**

$$\frac{\partial S_z}{\partial t} + \nabla \cdot \mathbf{J}_s = \mathcal{T}_z.$$

Torque density

**and definition of spin current remains an issue  
(Shi J, Zhang P, Xiao D, and Nui Q, Phys. Rev.  
Lett. 96 76604(2006)).**

$$\vec{\tau} \equiv \frac{d\hat{s}_z}{dt} \equiv (1/i\hbar) [\hat{s}_z, \hat{H}]$$

**Experiments measure spin accumulation, not  
spin current.**

**Spin accumulation, not spin current, is the key  
physical quantity of our interest.**

## Derivation of a spin diffusion equation

$$H_{\text{SOI}} = \vec{h}_{\vec{p}} \cdot \vec{\sigma}$$

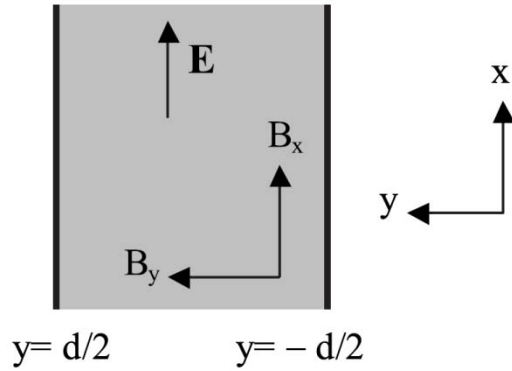
### Dresselhaus SOI:

$$h_k^x = \beta k_x (k_y^2 - \kappa^2);$$
$$h_k^y = -\beta k_y (k_x^2 - \kappa^2)$$

Dresselhaus SOI contains  
cubic term in  $k$

### Rashba SOI:

$$\vec{h}_{\vec{k}} = \alpha (\vec{k} \times \hat{z})$$



$$H' = V(\vec{r}, t) + \vec{B}(\vec{r}, t) \cdot \vec{\sigma} = \sum_i \Phi_i(\vec{r}, t) \tau^i$$

$$\text{where } \tau^0 = 1, \text{ and } \tau^i = \sigma^i \text{ for } i = x, y, z.$$

$$\mathbf{H}_B \cdot \boldsymbol{\sigma} = (\mathbf{h}_k + \tilde{\mathbf{B}}) \cdot \boldsymbol{\sigma}$$

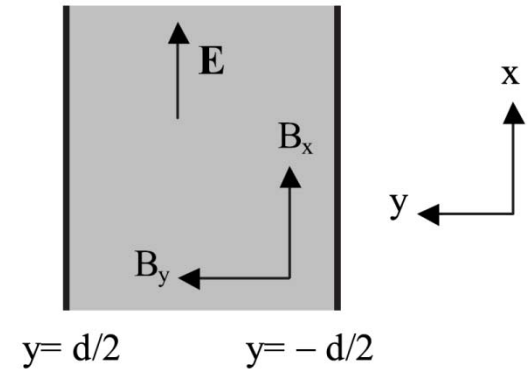
$$\tilde{\mathbf{B}} = g^* \mu_B \mathbf{B} / 2$$

$$D_i(\mathbf{r}, t) = -i \text{Tr}[\tau^j G^{-+}(\mathbf{r}, \mathbf{r}, t, t)]$$

$$\mathbf{D}_i(\mathbf{r}, \omega) = \int d^2 r' \sum_j \Pi_{ij}(\mathbf{r}, \mathbf{r}', \omega) \Phi_j(\mathbf{r}', \omega) + \mathbf{D}_i^0(\mathbf{r}, \omega)$$

$$D_i^0(\vec{q}, \omega) = -2N_0 \Phi_i(\vec{q}, \omega) \quad \text{is the local equilibrium densities}$$

$$\Pi_{ij}(\mathbf{q}, \omega) = i\omega \sum_{\mathbf{p}_1 \mathbf{k}_1} \int \frac{d\omega'}{2\pi} \frac{\partial f_{\text{FD}}(\omega')}{\partial \omega'} \langle \text{Tr}[G^a(\mathbf{k}_1, \mathbf{p}_1 - \mathbf{q}, \omega) \times \boldsymbol{\tau}^i G^r(\mathbf{p}_1, \mathbf{k}_1 + \mathbf{q}, \omega + \omega') \boldsymbol{\tau}^j] \rangle,$$



$$\Pi_{ij}(\mathbf{q}, \omega) = \frac{i\omega}{2\pi} \sum_j \int d\omega' \frac{\partial f_{\text{FD}}}{\partial \omega'} \left( \frac{\pi N_0}{\Gamma} \right) \tau_{\mu\alpha}^i \tau_{\beta\nu}^j \Psi_{\mu\lambda}^{\alpha\gamma}(\omega, \omega', \mathbf{q}) \times \{ [1 - \Psi(\omega, \omega', \mathbf{q})]^{-1} \}_{\lambda\nu}^{\gamma\beta},$$

$$\Psi^{il} = \frac{\Gamma}{2\pi N_0} \sum_{\mathbf{p}'} \text{Tr}[\boldsymbol{\tau}^i G^{r(0)}(\mathbf{p}', \omega + \omega') \boldsymbol{\tau}^l G^{a(0)}(\mathbf{p}' - \mathbf{q}, \omega')]$$

$$\Gamma / (\pi N_0) = c_i |V_{\text{sc}}|^2 / V$$

$$\mathbf{D}_i(\mathbf{r}, \omega) = \int d^2r' \sum_j \Pi_{ij}(\mathbf{r}, \mathbf{r}', \omega) \Phi_j(\mathbf{r}', \omega) + \mathbf{D}_i^0(\mathbf{r}, \omega)$$

$$\begin{aligned} \Pi_{ij}(\mathbf{q}, \omega) = & \frac{i\omega}{2\pi} \sum_j \int d\omega' \frac{\partial f_{\text{FD}}}{\partial \omega'} \left( \frac{\pi N_0}{\Gamma} \right) \boldsymbol{\tau}_{\mu\alpha}^j \boldsymbol{\tau}_{\beta\nu}^j \Psi_{\mu\lambda}^{\alpha\gamma}(\omega, \omega', \mathbf{q}) \\ & \times \{[1 - \Psi(\omega, \omega', \mathbf{q})]^{-1}\}_{\lambda\nu}^{\gamma\beta}, \end{aligned}$$

$$\Psi^{il} = \frac{\Gamma}{2\pi N_0} \sum_{\mathbf{p}'} \text{Tr}[\boldsymbol{\tau}^j G^{r(0)}(\mathbf{p}', \omega + \omega') \boldsymbol{\tau}^l G^{a(0)}(\mathbf{p}' - \mathbf{q}, \omega')]$$

$$(1 - \Psi)^{il} (\mathbf{D}_l - \mathbf{D}_l^0) = i\omega \tau \Psi^{il} \mathbf{D}_l^0,$$

Expansion of  $\Psi^{il}$  over  $\vec{q}$  leads to the Spin Diffusion equation

$$\Psi^{is}(\omega, \omega', \vec{q}) = \frac{1}{2} \frac{c_i}{V} |V_s|^2 \sum_{\vec{p}} \text{Tr} \left[ \tau^i G^a(\vec{p} - \vec{q}, \omega') \tau^s G^r(\vec{p}, \omega + \omega') \right]$$

**To get some feeling, let's consider the case  $\hbar \rightarrow 0$ :**

$$\Psi^{is}(\omega, \omega', \vec{q}) \Big|_{\hbar=0} = \delta^{is} \left[ 1 + i\omega\tau - Dq^2\tau \right]$$

$$\tau = \frac{1}{2\Gamma}$$

$$\Gamma = \pi c_i |V_s|^2 N_0(E_F)$$

$$D = v_F^2 \tau / 2$$

Dirty limit:  $\hbar_p \ll \Gamma$

$$\omega \ll \Gamma, \quad \vec{v}_F \cdot \vec{q} \ll \Gamma,$$

$$\Gamma \ll E_F$$

$$\Psi^{is}(\omega, \omega', \vec{q}) \Big|_{\text{linear in } h \text{ and } \omega=0} = \frac{-i\varepsilon^{ism}}{\Gamma^2} (\vec{q} \cdot \vec{v}_F) h_{p_F}^m$$

**Precession of the inhomogeneous spin polarization about the effective SOI field.**

$$\Psi^{is}(\omega, \omega', \vec{q}) \Big|_{h=0} = \delta^{is} [1 + i\omega\tau - Dq^2\tau]$$

**Angular average**

$$\Psi^{ij}(\omega, \omega', \vec{q}) \Big|_{\substack{q=0, \omega=0 \\ h^2 \text{ term}}} = -4\tau^2 h_{p_F}^2 (\delta^{ij} - n_k^i n_k^j)$$

**D'akonov-Perel spin relaxation**

$$\Psi^{l0}(\omega, \omega', \vec{q}) = \frac{\tau}{\Gamma^2} h_{p_F}^3 \frac{\partial n_{p_F}^l}{\partial \vec{p}} \cdot (i\vec{q}) = \Psi^{l0}(\omega, \omega', \vec{q})$$

$$\hat{n}_{\vec{k}} = \vec{h}_{\vec{k}} / h_{\vec{k}}$$

**Charge-spin coupling**

$$D_i(\vec{r}, \omega) - D_i^0(\vec{r}, \omega) = \int d^2 r' \sum_j \Pi_{ij}(\vec{r}, \vec{r}', \omega) \Phi_j(\vec{r}', \omega)$$

$$D^{ij} (D - D^0)_j = -i\omega D_i$$

$$D^{ij} = \delta^{ij} D \nabla^2 + \underbrace{4\tau \varepsilon^{ijm} \overline{h_{p_F}^m v_F^m}}_{R^{ijm} \nabla_m} - \underbrace{4\tau \overline{h_{p_F}^2 (\delta^{ij} - n_p^i n_p^j)}}_{\Gamma^{ij}} + \underbrace{\frac{h_{p_F}^3}{\Gamma^2} \frac{\partial n_{p_F}^i}{\partial \vec{p}} \cdot \vec{\nabla}}_{M^{i0}}$$

***D*** is the diffusion constant



## Spin densities Diffusion equation for Rashba-type semiconductor strip

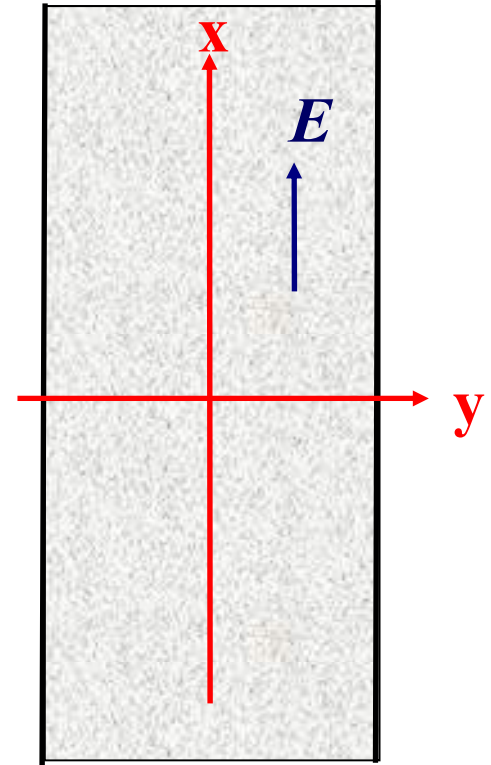
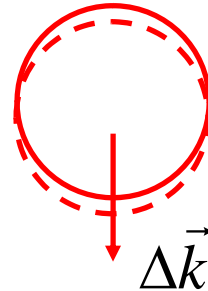
$$D \frac{\partial^2 S^z}{\partial y^2} - \Gamma^{zz} S^z = -R^{zyy} \frac{\partial S^y}{\partial y}$$

$$D \frac{\partial^2 S^y}{\partial y^2} - \Gamma^{yy} S^y = -R^{yzy} \frac{\partial S^z}{\partial y} + \frac{M_x^{y0}}{2} \frac{\partial D_0^0}{\partial x}$$

$$D \frac{\partial^2 S^x}{\partial y^2} - \Gamma^{xx} S^x = 0$$

**Bulk spin density :  $S^x = S^z = 0$**

$$S_b^y = - \left( M_x^{y0} / 2\Gamma^{yy} \right) \frac{\partial D_0^0}{\partial x} = -N_0 e E \alpha \tau$$



V.M. Edelstein  
Solid State Comm. 1990  
J.I. Inoue *et al*, PRB 2003

## Relating the spin flux to the spin densities

$$I_i^y(\vec{r}) = -D \frac{\partial S^i}{\partial y} - \frac{1}{2} R^{ijy} (S^j - S_b^j) + \delta_{iz} I_{SH}$$

$$I_{SH} = -\frac{1}{2} R^{zjy} S_b^j + eE \frac{N_0}{2\Gamma^2} v_F^y \overline{\left( \frac{\partial \vec{h}_k}{\partial k_x} \times \vec{h}_k \right)}_z$$

Boundary condition :

$$I_i^y(\pm d/2) = 0$$

**More recent work on the boundary conditions for the spin diffusion equation:**

**\*G. Bleibaum, Phys. Rev. B 74, 113309 (2006)**

**“Boundary conditions for spin-diffusion equations with Rashba spin-orbit interaction”**

**V.M. Galitski, A.A. Burkov, and S. Das Sarma,  
Phys. Rev. B 74, 115331 (2006)**

**“Boundary conditions for spin diffusion in disordered systems”**

**\*Y. Tserkovnyak, B.I. Halperin, A.A. Kovalev, A. Brataas,  
New Journal of Physics 9, 345 (2007)**

**“Boundary spin Hall effect in a two-dimensional semiconductor system with Rashba spin-orbit coupling”**

**\* Work that agrees with our result for hard wall boundary.**

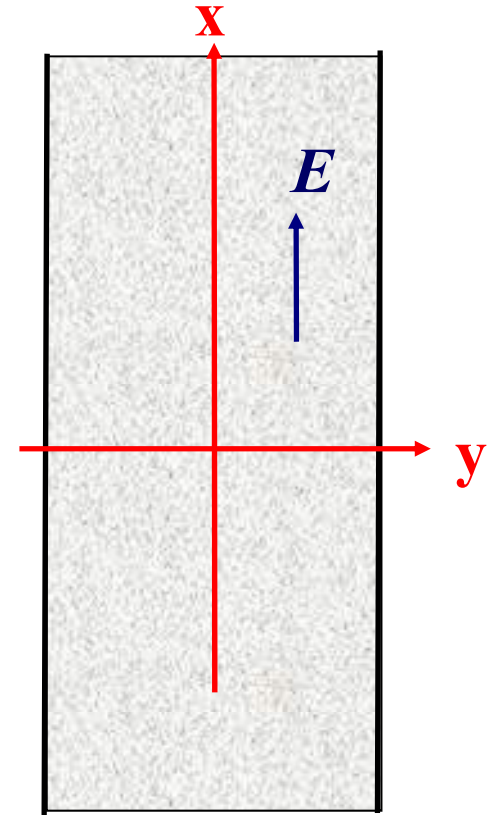
$$D \frac{\partial^2 S^z}{\partial y^2} - \Gamma^{zz} S^z = -R^{zyy} \frac{\partial S^y}{\partial y}$$

$$D \frac{\partial^2 S^y}{\partial y^2} - \Gamma^{yy} S^y = -R^{yzy} \frac{\partial S^z}{\partial y} + \frac{M_x^{y0}}{2} \frac{\partial D_0^0}{\partial x}$$

$$D \frac{\partial^2 S^x}{\partial y^2} - \Gamma^{xx} S^x = 0$$

**Bulk spin density :  $S^x = S^z = 0$**

$$S_b^y = - \left( M_x^{y0} / 2\Gamma^{yy} \right) \frac{\partial D_0^0}{\partial x} = -N_0 e E \alpha \tau$$



**NO Spin Accumulation at edges for Rashba-type strip.**

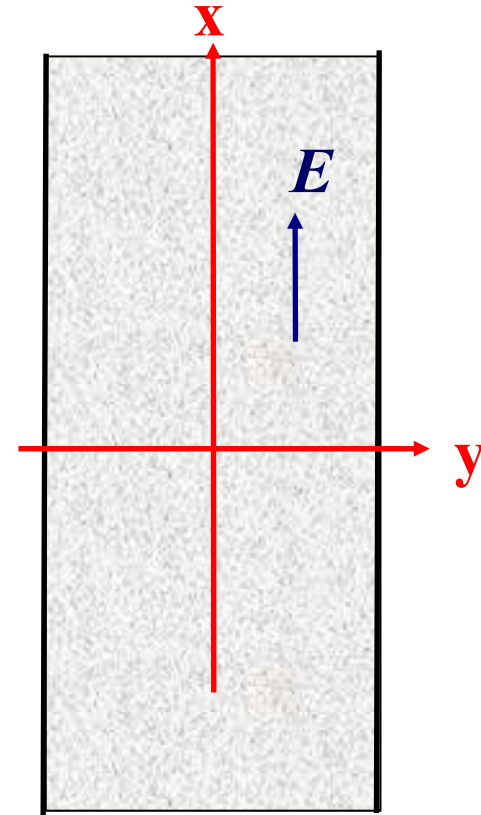
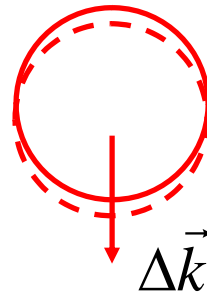
$$D \frac{\partial^2 S^z}{\partial y^2} - \Gamma^{zz} S^z = -R^{zxy} \frac{\partial S^x}{\partial y}$$

$$D \frac{\partial^2 S^x}{\partial y^2} - \Gamma^{xx} S^x = -R^{xzy} \frac{\partial S^z}{\partial y} + M_x^{x0} \frac{\partial D_0^0}{\partial x}$$

$$D \frac{\partial^2 S^y}{\partial y^2} - \Gamma^{yy} S^y = 0$$

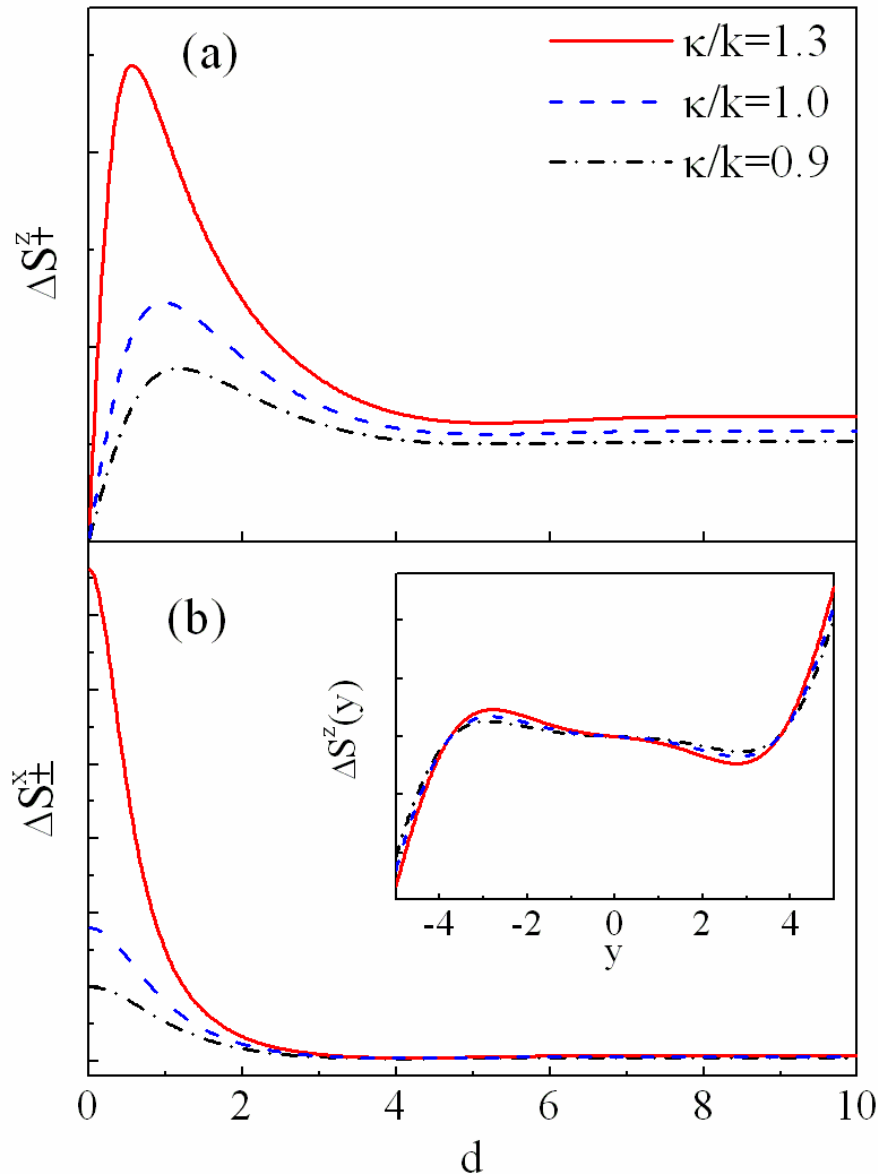
**Bulk spin density :  $S^y = S^z = 0$**

$$S_b^x = -\left(M_x^{x0} / 2\Gamma^{xx}\right) \frac{\partial D_0^0}{\partial x}$$



$$h_k^x = \beta k_x (k_y^2 - \kappa^2);$$

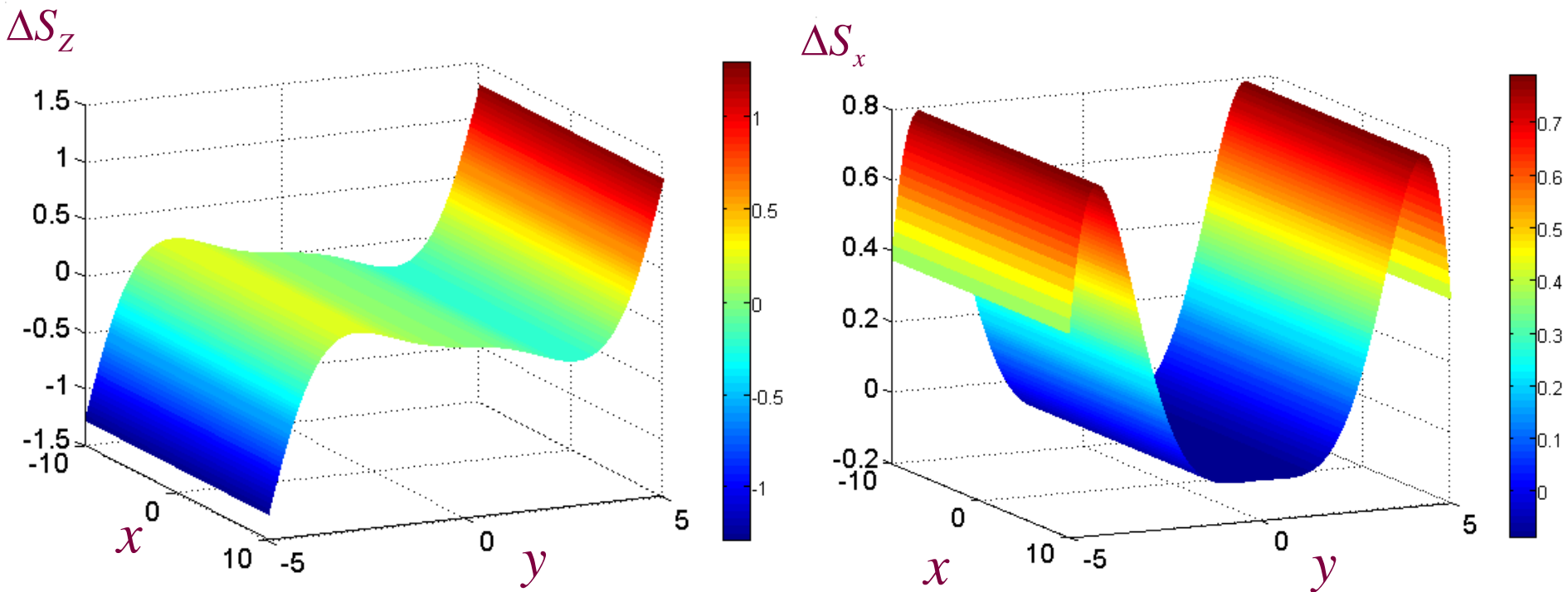
$$h_k^y = -\beta k_y (k_x^2 - \kappa^2)$$



Spin densities  
for  $i = x, z$  as a functions of its width  
 $d$ .

The inset shows the dependence of  
 $\Delta S_z(y)$  on the transverse coordinate  
 $y$ . Lengths are measured in unit of

Phys.Rev.Lett. 95, 146601(2005)  
Mal'shukov, Wang, Chu, Chao



Spin densities of  $\Delta S_z$  are of odd parity in a 2D strip with  $\kappa/k=1.3$  for the strip width  $d = 10$ .

**Spin accumulation in a Dresselhaus-type 2DEG has a comparable magnitude ( $\sim 17 \mu\text{m}^{-2}$  for GaAs)**

**At the time the semiconductor spintronic community gradually realized that disorder due to normal impurities removes completely the Rashba SOI Spin Hall Effect.**

## **SHE in Rashba-type spin-orbit systems vanishes in the presence of weak disorder**

**J.I. Inoue, *et al*, Phys. Rev. B 70, 041303 (2004)**  
**E.I. Rashba, Phys. Rev. B 70, 201309 (2004)**  
**O. Chalaev *et al*, Phys. Rev. B 71, 245318 (2005)**  
**E.G. Mishchenko, *et al*, Phys. Rev. Lett. 93, 226602 (2004)**  
**A.A. Burkov, *et al*, Phys. Rev. B 70, 155308 (2004)**  
**O.V. Dimitrova, Phys. Rev. B 71, 245327 (2005)**  
**R. Raimondi *et al*, Phys. Rev. B 71, 033311 (2005)**  
**A.G. Mal'shukov *et al*, Phys. Rev. B 71, 121308(R) (2005)**  
**B.A. Bernevig and S.C. Zhang, Phys. Rev. Lett. 95, 016801 (2005)**

**Cubic dependence on  $k$  is crucial.**



# Spin-Hall Effect for Dresselhaus SOI 2DEG in a magnetic field

## Spin diffusion equation for Dresselhaus SOI 2DEG

$$\left\{ \begin{array}{l} D \frac{\partial^2}{\partial y^2} S_x + \frac{R^{xzy}}{\hbar} \frac{\partial}{\partial y} S_z - \frac{\Gamma^{xx}}{\hbar^2} S_x + \frac{2}{\hbar} \tilde{B}_y S_z - \frac{C_1}{\hbar^2} = 0, \\ D \frac{\partial^2}{\partial y^2} S_y - \frac{\Gamma^{yy}}{\hbar^2} S_y - \frac{2}{\hbar} \tilde{B}_x S_z = 0, \\ D \frac{\partial^2}{\partial y^2} S_z + \frac{R^{zxy}}{\hbar} \frac{\partial}{\partial y} S_x - \frac{\Gamma^{zz}}{\hbar^2} S_z - \frac{2}{\hbar} \tilde{B}_y S_x + \frac{2}{\hbar} \tilde{B}_x S_y - \frac{\tilde{B}_y}{\hbar} C_2 = 0, \end{array} \right.$$

$$C_2 = \overline{\tau(\partial h_k^x / \partial k_x)} (\partial D_0^0 / \partial x)$$

$$C_1 = M^{x0} D_0^0 / 2$$

$$D_0^0 = -2N_0 e E x$$

**Precession of  
Inhomogeneous  
Spin**

$$d\boldsymbol{\sigma} / dt = (2 / \hbar) \tilde{\mathbf{B}} \times \boldsymbol{\sigma}$$

**D'akonov-Perel  
spin relaxation**

## Spin current for Dresselhaus SOI 2DEG

$$I_y^i(\mathbf{r}) = -2D \frac{\partial S_i}{\partial y} - \frac{R^{ijy}}{\hbar} (S_j - S_j^b) + \frac{I_{sH}}{\hbar} \delta_{iz}$$

$$I_{sH} = -R^{zjy} S_j^b + 4\tau^2 e E N_0 v_F \overline{\left( \frac{\partial \mathbf{h}_{\mathbf{k}}}{\partial k_x} \times \mathbf{h}_{\mathbf{k}} \right)_z}$$

Boundary condition :

$$I_i^y(\pm d/2) = 0$$

# Spatial profile of the spin densities for the case of longitudinal $B$

Numerical parameters:

GaAs

$$m^* = 0.067m_0$$

$$g^* = 0.44$$

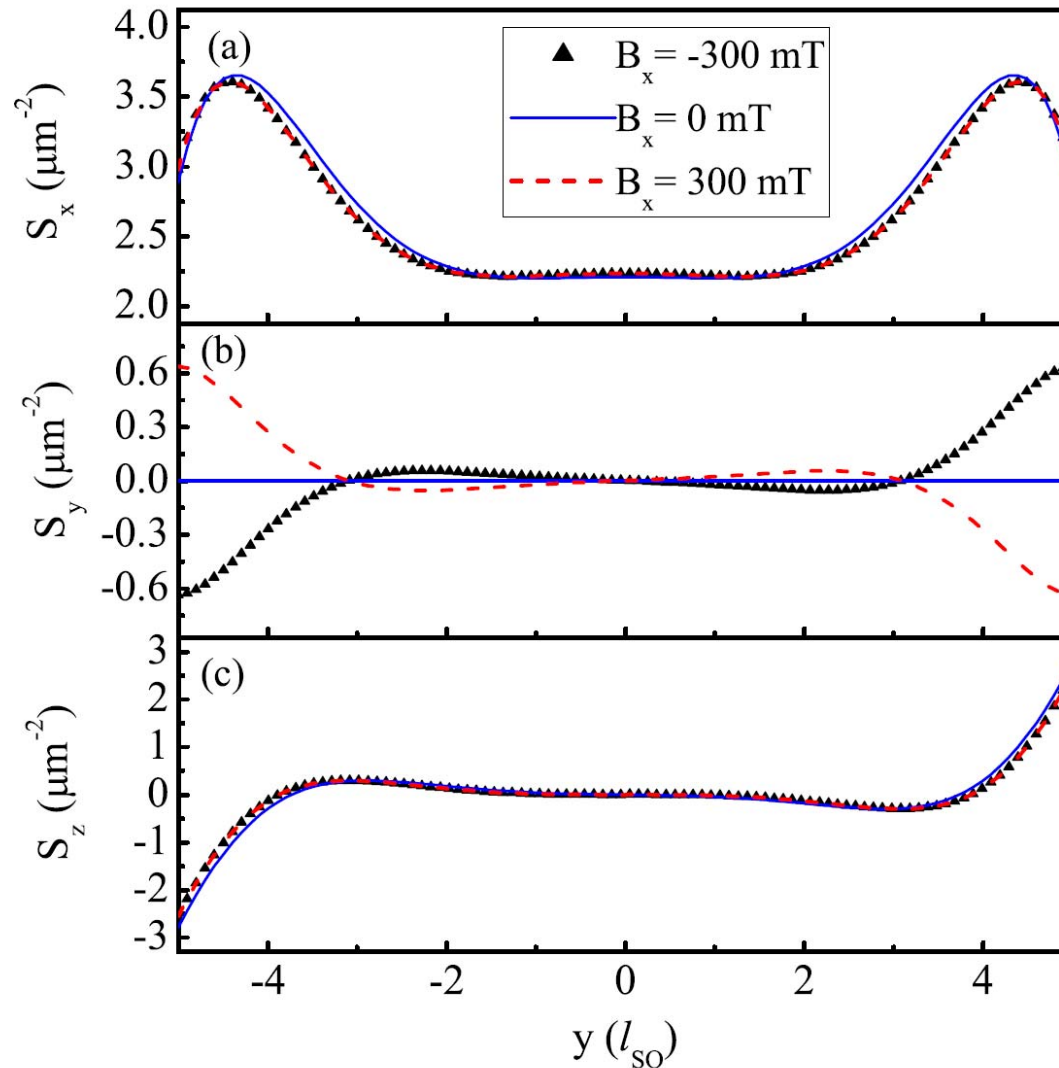
$$\beta = 27.5 \text{ eV}\text{\AA}^3$$

$$n = 2.4 \times 10^{11} \text{ cm}^{-2}$$

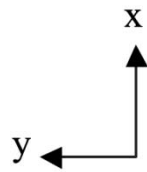
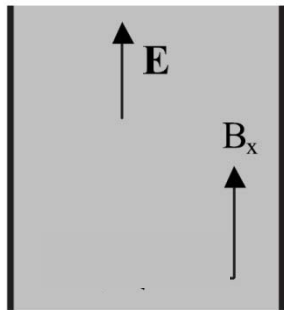
$$w = 300 \text{ \AA}$$

$$l_e = 1 \text{ }\mu\text{m}$$

$$l_{\text{so}} = 2.9 \text{ }\mu\text{m}$$



$S_y$  changes most drastically: contribution from precession of  $S_z$

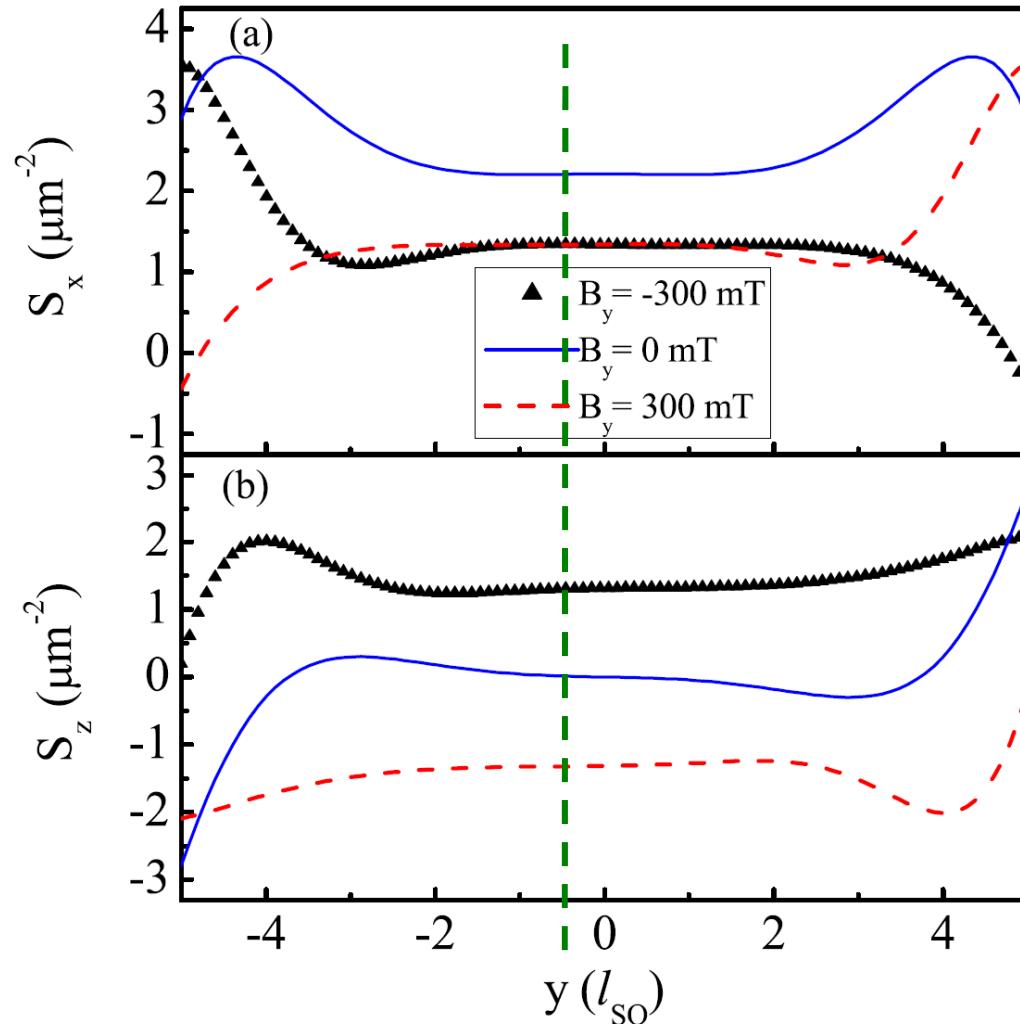
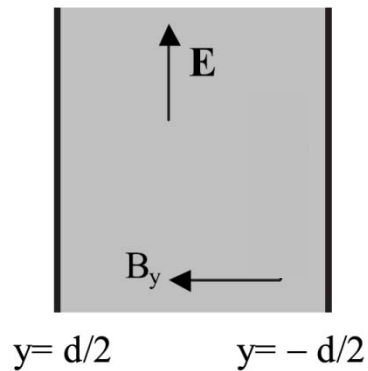


$y = d/2$

$y = -d/2$

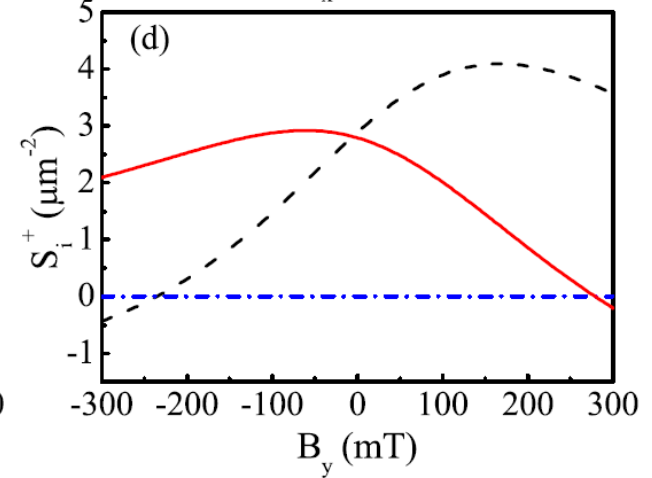
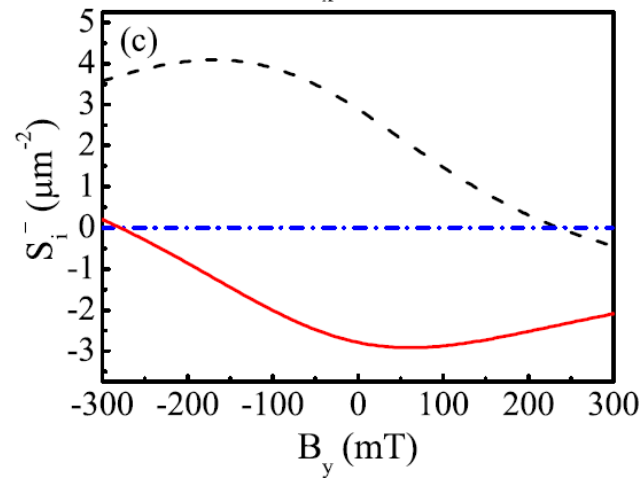
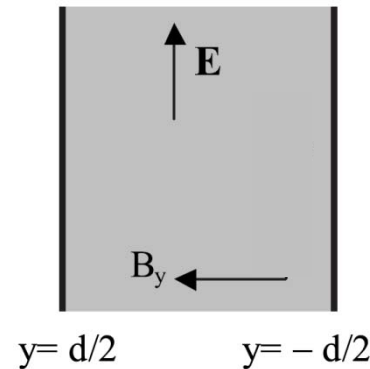
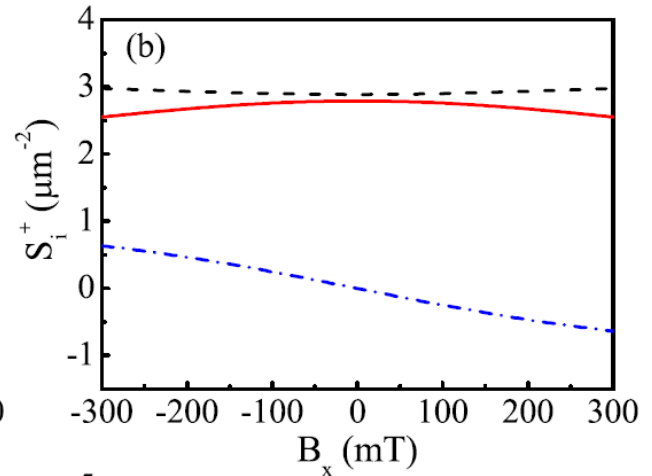
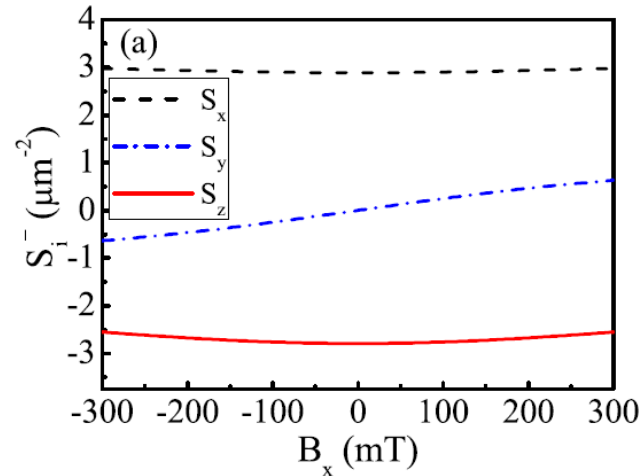
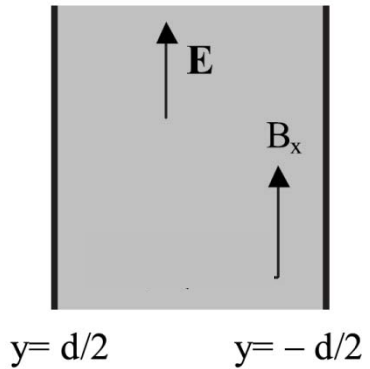
## Spatial profile of the spin densities for the case of transverse $B$

Asymmetry in the Spin density spatial profiles is related to the spin polarization.



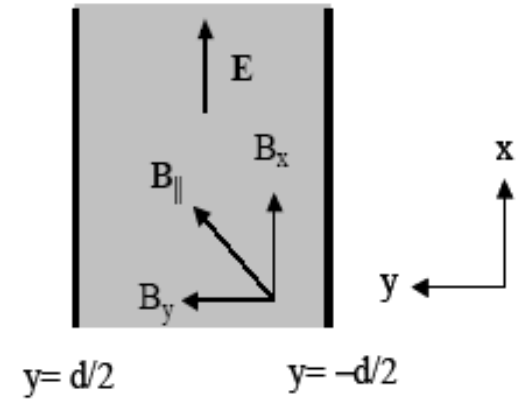
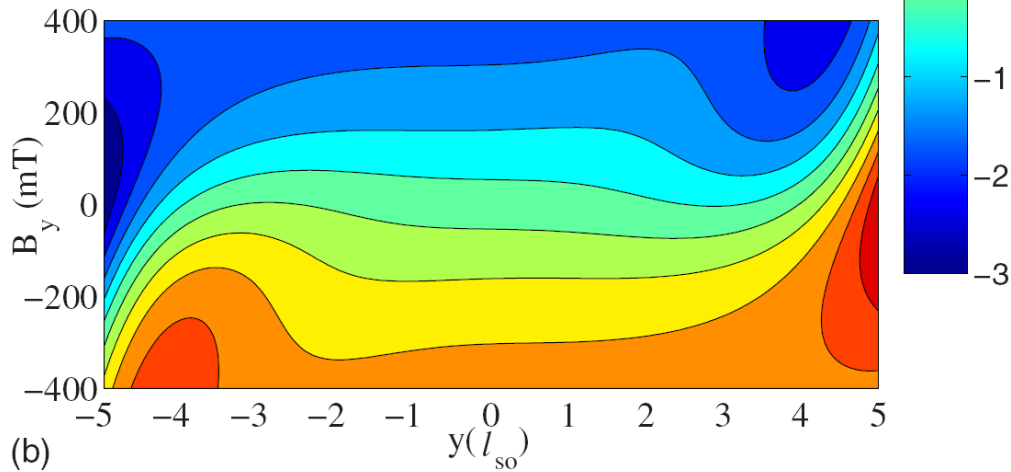
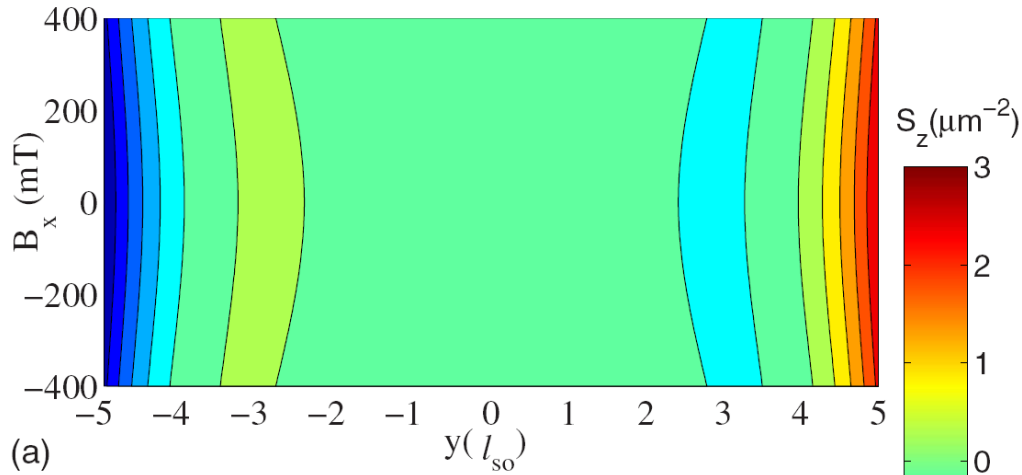
Asymmetry arises from competition between DP relaxation and spin precessions.

# Magnetic field dependences of the spin densities at the transverse edges



Asymmetry arises from competition between DP relaxation and spin precessions.

# Out-of-plane $S_z$ Asymmetries in both $y$ and $B$



$$S_z(B_y, y) = -S_z(-B_y, -y)$$

## Summary

The strong in-plane magnetic-field anisotropy in the symmetry characteristics of the  $S_z$  profile is distinct for the Dresselhaus SOI.

Out-of-plane spin density can be generated in the case of Dresselhaus SOI by a transverse in-plane magnetic field.

The out-of-plane spin density is closely related to the spin polarizations.

We commence the notion of utilizing low in-plane magnetic field for the determination of the underlying SOI in a particular sample, without the need to prepare controlling samples of different crystal orientations.



PRL 95, 166605 (2005)

PHYSICAL REVIEW LETTERS

week ending  
14 OCTOBER 2005

## Theory of Spin Hall Conductivity in $n$ -Doped GaAs

Hans-Andreas Engel, Bertrand I. Halperin, and Emmanuel I. Rashba

*Department of Physics, Harvard University, Cambridge, Massachusetts 02138, USA*

(Received 21 May 2005; published 13 October 2005)

We develop a theory of extrinsic spin currents in semiconductors, resulting from spin-orbit coupling at charged scatterers, which leads to skew-scattering and side-jump contributions to the spin-Hall conductivity. Applying the theory to bulk  $n$ -GaAs, without any free parameters, we find spin currents that are in reasonable agreement with experiments by Kato *et al.* [Science **306**, 1910 (2004)].

DOI: [10.1103/PhysRevLett.95.166605](https://doi.org/10.1103/PhysRevLett.95.166605)

PACS numbers: 72.25.Dc, 71.70.Ej



What should be the distribution of electrons in the momentum space if there is spin-orbit scatterers in the system (extrinsic SOI) ?

Physical Review Letters 95, 166605 (2005)

We start by refreshing our understanding on the normal Boltzmann equation.

$$-\frac{e\vec{E}}{\hbar} \cdot \frac{\partial f(\vec{k})}{\partial \vec{k}} = -\sum_{\vec{k}'} \frac{2\pi}{\hbar} |W_{\vec{k}\vec{k}'}|^2 \delta(\varepsilon_{\vec{k}} - \varepsilon_{\vec{k}'}) \frac{1}{V^2} [f(\vec{k}) - f(\vec{k}')] ]$$

Connection to differential cross - section :

$$\frac{1}{V} \frac{\hbar k}{m^*} \frac{d\sigma}{d\Omega} d\Omega_{\hat{k}'} = \int \frac{2\pi}{\hbar} |W_{\vec{k}\vec{k}'}|^2 \delta(\varepsilon_{\vec{k}} - \varepsilon_{\vec{k}'}) \frac{1}{V^2} d\Omega_{\hat{k}'} k'^2 dk' \frac{V}{(2\pi)^3}$$

$$\frac{d\sigma}{d\Omega} = \frac{m^{*2}}{4\pi^2 \hbar^4} |W_{\vec{k}\vec{k}'}|^2$$

RHS of the Boltzmann equation : the scattering rate

$$\begin{aligned}
 & - \sum_{\vec{k}} \frac{2\pi}{\hbar} \frac{4\pi^2 \hbar^4}{m^{*2}} \frac{d\sigma}{d\Omega} \delta(\varepsilon_{\vec{k}} - \varepsilon_{\vec{k}'}) \frac{1}{V^2} [f(\vec{k}) - f(\vec{k}')] \\
 & = - \frac{\hbar}{m^*} \frac{1}{V} \int d\Omega_{\hat{k}, k'} \frac{d\sigma}{d\Omega} [f(\vec{k}) - f(\vec{k}')]
 \end{aligned}$$

For a total of  $N_i$  impurities, the total scattering rate is

$$- \frac{e\vec{E}}{\hbar} \cdot \frac{\partial f(\vec{k})}{\partial \vec{k}} = -n_i \int d\Omega_{\hat{k}, k'} \frac{\hbar k'}{m^*} \frac{d\sigma}{d\Omega} [f(\vec{k}) - f(\vec{k}')]$$

$$\begin{aligned}
 & - \frac{e\vec{E}}{\hbar} \cdot \frac{\partial f(\vec{k})}{\partial \vec{k}} = - \frac{\delta f(\vec{k})}{\tau} \\
 \Rightarrow \delta f(\vec{k}) & = \frac{\tau e \hbar}{m^*} \vec{E} \cdot \vec{k} \frac{df_0}{d\varepsilon_k}
 \end{aligned}$$

$$f(\vec{k}) = f_0(\vec{k}) + \delta f(\vec{k})$$

For isotropic scatterers, we have  $\int d\Omega_{\vec{k}}, \delta f(\vec{k}') = 0$

When the impurities are spin-orbit scatterers, the distribution  $f(\vec{k})$  will become a matrix, a 2X2 matrix.

$$\hat{f}(\vec{k}) = f_0(\vec{k}) 1_{2 \times 2} + \left( \phi(\vec{k}) 1_{2 \times 2} + \vec{f}(\vec{k}) \cdot \vec{\sigma} \right)$$

We may expect the scattering rate to become a scattering rate matrix.

$$-\frac{e\vec{E}}{\hbar} \cdot \frac{\partial \hat{f}(\vec{k})}{\partial \vec{k}} = -n_i \int d\Omega_{\hat{k}'} \frac{\hbar k'}{m^*} \frac{d\vec{\sigma}}{d\Omega} \left[ \hat{f}(\vec{k}) - \hat{f}(\vec{k}') \right]$$

How do we come up with an appropriate definition of the scattering rate matrix ?

Before we go on to find the scattering rate matrix expression, it is beneficial for us to look at the physical meaning of the scattering from a spin-orbit scatterer.

$$\begin{aligned} & \lambda \vec{\sigma} \cdot (\vec{k} \times \vec{\nabla} V) \\ & \rightarrow \lambda \vec{\sigma} \cdot \left[ \frac{1}{2} (\vec{k} + \vec{k}') \times (\vec{k} - \vec{k}') \right] V((\vec{k} + \vec{k}')/2) \\ & \rightarrow \frac{\lambda}{2} \vec{\sigma} \cdot (\vec{k} \times \vec{k}' - \vec{k}' \times \vec{k}) V((\vec{k} + \vec{k}')/2) \\ & \rightarrow \lambda \vec{\sigma} \cdot (\vec{k} \times \vec{k}') V((\vec{k} + \vec{k}')/2) \\ & \Rightarrow \text{the effective magnetic field due to} \\ & \quad \text{scattering event } \vec{k} \rightarrow \vec{k}' \text{ is along the} \\ & \quad \text{direction } \vec{k} \times \vec{k}'. \end{aligned}$$



We first consider the scattering matrix of a spin-orbit scattering event.

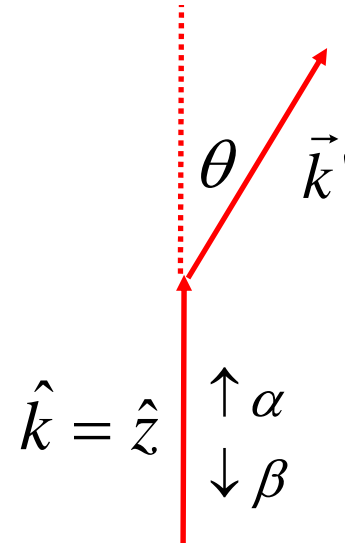
Without loss of generality, we can assume that the particle is incident along  $z$  and the spin is either parallel or anti-parallel to  $z$ .

$$\psi_{\text{inc}} = e^{ikz} \alpha$$

$$\rightarrow e^{ikz} \alpha + [S_{11} \alpha + S_{21} \beta] \frac{e^{ikr}}{r};$$

$$\psi_{\text{inc}} = e^{ikz} \beta$$

$$\rightarrow e^{ikz} \beta + [S_{12} \alpha + S_{22} \beta] \frac{e^{ikr}}{r}$$



The scattering matrix  $S_{ij}$  are functions of  $\theta$  and  $\phi$ .

To find the  $\phi$  dependence of  $S_{ij}$  we look at the total angular momentum along  $z$ .

$$\hbar \left( \frac{1}{i} \frac{\partial}{\partial \phi} + \frac{1}{2} \sigma_z \right) \left[ e^{ikz} \alpha + (S_{11} \alpha + S_{21} \beta) \frac{e^{ikr}}{r} \right] = \frac{\hbar}{2} \left[ e^{ikz} \alpha + (S_{11} \alpha + S_{21} \beta) \frac{e^{ikr}}{r} \right]$$

$$\left( \frac{1}{i} \frac{\partial}{\partial \phi} + \frac{1}{2} \sigma_z \right) (S_{11} \alpha + S_{21} \beta) = \frac{1}{2} (S_{11} \alpha + S_{21} \beta)$$

$$\left( \frac{1}{i} \frac{\partial}{\partial \phi} + \frac{1}{2} \right) S_{11} = \frac{1}{2} S_{11}$$

$$\Rightarrow \frac{\partial S_{11}}{\partial \phi} = 0$$

$$\left( \frac{1}{i} \frac{\partial}{\partial \phi} - \frac{1}{2} \right) S_{21} = \frac{1}{2} S_{21}$$

$$\Rightarrow \frac{\partial S_{21}}{\partial \phi} = i S_{21}$$

$$\Rightarrow S_{21} \propto e^{i\phi}$$

Similarly, we have

$$S_{12} \propto e^{-i\phi} \quad \text{and} \quad \frac{\partial S_{22}}{\partial \phi} = 0$$

To find the  $\theta$  dependence of  $S_{ij}$  we look at the “reflection symmetry” in the  $yz$  plane.

Symmetry operator for the reflection in the  $yz$  plane :

$$P_x \sigma_x$$

$P_x$  make changes  $x \rightarrow -x$  to any function at its right hand side.

$$\sigma_x \sigma_x \sigma_x = \sigma_x \quad ; \quad \sigma_x \sigma_y \sigma_x = -\sigma_y \quad ; \quad \sigma_x \sigma_z \sigma_x = -\sigma_z$$

$$P_x \sigma_x (\vec{L} \cdot \vec{s}) P_x \sigma_x = \vec{L} \cdot \vec{s}$$

Applying our reflection operator to our scattering state :

$$P_x \sigma_x \left\{ e^{ikz} \alpha + [S_{11}(\theta, \phi) \alpha + S_{21}(\theta, \phi) \beta] \frac{e^{ikr}}{r} \right\}$$

$$\rightarrow e^{ikz} \beta + [S_{11}(\theta, \pi - \phi) \beta + S_{21}(\theta, \pi - \phi) \alpha] \frac{e^{ikr}}{r}$$



From reflection symmetry, we have

$$\rightarrow e^{ikz} \beta + [S_{11}(\theta, \pi - \phi) \beta + S_{21}(\theta, \pi - \phi) \alpha] \frac{e^{ikr}}{r}$$

From our previous scattering convention, we have

$$\rightarrow e^{ikz} \beta + [S_{12}(\theta, \phi) \alpha + S_{22}(\theta, \phi) \beta] \frac{e^{ikr}}{r}$$

$$S_{12}(\theta, \phi) = h(\theta) e^{-i\phi} \quad ; \quad S_{21}(\theta, \phi) = h'(\theta) e^{i\phi}$$

$$\Rightarrow h(\theta) = -h'(\theta)$$

$$\hat{n} = \frac{\vec{k} \times \vec{k}'}{|\vec{k} \times \vec{k}'|}$$

Scattering matrix :

$$\hat{S} = \begin{pmatrix} g(\theta) & h(\theta) e^{-i\phi} \\ -h(\theta) e^{i\phi} & g(\theta) \end{pmatrix} = g(\theta) 1_{2 \times 2} + ih(\theta) \hat{n} \cdot \vec{\sigma}$$

The scattering wavefunction becomes :

$$e^{ikz} \chi_{\eta} + \hat{S} \chi_{\eta} \frac{e^{ikr}}{r}$$

Scattering rate for such a scattering wave is :

$$\psi_{sc} = \hat{S} \chi_{\eta} \frac{e^{ikr}}{r}$$

$$j_r = \frac{\hbar}{2mi} \psi_{sc}^+ \frac{\partial}{\partial r} \psi_{sc} + c.c.$$

$$= \frac{\hbar k}{mr^2} \chi_{\eta}^+ \hat{S}^+ \hat{S} \chi_{\eta}$$

$$\text{scattering rate} = \frac{j_r r^2 d\Omega}{V} = \frac{\hbar k}{mV} \chi_{\eta}^+ \hat{S}^+ \hat{S} \chi_{\eta} d\Omega$$

Define the scattering rate matrix as follows :

$$\begin{aligned}
 -\frac{e\hbar}{m^*} \vec{E} \cdot \vec{k} \frac{\partial f_0(\vec{k})}{\partial \varepsilon_k} 1_{2 \times 2} = & -n_i \sum_{\eta} \int d\Omega_{\hat{k}'} \frac{\hbar k}{m^*} \hat{S} \chi_{\eta} \chi_{\eta}^+ \hat{S}^+ \delta f_{\eta}(\vec{k}) \\
 & + n_i \sum_{\eta} \int d\Omega_{\hat{k}'} \frac{\hbar k}{m^*} \hat{S}(-\hat{n}) \chi_{\eta} \chi_{\eta}^+ \hat{S}^+(-\hat{n}) \delta f_{\eta}(\vec{k}')
 \end{aligned}$$

$$\begin{aligned}
 -\frac{e\hbar}{m^*} \vec{E} \cdot \vec{k} \frac{\partial f_0(\vec{k})}{\partial \varepsilon_k} 1_{2 \times 2} = & -n_i \sum_{\eta} \int d\Omega_{\hat{k}'} \frac{\hbar k}{m^*} \hat{S}(\hat{n}) \delta \hat{f}(\vec{k}) \hat{S}^+(\hat{n}) \\
 & + n_i \sum_{\eta} \int d\Omega_{\hat{k}'} \frac{\hbar k}{m^*} \hat{S}(-\hat{n}) \delta \hat{f}(\vec{k}') \hat{S}^+(-\hat{n})
 \end{aligned}$$

$$\hat{S}(\hat{n}) \hat{\sigma} \hat{f}(\vec{k}) \hat{S}^+(\vec{k})$$

$$= [g(\theta) 1_{2 \times 2} + ih(\theta) \hat{n} \cdot \vec{\sigma}] [\phi(\vec{k}) 1_{2 \times 2} + \vec{f}(\vec{k}) \cdot \vec{\sigma}] [g(\theta)^* 1_{2 \times 2} - ih(\theta)^* \hat{n} \cdot \vec{\sigma}]$$

$$\hat{S} \hat{S}^+ = |g|^2 + i(hg^* - gh^*) \hat{n} \cdot \vec{\sigma} + |h|^2$$

$$\hat{S} \vec{\sigma} \hat{S}^+ = |g|^2 \vec{\sigma} + i[hg^* (\hat{n} \cdot \vec{\sigma}) \vec{\sigma} - gh^* \vec{\sigma} (\hat{n} \cdot \vec{\sigma})] + |h|^2 (\hat{n} \cdot \vec{\sigma}) \vec{\sigma} (\hat{n} \cdot \vec{\sigma})$$

$$-\frac{e\hbar}{m^*} \vec{E} \cdot \vec{k} \frac{\partial f_0(\vec{k})}{\partial \varepsilon_k} 1_{2 \times 2}$$

$$= -n_i \int d\Omega_{\hat{k}'} \frac{\hbar k}{m^*} \left\{ I(\theta) [\hat{f}(\vec{k}) - \hat{f}(\vec{k}')] + I(\theta) S(\theta) \hat{n} \cdot \vec{\sigma} [\phi(\vec{k}) + \phi(\vec{k}')] \right\}$$

Sherman function

$$S(\theta) = \frac{i[h(\theta)g(\theta)^* - g(\theta)h(\theta)^*]}{I(\theta)}$$

$$I(\theta) = |g|^2 + |h|^2$$

$$\begin{aligned}
 & -\frac{e\hbar}{m^*} \vec{E} \cdot \vec{k} \frac{\partial f_0(\vec{k})}{\partial \varepsilon_k} 1_{2 \times 2} \\
 & = -n_i \int d\Omega_{\hat{k}} \frac{\hbar k}{m^*} \left\{ I(\theta) [\hat{f}(\vec{k}) - \hat{f}(\vec{k}')] + I(\theta) S(\theta) \hat{n} \cdot \vec{\sigma} [\phi(\vec{k}) + \phi(\vec{k}')] \right\}
 \end{aligned}$$

$$\hat{f}(\vec{k}) = f_0(\vec{k}) 1_{2 \times 2} + \left( \phi(\vec{k}) 1_{2 \times 2} + \vec{f}(\vec{k}) \cdot \vec{\sigma} \right)$$

We can see that the following ansatz must be valid:

$$\phi(\vec{k}) = \vec{k} \cdot \vec{E} C_k$$

$$C_k = \frac{e\hbar\tau}{m^*} \frac{\partial f_0(\vec{k})}{\partial \varepsilon_k} ; \quad \frac{1}{\tau} = n_i \int d\Omega_{\hat{k}} \frac{\hbar k}{m^*} I(\theta) [1 - \cos \theta]$$

$$0 = -n_i \int d\Omega_{\hat{k}'} \frac{\hbar k}{m^*} I(\theta) \left\{ \left[ \vec{f}(\vec{k}) - \vec{f}(\vec{k}') \right] \cdot \vec{\sigma} + S(\theta) \hat{n} \cdot \vec{\sigma} \left[ \vec{k} + \vec{k}' \right] \cdot \vec{E} C_k \right\}$$

Another ansatz : since  $\vec{f}(\vec{k})$  must change sign if  $\vec{k} \rightarrow -\vec{k}$ , then we let  $\vec{f}(\vec{k}) = \vec{b}(\varepsilon_k) \times \vec{k}$

After some calculation, we get

$$\vec{b} = \frac{1}{2} C_k \gamma_k \vec{E} ; \quad \text{where} \quad \gamma_k = \frac{\int d\Omega_{\hat{k}'} I(\theta) S(\theta) \sin\theta}{\int d\Omega_{\hat{k}'} I(\theta) (1 - \cos\theta)}$$

$$\hat{f}(\vec{k}) = f_0(\vec{k}) 1_{2 \times 2} + C_k \vec{k} \cdot \left[ \vec{E} 1_{2 \times 2} + \frac{\gamma_k}{2} (\vec{\sigma} \times \vec{E}) \right] \quad C_k = \frac{e \hbar \tau}{m^*} \frac{\partial f_0(\vec{k})}{\partial \varepsilon_k}$$

Spin current:

$$\mathbf{j}_{SS}^{\mu} = n \langle \sigma_{\mu} \mathbf{v}_0 \rangle$$

$$\mathbf{v}_0 = \hbar \mathbf{k} / m^*$$

$$j_{SS,\kappa}^{\mu} = \text{Tr} \sigma_{\mu} \int \frac{d^3 k}{(2\pi)^3} \frac{\hbar k_{\kappa}}{m^*} \hat{f}(\mathbf{k}) = \frac{\gamma}{2e} \varepsilon^{\kappa\mu\nu} (\mathbf{J}_0)_{\nu},$$

where

$$\mathbf{J}_0 = 2e \int d^3 k (2\pi)^{-3} (\hbar \mathbf{k} / m^*) \mathbf{k} \cdot \mathbf{E} C_k$$

where  $\mathbf{J}_0$  is the charge current in the absence of SO coupling.

## Theory of Spin Hall Conductivity in $n$ -Doped GaAs

Hans-Andreas Engel, Bertrand I. Halperin, and Emmanuel I. Rashba

*Department of Physics, Harvard University, Cambridge, Massachusetts 02138, USA*

(Received 21 May 2005; published 13 October 2005)

We develop a theory of extrinsic spin currents in semiconductors, resulting from spin-orbit coupling at charged scatterers, which leads to skew-scattering and side-jump contributions to the spin-Hall conductivity. Applying the theory to bulk  $n$ -GaAs, without any free parameters, we find spin currents that are in reasonable agreement with experiments by Kato *et al.* [Science **306**, 1910 (2004)].

DOI: [10.1103/PhysRevLett.95.166605](https://doi.org/10.1103/PhysRevLett.95.166605)

PACS numbers: 72.25.Dc, 71.70.Ej

Next, we estimate the spin-Hall currents. The measurements were performed at electrical fields  $E \approx 20 \text{ mV } \mu\text{m}^{-1}$  where the conductivity increased to  $\sigma_{xx} \approx 3 \times 10^3 \Omega^{-1} \text{ m}^{-1}$  due to electron heating. We assume that  $\gamma$  is not very sensitive to these heating effects and we still use Eq. (8) but with the increased conductivity. For an electrical field  $\mathbf{E} = \hat{x}E_x$ , we find both contributions to the spin-Hall conductivity  $\sigma^{\text{SH}} \equiv -j_y^z/E_x$ , namely,  $\sigma_{\text{SS}}^{\text{SH}} = -(\gamma/2e)\sigma_{xx} \approx 1.7 \Omega^{-1} \text{ m}^{-1}/|e|$  and  $\sigma_{\text{SJ}}^{\text{SH}} = 2n\lambda e/\hbar \approx -0.8 \Omega^{-1} \text{ m}^{-1}/|e|$ . In total, we arrive at the extrinsic spin-Hall conductivity  $\sigma_{\text{theor}}^{\text{SH}} \approx 0.9 \Omega^{-1} \text{ m}^{-1}/|e|$ . The magnitude is within the error bars of the experimental value of  $|\sigma_{\text{expt}}^{\text{SH}}| \approx 0.5 \Omega^{-1} \text{ m}^{-1}/|e|$  found from spin accumulation near the free edges of the specimen [1,27].



## **Spin dipole around a local scatterer**

- **isotropic normal scatterer in a Rashba 2DEG**
- **extrinsic spin-orbit scatterer in a normal 2DEG**

R. Landauer

# Spatial Variation of Currents and Fields Due to Localized Scatterers in Metallic Conduction

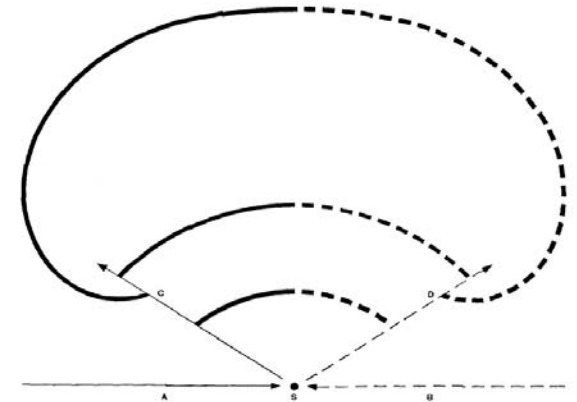
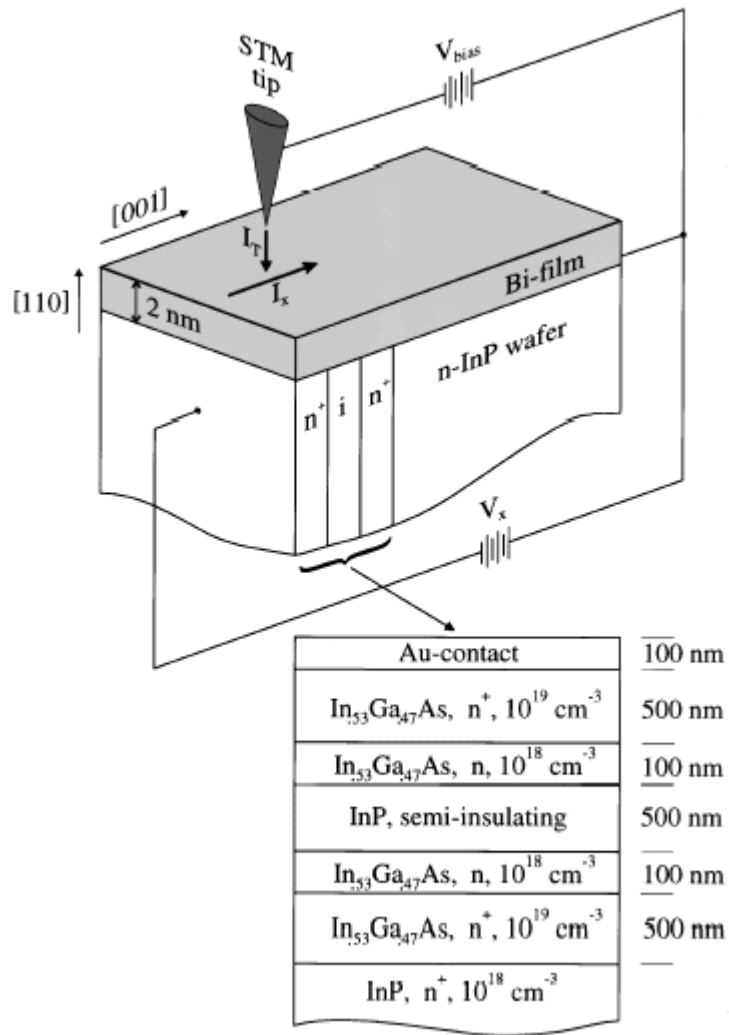


Figure 1 Schematic representation of current flow disturbed by the scatterer  $S$ . Electrons in excess numbers are incident along  $A$ , then are scattered to  $C$ , then scattered by the background. The number of electrons incident along  $B$  is less than the equilibrium number. The deficit is scattered to  $D$ , then scattered by the background. The excess and deficit diffuse together and recombine along the arc.

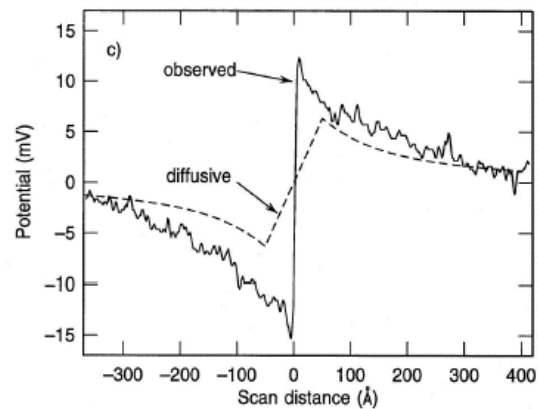
**Abstract:** Localized scatterers can be expected to give rise to spatial variations in the electric field and in the current distribution. The transport equation allowing for spatial variations is solved by first considering the homogeneous transport equation which omits electric fields. The homogeneous solution gives the purely diffusive motion of current carriers and involves large space charges. The electric field is then found, and approximate space charge neutrality is restored, by adding a particular solution of the transport equation in which the electric field is associated only with space charge but not with a current. The presence of point scatterers leads to a dipole field about each scatterer. The spatial average of a number of these dipole fields is the same as that obtained by the usual approach which does not explicitly consider the spatial variation. Infinite plane obstacles with a reflection coefficient  $r$  are also considered. These produce a resistance proportional to  $r/(1 - r)$ .



Topography image



Potential image



PRB 54, R5283 (1996)  
BG Briner, RM Feenstra  
*et al.*

# Isotropic normal scatterer in a Rashba 2DEG

**Scattering amplitude  
of the scatterer**

$$f(\mathbf{k}, \mathbf{k}') = -\frac{m^*}{\sqrt{2\pi}k_F} \int dr^2 U(\mathbf{r}) e^{i(\mathbf{k}-\mathbf{k}')\mathbf{r}},$$

$$G_{\mathbf{k}\mathbf{k}'}^r(\omega) = \delta_{\mathbf{k}\mathbf{k}'} G_{\mathbf{k}}^{r(0)}(\omega) + G_{\mathbf{k}\mathbf{k}'}^{r(1)}(\omega) + G_{\mathbf{k}\mathbf{k}'}^{r(2)}(\omega),$$

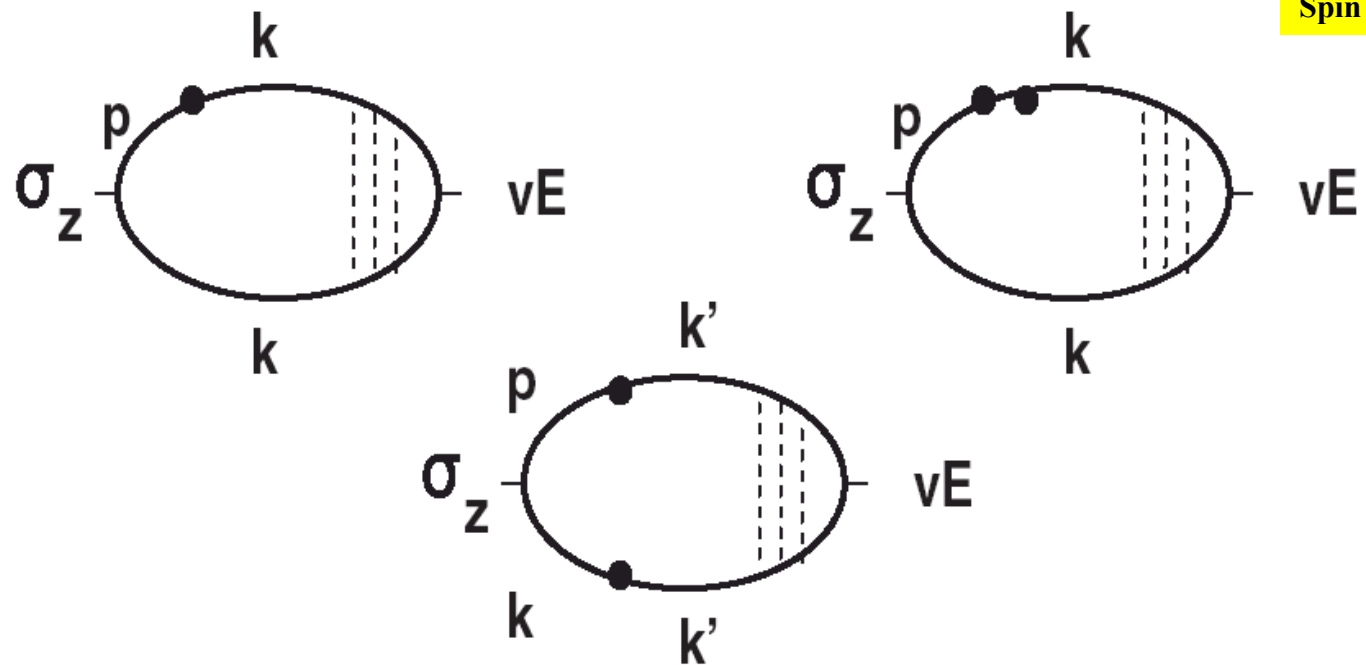
$$G_{\mathbf{k}\mathbf{k}'}^{r(1)}(\omega) = G_{\mathbf{k}}^{r(0)}(\omega) U_{\mathbf{k}\mathbf{k}'} G_{\mathbf{k}'}^{r(0)}(\omega),$$

$$G_{\mathbf{k}\mathbf{k}'}^{r(2)}(\omega) = G_{\mathbf{k}}^{r(0)}(\omega) \sum_{\mathbf{k}''} U_{\mathbf{k}\mathbf{k}''} G_{\mathbf{k}''}^{r(0)}(\omega) U_{\mathbf{k}''\mathbf{k}'} G_{\mathbf{k}'}^{r(0)}(\omega).$$

**Spin density in the vicinity of the scatterer**

$$\sigma_z(\mathbf{r}) = \sum_{\mathbf{k}, \mathbf{k}', \mathbf{p}} e^{i(\mathbf{p}-\mathbf{k})\cdot\mathbf{r}} \int \frac{d\omega}{2\pi} \frac{dn_F(\omega)}{d\omega} \times \text{Tr}[G_{\mathbf{k}'\mathbf{k}}^a(\omega) \sigma_z G_{\mathbf{p}\mathbf{k}'}^r(\omega) \mathcal{T}(\omega, \mathbf{k}')],$$

**Vertex part**



**Spin dipole in the ballistic regime: (PRL 97, 76601 (2006))**

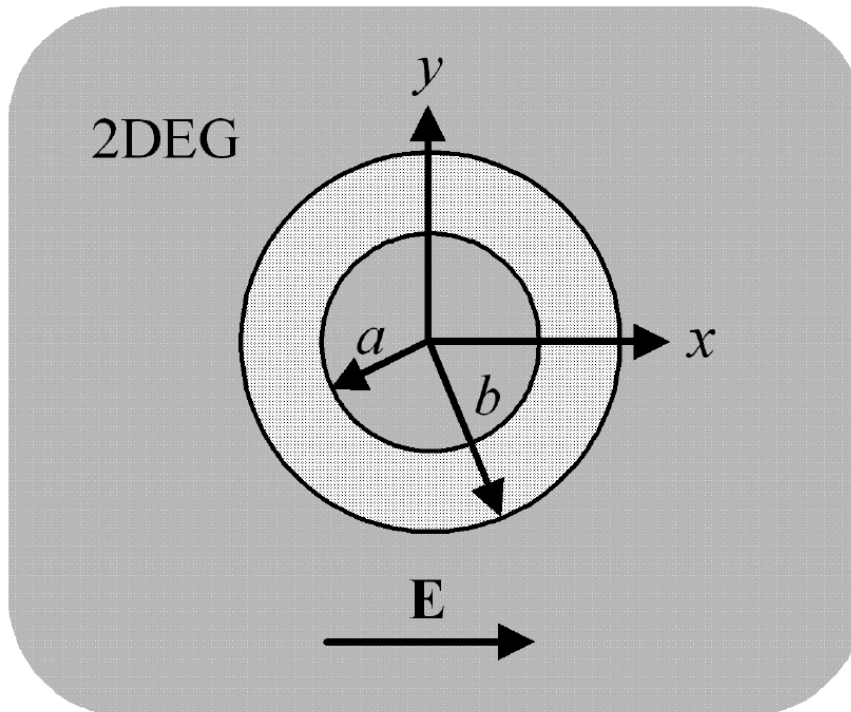
**spin accumulation occurs regardless of zero spin current in the bulk**

$$\sigma_z(\mathbf{r}) = -\frac{m^* v_d \sigma_t}{2\pi^2 R L_{so}} \sin\left(\frac{2R}{L_{so}}\right) \sin\theta + \frac{m^* v_d}{2\pi^2 R^2} \sin^2\left(\frac{R}{L_{so}}\right) \\ \times \sin^3\theta \left( \sigma_{tot} + \sqrt{\frac{8\pi}{k_F}} \text{Re}[f(\pi) e^{2ik_F R}] \right),$$



We invoke both the **in-plane potential gradient SOI** and the **resonant effects** for the amplification of the spin accumulation.

Chen, Chu, and Mal'shukov (Phys. Rev. B 76, 2007)



A ring-shaped potential pattern is embedded in a 2DEG. An electric field  $E$  sets up a current in the 2DEG.

$$H_{\text{SO}} = \lambda \vec{\sigma} \cdot (\vec{k} \times \vec{\nabla} V)$$

$$V(\rho) = V_o [\theta(\rho - a) - \theta(\rho - b)]$$

$$S_z(\boldsymbol{\rho}) = \frac{1}{4\pi^2} \int d\mathbf{k} g(\mathbf{k}) \sum_{\sigma} \sigma \Psi_{\mathbf{k}\sigma}^{\dagger}(\boldsymbol{\rho}) \Psi_{\mathbf{k}\sigma}(\boldsymbol{\rho}),$$

**Sorbello and Chu, IBM J. Res. Dev. 32, 58 (1988)**

**Chu and Sorbello, Phys. Rev. B 38, 7260 (1988)**

**Dipole-like**

$$S_z(\boldsymbol{\rho}) = n_E \operatorname{Re} \sum_{\sigma} \sigma \sum_{l=0}^{\infty} R_l^{\sigma}(\rho) R_{l+1}^{\sigma*}(\rho) \sin\phi_{\rho}$$

**Radial wavefunction**

**Asymptotic  
form:**

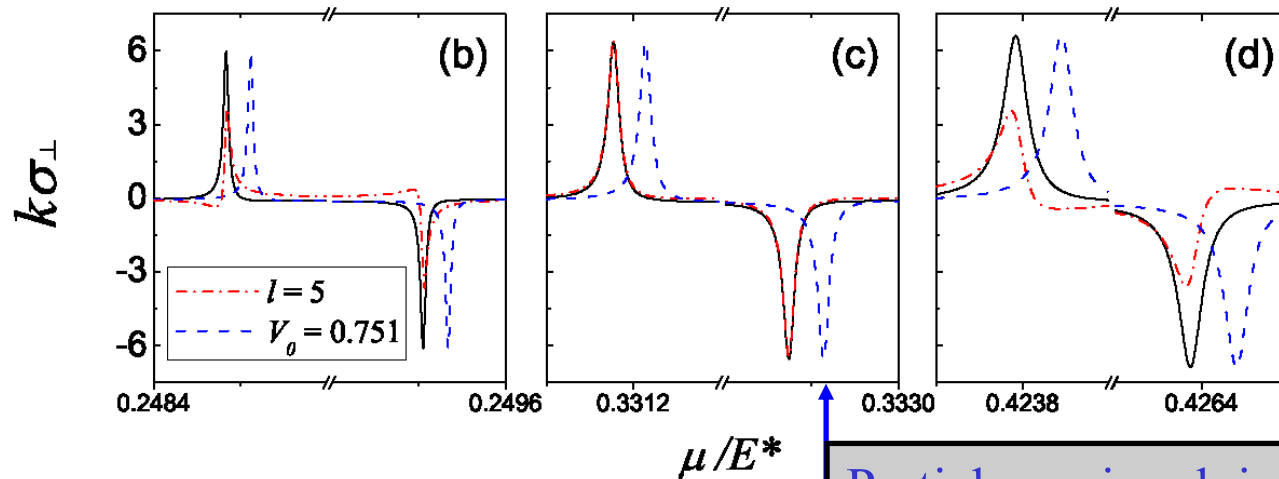
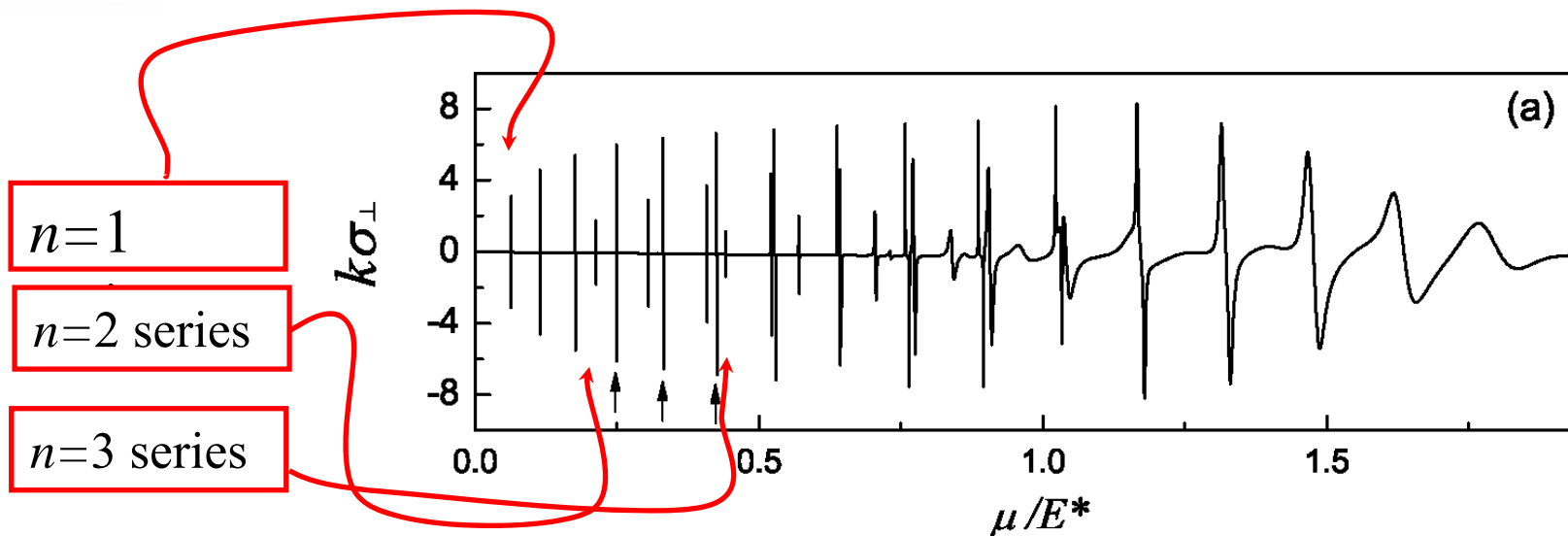
$$S_z = \frac{\sin\phi_\rho}{k^*\rho} \left[ p_s + \frac{\wp_s}{k^*\rho} \right]$$

$$p_s = -\frac{n_E^* k \sigma_\perp}{4\pi}$$

$$n_E^* = \frac{m^* e E_0 l_0^*}{\pi \hbar^2}$$

$$\sigma_\perp = \frac{2}{k} \sum_\sigma \sigma \sum_{l=0}^{\infty} \sin [2 (\delta_l^\sigma - \delta_{l+1}^\sigma)]$$





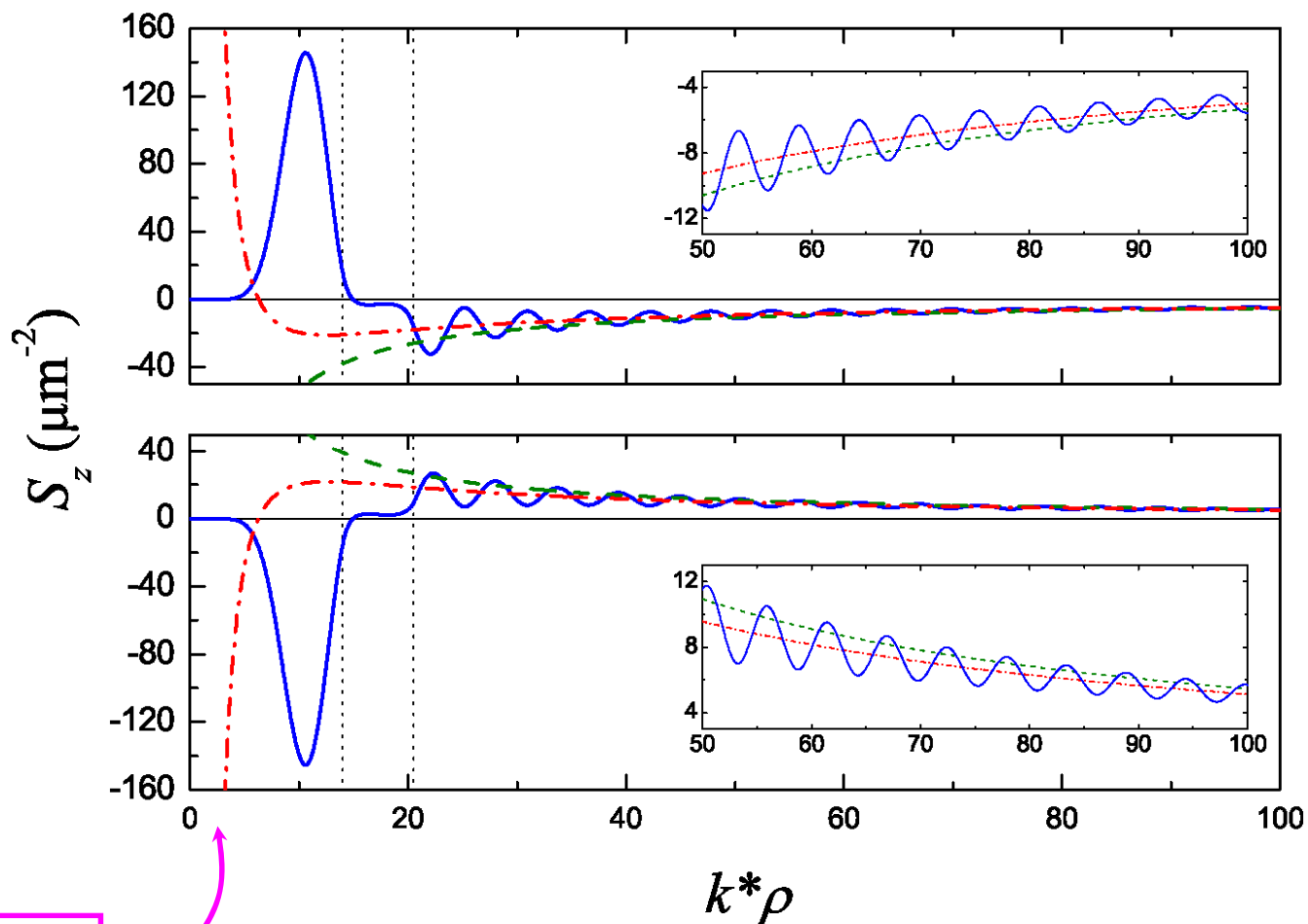
$E^* = 77.1 \text{ meV}$

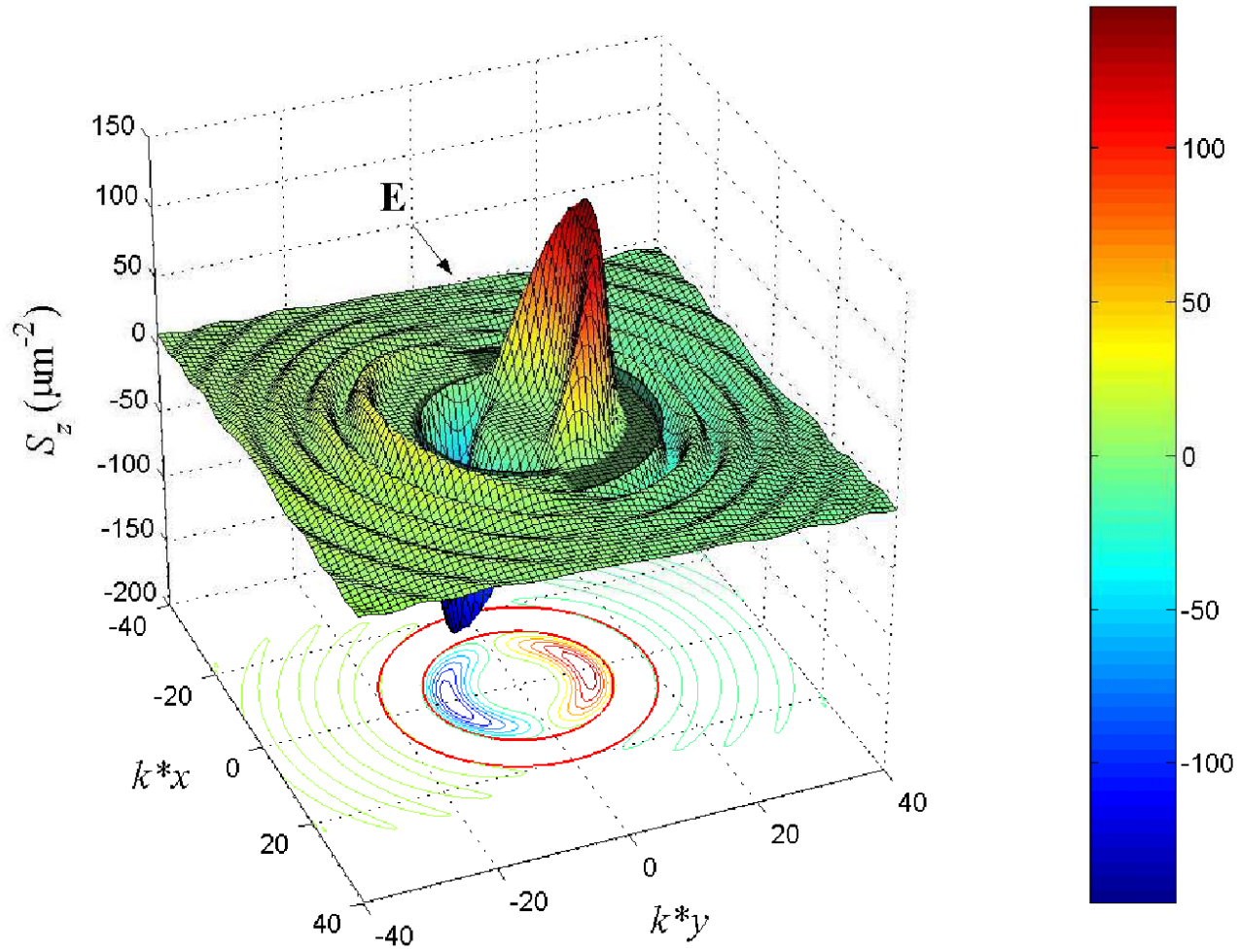
Partial sum involving  $\delta_l=5$

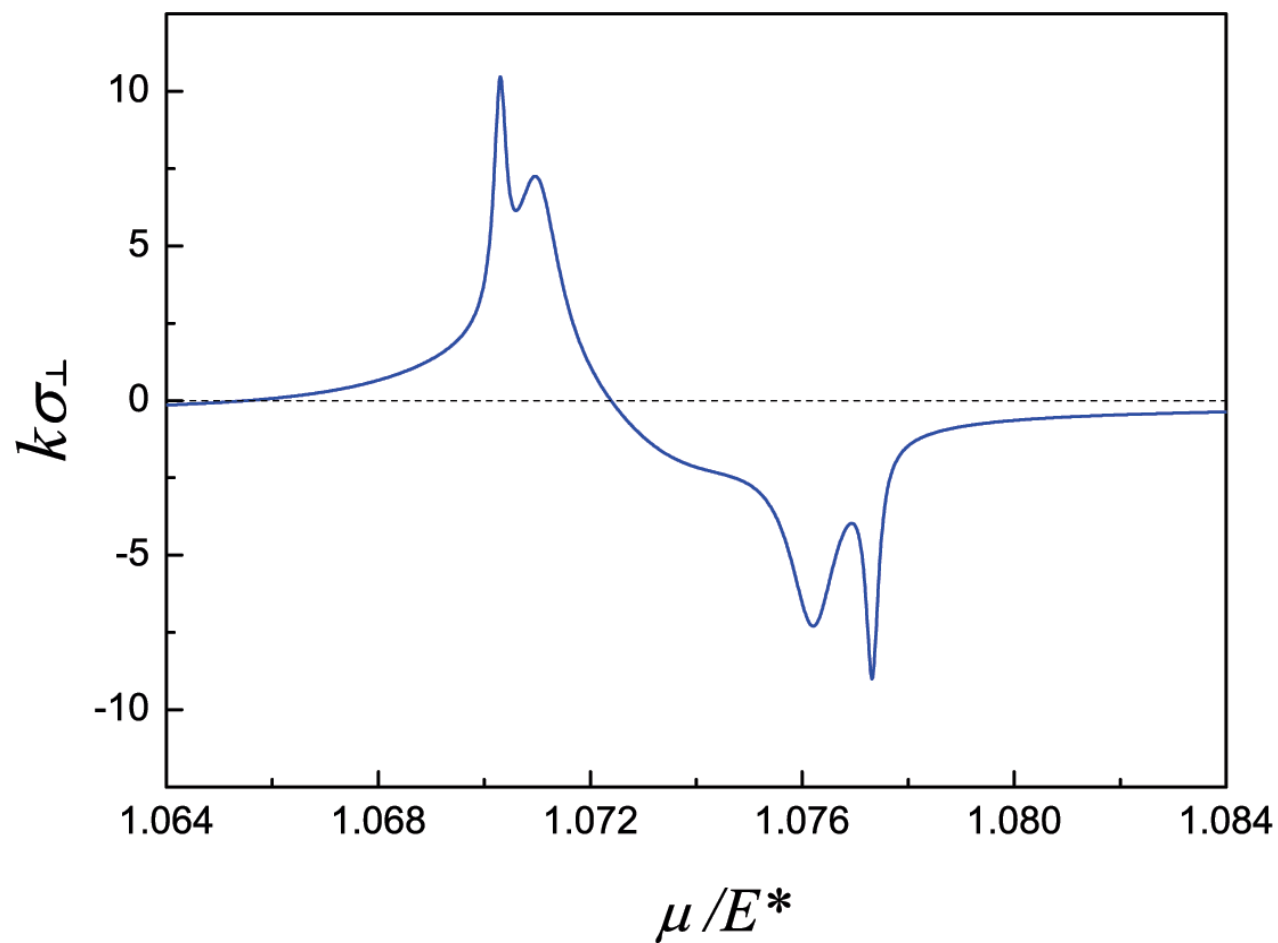
$n=1,$   
 $l=5$

Length  
scale =  
 $46.3 \text{ \AA}$

Asymptotic



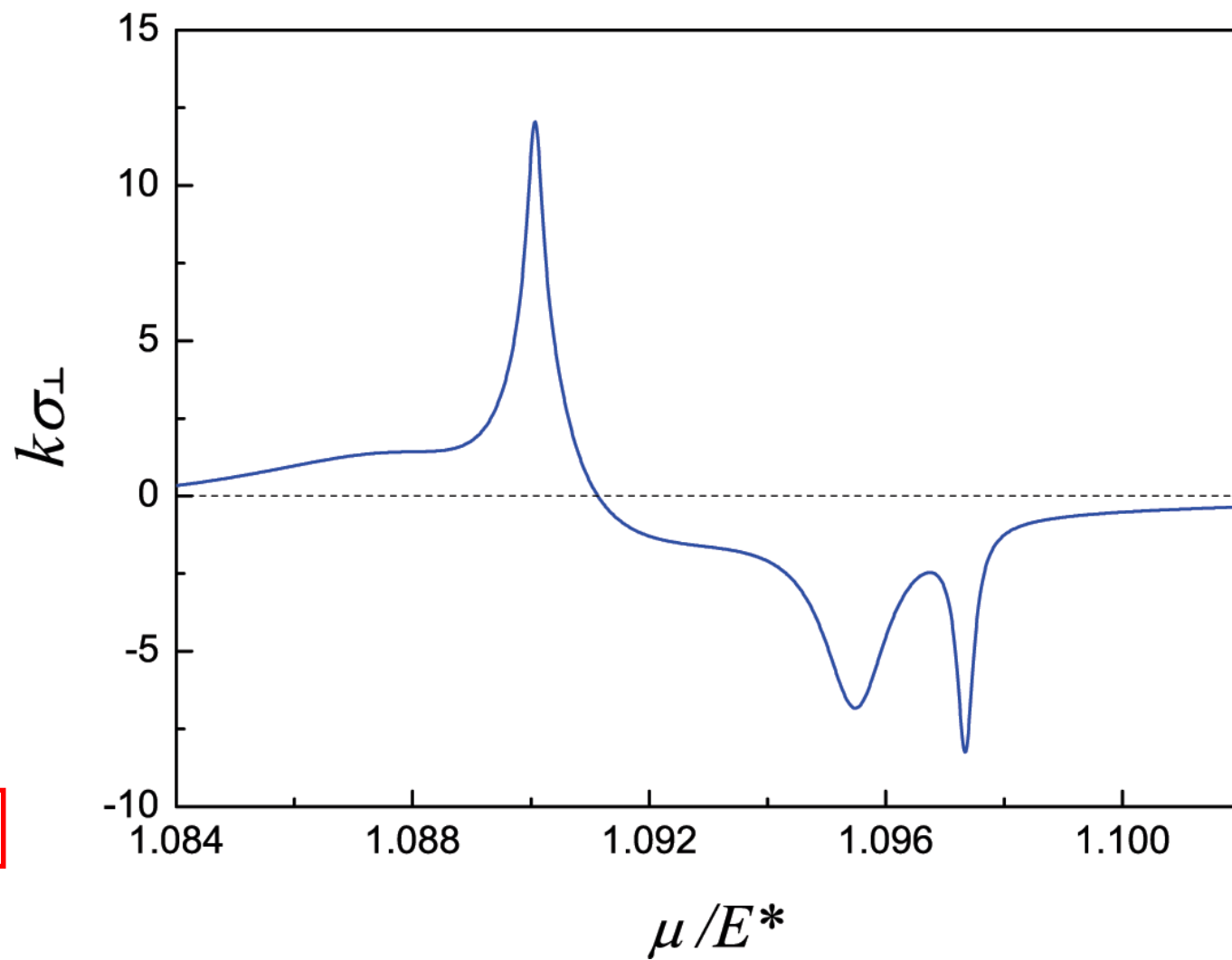




$$V_0 = 1$$

$$a = 20$$

$$b = 26.5$$



$$V_0 = 1$$

$$a = 19.8$$

$$b = 26.3$$

## **Possible realization of the microstructure:**

- 1. Gate-patterning on the 2DEG**
- 2. Carrier distribution profiles in Si-doped layers formed by focused ion beam implanatation and successive overlayer growth**

**Ref. J. Vac. Sci. Technol. B 18, 3158 (2000)**

## Summary

- 1. Nonequilibrium spin accumulation (spin cloud or spin dipole) is found in the absence of bulk “spin current”.**
- 2. For the case of Rashba SOI, nonequilibrium spin cloud is formed around a normal impurity.**
- 3. For the case of a normal 2DEG, nonequilibrium spin cloud is formed around a local SOI structure.**
- 4. The interplay between the in-plane potential gradient SOI and quantum resonances can lead to significant effects.**

## Other recent work that invoked the importance of in-plane potential gradient:

**Phys. Rev. Lett. 98, 186807 (2007)**

### **Giant Spin Splitting through Surface Alloying**

Christian R. Ast,<sup>1,2,\*</sup> Jürgen Henk,<sup>3</sup> Arthur Ernst,<sup>3</sup> Luca Moreschini,<sup>2</sup> Mihaela C. Falub,<sup>2</sup> Daniela Pacilé,<sup>2,†</sup>  
Patrick Bruno,<sup>3</sup> Klaus Kern,<sup>1,2</sup> and Marco Grioni<sup>2</sup>

<sup>1</sup>*Max-Planck-Institut für Festkörperforschung, D-70569 Stuttgart, Germany*

<sup>2</sup>*Ecole Polytechnique Fédérale de Lausanne (EPFL), Institut de Physique des Nanostructures, CH-1015 Lausanne, Switzerland*

<sup>3</sup>*Max-Planck-Institut für Mikrostrukturphysik, D-06120 Halle (Saale), Germany*

(Received 26 October 2006; published 3 May 2007)

The long-range ordered surface alloy **Bi/Ag(111)** is found to exhibit a giant spin splitting of its surface electronic structure due to spin-orbit coupling, as is determined by angle-resolved photoelectron spectroscopy. First-principles electronic structure calculations fully confirm the experimental findings. The effect is brought about by a strong in-plane gradient of the crystal potential in the surface layer, in interplay with the structural asymmetry due to the surface-potential barrier. As a result, the spin polarization of the surface states is considerably rotated out of the surface plane.

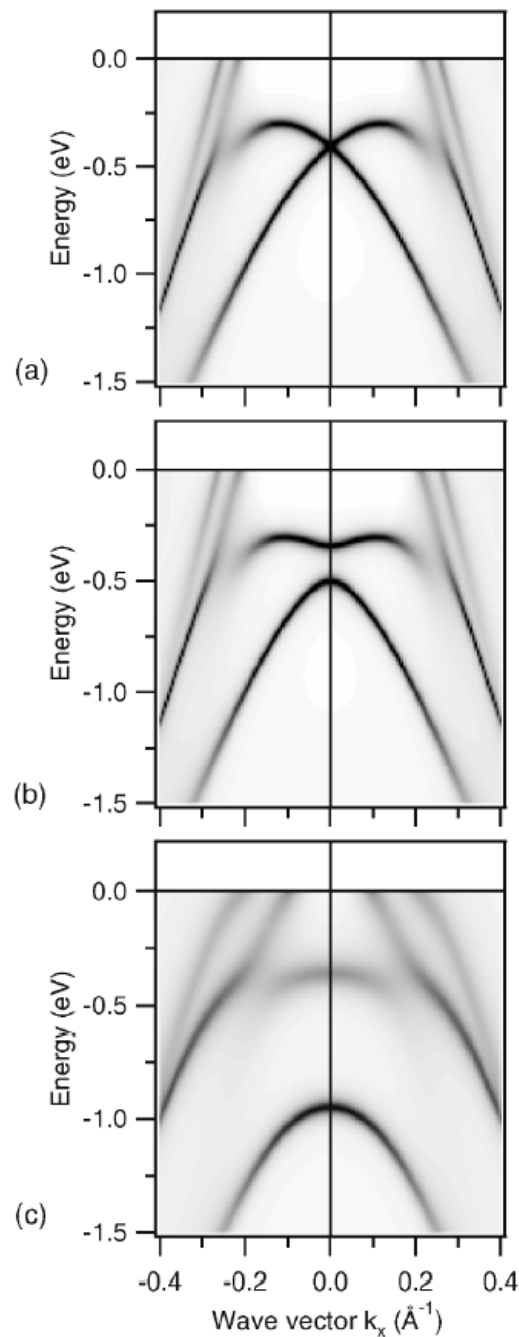
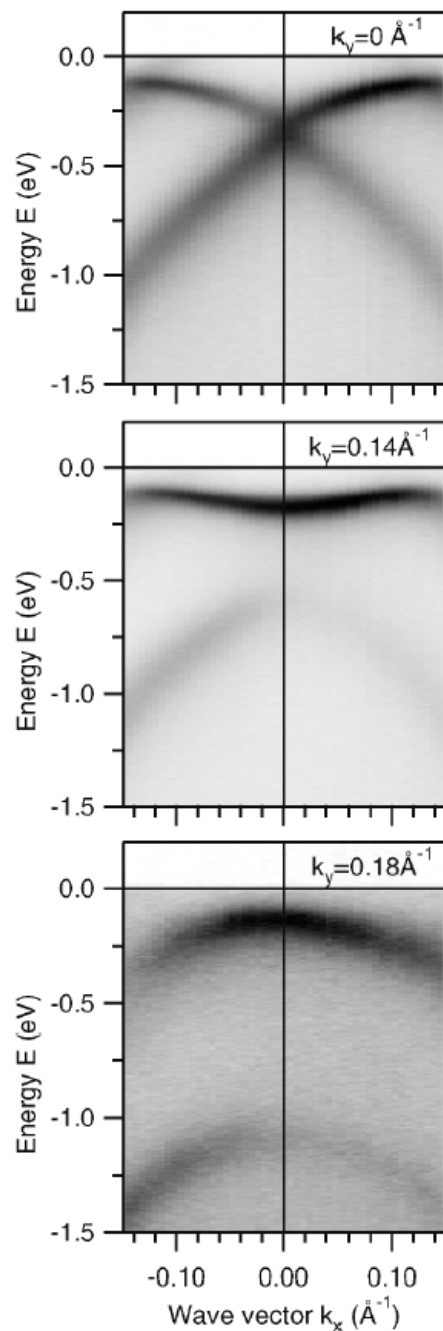


TABLE I. Selected materials and parameters characterizing the spin splitting: Rashba energy of split states  $E_R$ , wave number offset  $k_0$ , and Rashba parameter  $\alpha_R$ .

Material	$E_R$ (meV)	$k_0$ ( $\text{\AA}^{-1}$ )	$\alpha_R$ (eV $\text{\AA}$ )	Reference
InGaAs/InAlAs heterostructure	$<1$	0.028	0.07	[4]
Ag(111) surface state	$<0.2$	0.004	0.03	[5,6]
Au(111) surface state	2.1	0.012	0.33	[6,7]
Bi(111) surface state	$\sim 14$	$\sim 0.05$	$\sim 0.56$	[8]
Bi/Ag(111) surface alloy	200	0.13	3.05	This work

Band structure measurements by ARPES (left-hand panels) and calculations (right-hand panels) in the vicinity of the  $\Gamma$  point.

Note the different horizontal scales.



PHYSICAL REVIEW B 77, 081407(R) (2008)

**Spin-orbit split two-dimensional electron gas with tunable Rashba and Fermi energy**Christian R. Ast,<sup>1,2,\*</sup> Daniela Pacilé,<sup>2,†</sup> Luca Moreschini,<sup>2</sup> Mihaela C. Falub,<sup>2</sup> Marco Papagno,<sup>2</sup> Klaus Kern,<sup>1,2</sup> and  
Marco Grioni<sup>2</sup><sup>1</sup>*Max-Planck-Institut für Festkörperforschung, D-70569 Stuttgart, Germany*<sup>2</sup>*Ecole Polytechnique Fédérale de Lausanne (EPFL), Institut de Physique des Nanostructures, CH-1015 Lausanne, Switzerland*Jürgen Henk, Arthur Ernst, Sergey Ostanin, and Patrick Bruno  
*Max-Planck-Institut für Mikrostrukturphysik, D-06120 Halle (Saale), Germany*

(Received 15 January 2008; published 15 February 2008)

We demonstrate that it is possible to tune the Rashba energy, introduced by a strong spin-orbit splitting, and the Fermi energy in a two-dimensional electron gas by a controlled change of stoichiometry in an artificial surface alloy. In the  $\text{Bi}_x\text{Pb}_{1-x}/\text{Ag}(111)$  surface alloy, the spin-orbit interaction maintains a dramatic influence on the band dispersion for arbitrary Bi concentration  $x$ , as is shown by angle-resolved photoelectron spectroscopy. The Rashba energy  $E_R$  and the Fermi energy  $E_F$  can be tuned to achieve values larger than one for the ratio  $E_R/E_F$ , which opens up the possibility for observing phenomena, such as corrections to the Fermi liquid or a superconducting state. Relativistic first-principles calculations explain the experimental findings.

DOI: [10.1103/PhysRevB.77.081407](https://doi.org/10.1103/PhysRevB.77.081407)

PACS number(s): 73.20.At, 79.60.-i, 71.70.Ej

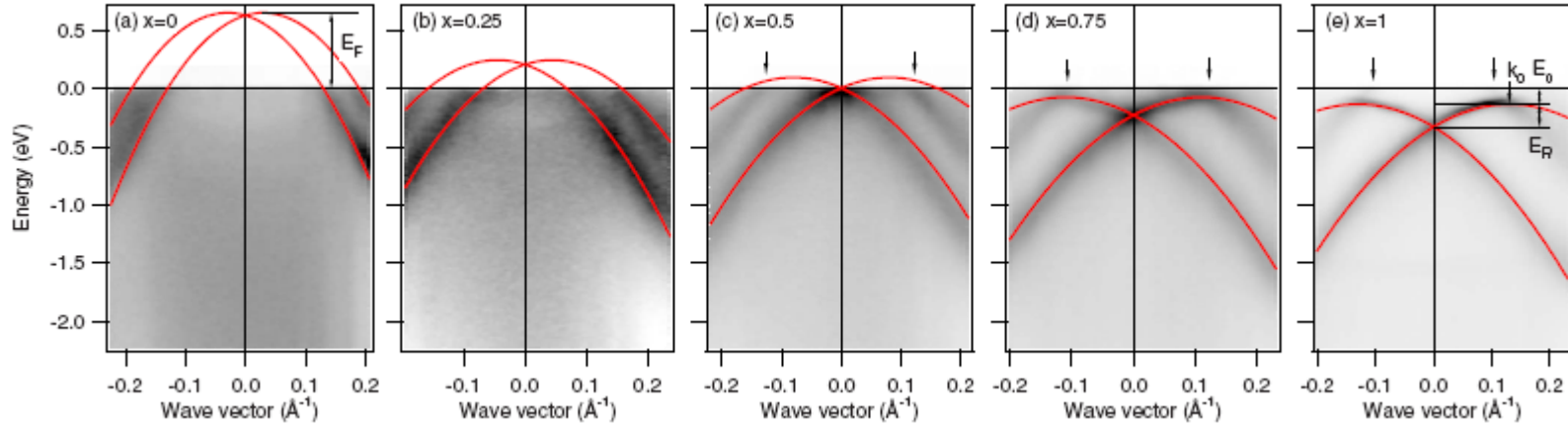
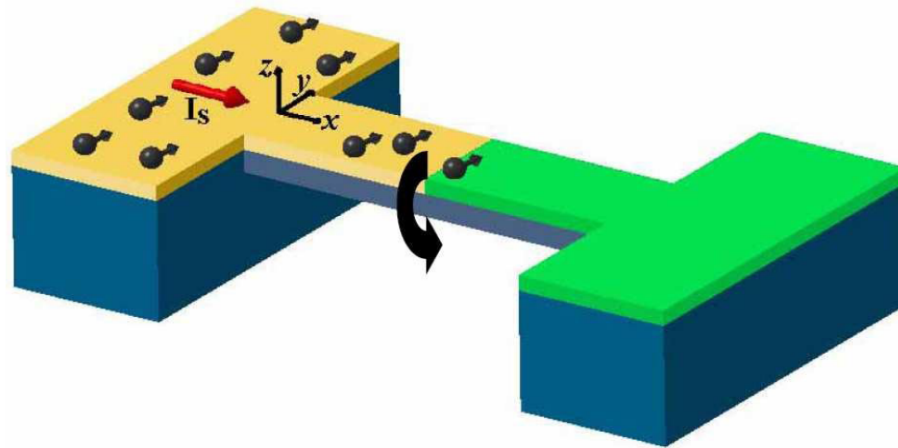


FIG. 1. (Color online) Experimental band structures of  $\text{Bi}_x\text{Pb}_{1-x}/\text{Ag}(111)$  surface alloys for  $x$  as indicated. The photoemission intensity is depicted as linear gray scale, with dark corresponding to high intensity, versus energy  $E$  and wave vector  $k$  along  $\bar{\text{K}}\bar{\Gamma}\bar{\text{K}}$ . Data are taken at 21.2 eV (HeI). Red (dark gray) lines represent parabolic fits to the surface-state bands. The Fermi energy of the holes is indicated in (a). The spin-orbit splitting  $k_0$ , the Rashba energy  $E_R$  as well as the energy offset  $E_0$  are defined in (e).

## Spin Current Detection

- **A nano-mechanical proposal**
- **An Inverse spin-Hall proposal and experiment**

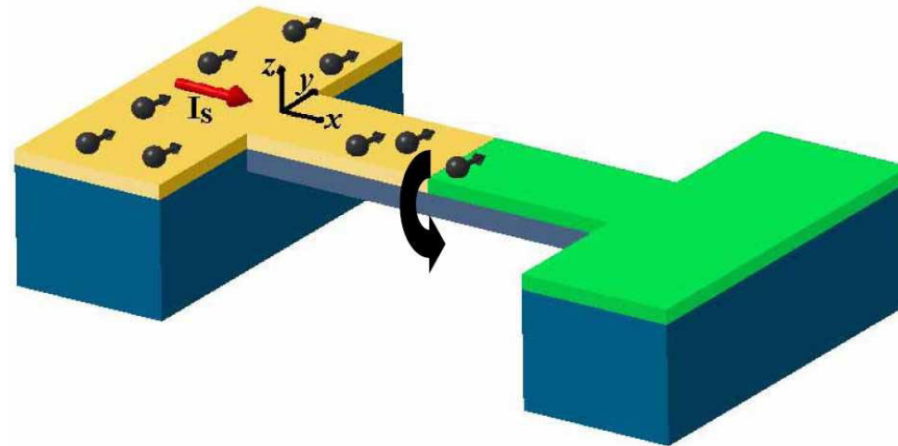
Nanobridge consists of:  
Semiconductor (yellow region); Metal (green region);  
Insulator (blue region)



**Semiconductor** provides the strain-induced SOI;  
**Metal** provides a rapid spin relaxation;  
Insulator is to provide an asymmetric environment for the semiconductor so as to allow for a net torsional stress.

- Relate torsional energy to spin current
- Derive equation of motion for the torsion angle
- Relate the spin current to the spin density
- Estimate torsion angle and its thermal fluctuation

**Target:** To study the torsion angle the nanobridge is to twist upon the diffusion of electron spin into the nanobridge from the semiconductor side.



### Dimension of the Nanobridge:

- $b$  : the width
- $c/2$  : thickness of the semiconductor
- $L$  : length of the semiconductor in the nanobridge
- $c/2$  : thickness of the insulator
- $L_t$  : total length of the nanobridge

## Strain-induced SOI in semiconductor

$$H_{\text{SOI}} = \alpha \left[ \sigma_x (u_{zx} k_z - u_{xy} k_y) + \sigma_y (u_{xy} k_x - u_{yz} k_z) + \sigma_z (u_{yz} k_y - u_{zx} k_x) \right] \\ + \beta \left[ \sigma_x k_x (u_{yy} - u_{zz}) + \sigma_y k_y (u_{zz} - u_{xx}) + \sigma_z k_z (u_{xx} - u_{yy}) \right]$$

$u_{ij}$  are elements of the strain tensor

$\alpha$  is the coupling constant for torsional motions

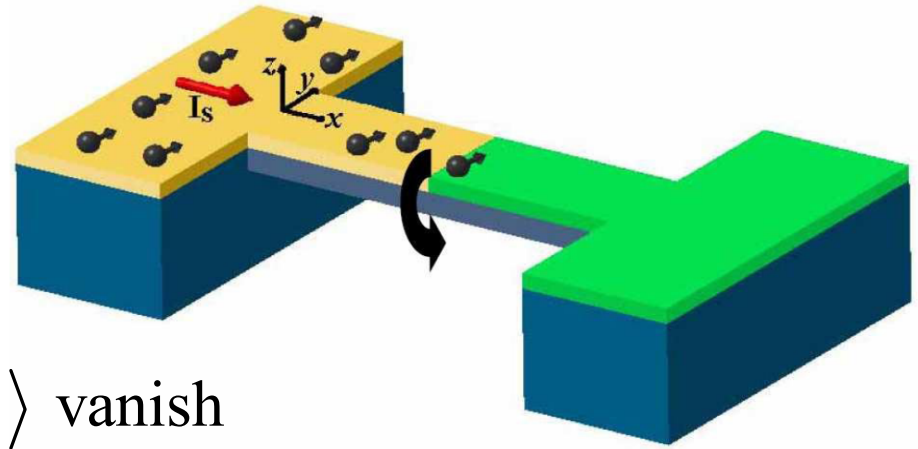
$\beta$  is the coupling constant for flexural motions

$\beta \ll \alpha$  for narrow gap semiconductors



$$H_{\text{SOI}} = \alpha \left[ \sigma_x (u_{zx} k_z - u_{xy} k_y) + \sigma_y (u_{xy} k_x - u_{yz} k_z) + \sigma_z (u_{yz} k_y - u_{zx} k_x) \right]$$

$u_{yz} = 0$  for torsional motion  
along  $x$  axis



terms involving  $\langle k_y \rangle$  and  $\langle k_z \rangle$  vanish

$$H_{\text{SOI}} = \alpha \left[ \sigma_y u_{xy} - \sigma_z u_{zx} \right] k_x$$

$$H_{\text{SOI}} = \alpha \left[ \sigma_y u_{xy} - \sigma_z u_{zx} \right] k_x$$

$$u_{yx} = \tau(x) \frac{\partial \chi}{\partial z}; \quad u_{zx} = -\tau(x) \frac{\partial \chi}{\partial y}$$

$$\tau(x) = \frac{\partial \theta}{\partial x}$$

$$\nabla^2 \chi(y, z) = -1 \quad \text{with the boundary condition } \chi = 0$$

**An influx of diffusive spin current can be represented by a Boltzmann distribution function  $F_k^i(r)$  from which we can calculate the spin distribution function  $P_k^i(r)$ . We assume  $P_k^i(r)$  to be uniform within the cross section of the semiconductor.**

**Torsional energy:**

$$\begin{aligned}
 E_{\text{SO}} &= \int \sum_{\vec{k}} \text{Tr} \left[ \hat{F}_{\vec{k}}(\vec{r}) H_{\text{SOI}} \right] dx dy dz \\
 &= 2\alpha \int_0^L dx \frac{\partial \theta}{\partial x} \sum_{\vec{k}} k_x \left[ P_{\vec{k}}^y \frac{\partial \chi}{\partial z} + P_{\vec{k}}^z \frac{\partial \chi}{\partial y} \right] dy dz
 \end{aligned}$$

**From the above expression it is clear that the insulator plays a very important role in providing a net torsional stress.**

$$J^y(x) = S \sum_{\vec{k}} v_x P_{\vec{k}}^y(x)$$

$$E_{\text{SO}} = -\gamma \int_0^L dx J^y(x) \frac{\partial \theta}{\partial x}$$

$$\rho I \frac{d^2 \theta}{dt^2} - K \frac{d^2 \theta}{dx^2} - \gamma \frac{d}{dx} [J^y(x) \eta(L-x)] = 0$$

$$\theta_L = \frac{L(L_t - L)}{L_t} \frac{\mathfrak{T}}{K}$$

The SOI torque on the nanobridge  $\mathfrak{T} = \gamma \frac{1}{L} \int_0^L dx J^y(x)$

$$\bar{J}^y \equiv \frac{1}{L} \int_0^L dx J^y(x) = \frac{D_S P^y(0) S}{L}$$

$$\overline{\delta\theta_L^2} = \frac{k_B T L_t}{\pi^2 K} \sum_{n \geq 1} \frac{1}{n^2} \sin^2 \left( \frac{\pi n L}{L_t} \right)$$

$$\theta_L = \frac{L(L_t - L)}{L_t} \frac{\mathfrak{I}}{K}$$

$$b = 400 \text{ nm}$$

$$c = 200 \text{ nm}$$

$$\alpha/\hbar = 4 \times 10^5 \text{ m/s (GaAs)}$$

$$\gamma = 2.4 \times 10^{-32} \text{ J sec}$$

$$\text{For } e\bar{J}^y = 10^{-8} \text{ Amp.}$$

$$\mathfrak{I} = 1.5 \times 10^{-21} \text{ Nm}$$

**within the sensitivity of  
P. Mohanty's group,  
Phys. Rev. B 70, 195301  
(2004)**

**A.G. Mal'shukov, C.S. Tang,  
C.S. Chu, K.A. Chao,  
Phys. Rev. Lett. 95, 107203  
(2005)**

$$\text{For } L_t = 5 \text{ } \mu\text{m}$$

$$L = 2 \text{ } \mu\text{m}$$

$$Q \approx 10^4$$

$$\delta\theta \approx 0.5 \times 10^{-4} \text{ }^\circ$$

## **Summary**

- 1. Strain-induced SOI provides a nanomechanical scheme for the detection of spin current**
- 2. The effect can be inverted for the generation of spin current from torsional motion**

## LETTERS

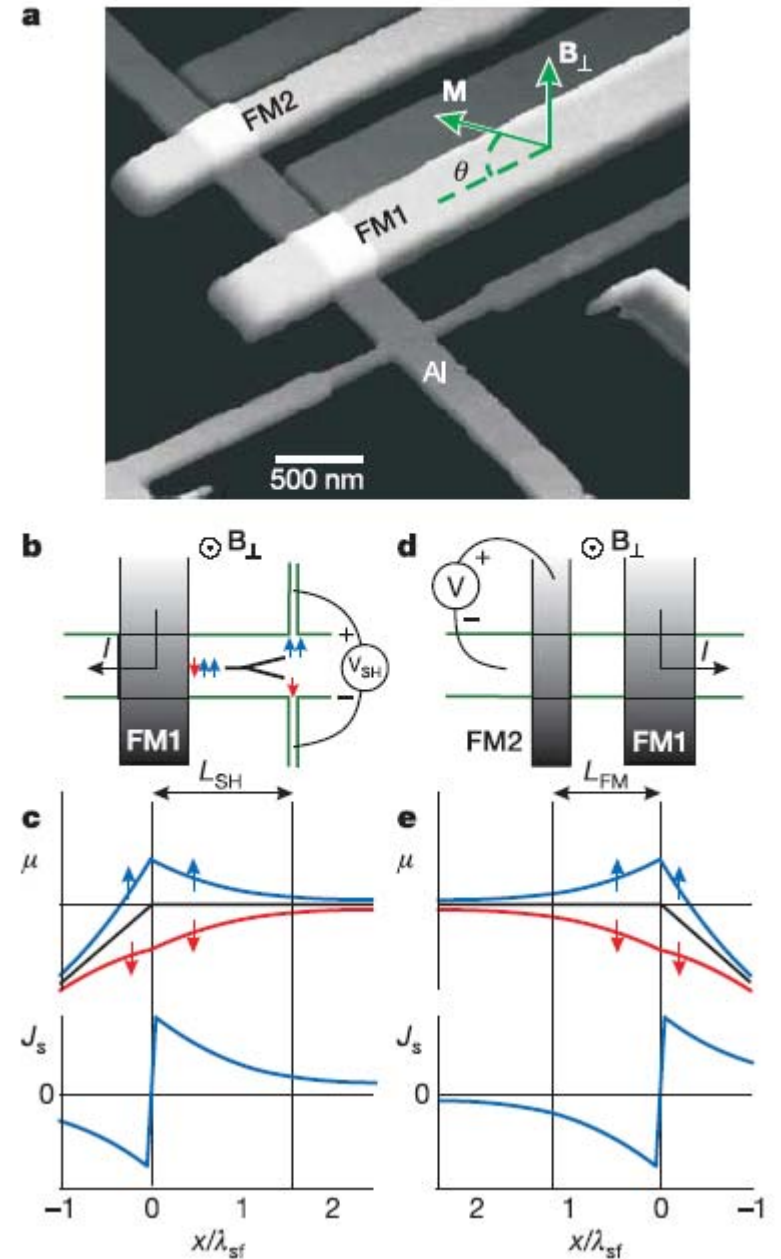
## Direct electronic measurement of the spin Hall effect

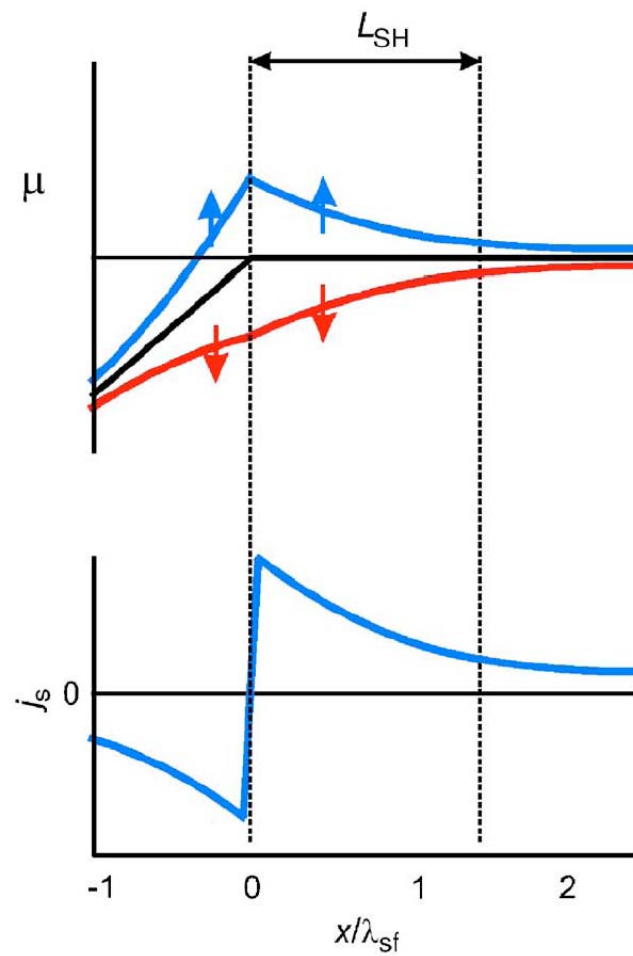
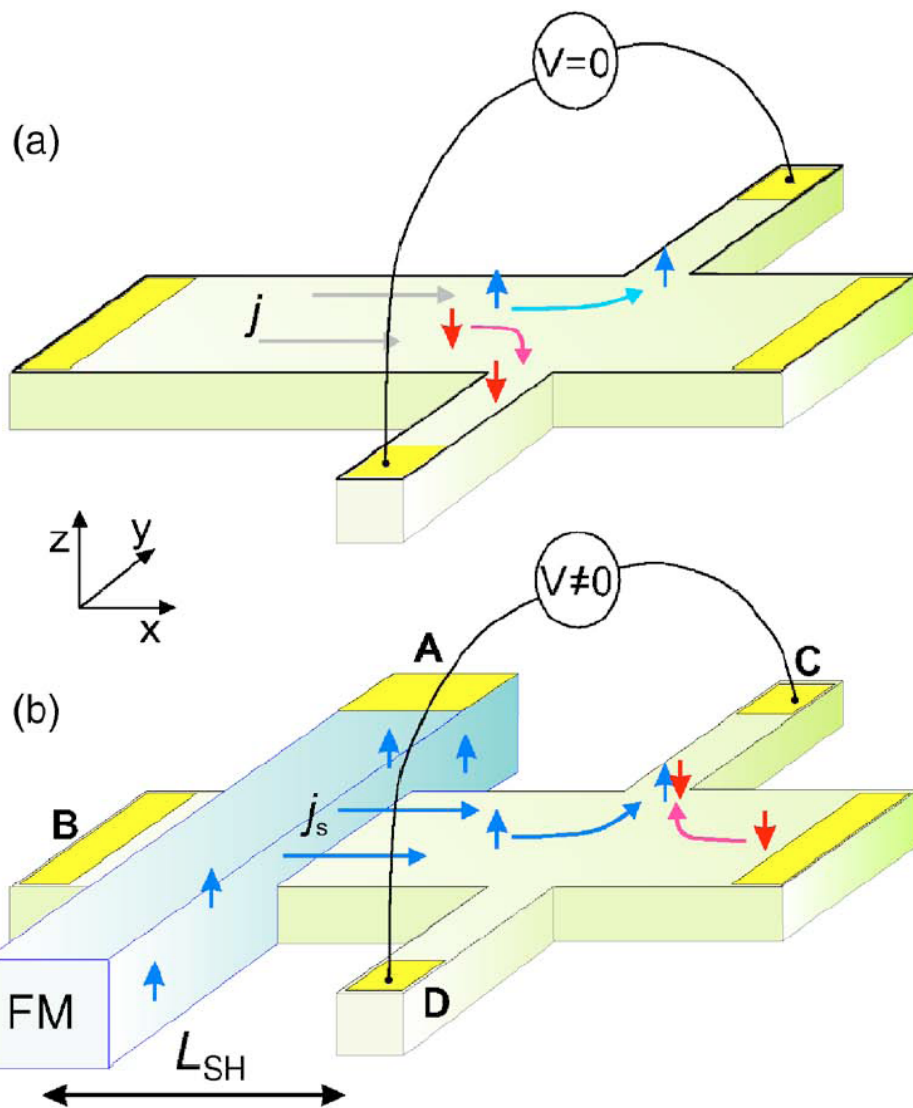
S. O. Valenzuela<sup>1</sup>† & M. Tinkham<sup>1</sup>

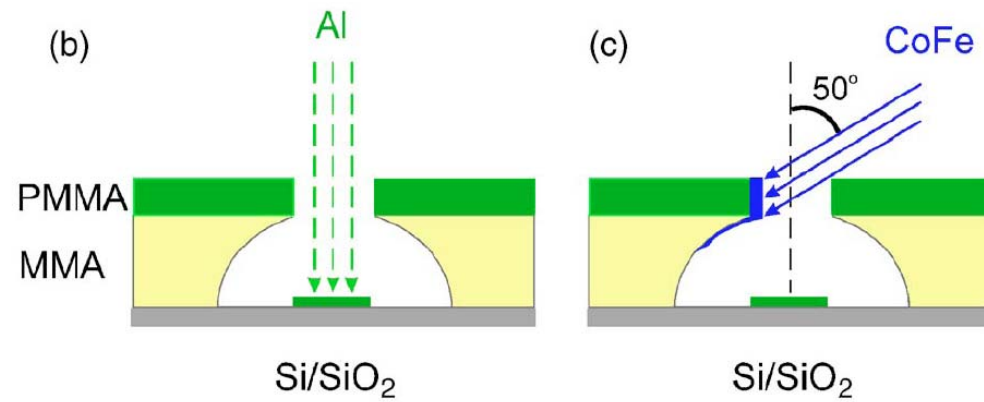
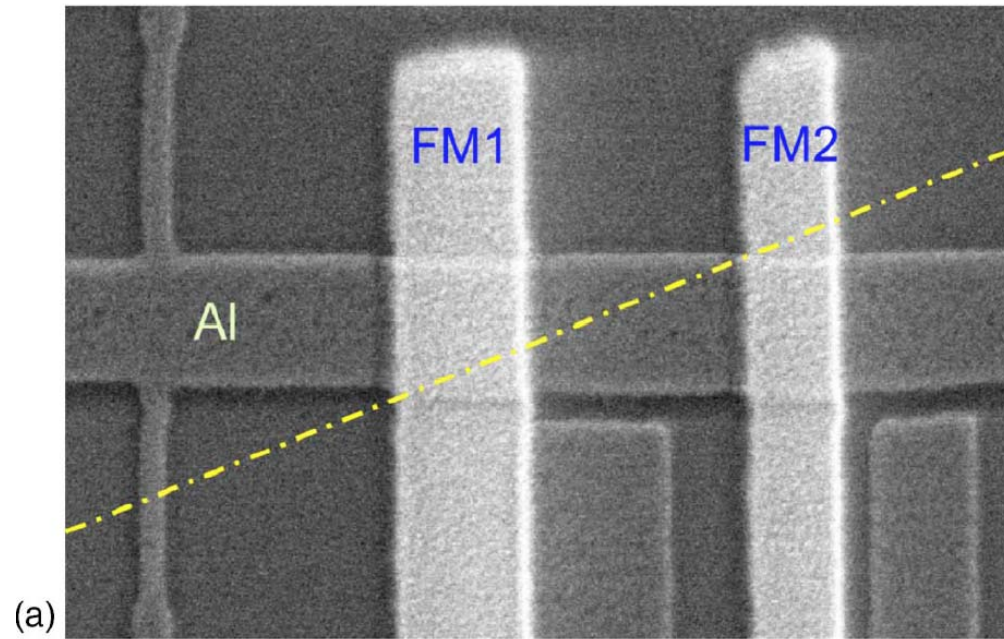
The generation, manipulation and detection of spin-polarized electrons in nanostructures define the main challenges of spin-based electronics<sup>1</sup>. Among the different approaches for spin generation and manipulation, spin-orbit coupling—which couples the spin of an electron to its momentum—is attracting considerable interest. In a spin-orbit-coupled system, a non-zero spin current is predicted in a direction perpendicular to the applied electric field, giving rise to a spin Hall effect<sup>2–4</sup>. Consistent with this effect, electrically induced spin polarization was recently detected by optical techniques at the edges of a semiconductor channel<sup>5</sup> and in two-dimensional electron gases in semiconductor heterostructures<sup>6,7</sup>. Here we report electrical measurements of the spin Hall effect in a diffusive metallic conductor, using a ferromagnetic electrode in combination with a tunnel barrier to inject a spin-polarized current. In our devices, we observe an induced voltage that results exclusively from the conversion of the injected spin current into charge imbalance through the spin Hall effect. Such a voltage is proportional to the component of the injected spins that is perpendicular to the plane defined by the spin current direction and the voltage probes. These experiments reveal opportunities for efficient spin detection without the need for magnetic materials, which could lead to useful spintronics devices that integrate information processing and data storage.



**Figure 1 | Geometry of the devices and measurement schemes.** **a**, Atomic force microscope image of a device. A thin aluminium (Al) Hall cross is oxidized and contacted with two ferromagnetic electrodes with different widths (FM1 and FM2). A magnetic field perpendicular to the substrate,  $B_{\perp}$ , sets the orientation of the magnetization  $M$  of FM1 (and FM2), which is characterized by an angle  $\theta$ . **b**, Spin Hall measurement. A current  $I$  is injected out of FM1 into the Al film and away from the Hall cross. A spin Hall voltage,  $V_{SH}$ , is measured between the two Hall probes at a distance  $L_{SH}$  from the injection point.  $V_{SH}$  is caused by the separation of up and down spins due to spin-orbit interaction in combination with a pure spin current. **c**, Top: spatial dependence of the spin-up and spin-down electrochemical potentials,  $\mu_{\uparrow, \downarrow}$ . The black line represents the electrochemical potential of the electrons in the absence of spin injection.  $\lambda_{sf}$  is the spin diffusion length. Bottom: associated spin current,  $J_s$ . The polarized spins are injected near  $x = 0$  and diffuse in both Al branches in opposite directions. The sign change in  $J_s$  reflects the flow direction. **d**, Spin-transistor measurement for device characterization.  $I$  is injected out of FM1 into the Al film and away from FM2, which is located at a distance  $L_{FM}$  from FM1. A voltage  $V$  is measured between FM2 and the left side of the Al film. **e**, As in **c** but for the conditions shown in **d**. Note that both  $V_{SH}$  in **b** and  $V$  in **d** vary with  $\theta$ .







$$\nabla^2 \delta\mu(\mathbf{r}) = \frac{\delta\mu(\mathbf{r})}{\lambda_{sf}^2}, \quad \delta\mu(\mathbf{r}) = \frac{\mu^\uparrow(\mathbf{r}) - \mu^\downarrow(\mathbf{r})}{2}$$

$$\mathbf{j}_c(\mathbf{r}) = \sigma_c \mathbf{E}(\mathbf{r}) + \frac{\sigma_{SH}}{\sigma_c} (\hat{\mathbf{z}} \times \mathbf{j}_s),$$

$$\mathbf{j}_s(\mathbf{r}) = -\sigma_c \nabla \delta\mu(\mathbf{r})$$

$$j_s(x) = \frac{1}{2} P \frac{I}{A_N} e^{-x/\lambda_{sf}},$$

# New Journal of Physics

The open-access journal for physics

## Extracting current-induced spins: spin boundary conditions at narrow Hall contacts

i Adagideli<sup>1,3</sup>, M Scheid<sup>1</sup>, M Wimmer<sup>1</sup>, G E W Bauer<sup>2</sup>  
and K Richter<sup>1</sup>

<sup>1</sup> Institut für Theoretische Physik, Universität Regensburg, D-93040, Germany

<sup>2</sup> Kavli Institute of Nanoscience, TU Delft, Lorentzweg 1,  
2628 CJ Delft, The Netherlands

E-mail: [inanc.adagideli@physik.uni-regensburg.de](mailto:inanc.adagideli@physik.uni-regensburg.de)

*New Journal of Physics* 9 (2007) 382

Received 30 July 2007

Published 24 October 2007

Online at <http://www.njp.org/>

doi:10.1088/1367-2630/9/10/382

**Abstract.** We consider the possibility to extract spins that are generated by an electric current in a two-dimensional electron gas with Rashba–Dresselhaus spin–orbit interaction (R2DEG) in the Hall geometry. To this end, we discuss boundary conditions for the spin accumulations between a spin–orbit (SO) coupled region and a contact without SO coupling, i.e. a normal two-dimensional electron gas (2DEG). We demonstrate that in contrast to contacts that extend along the whole sample, a spin accumulation can diffuse into the normal region through finite contacts and be detected by e.g. ferromagnets. For an impedance-matched narrow contact the spin accumulation in the 2DEG is equal to the current induced spin accumulation in the bulk of R2DEG up to a geometry-dependent numerical factor.

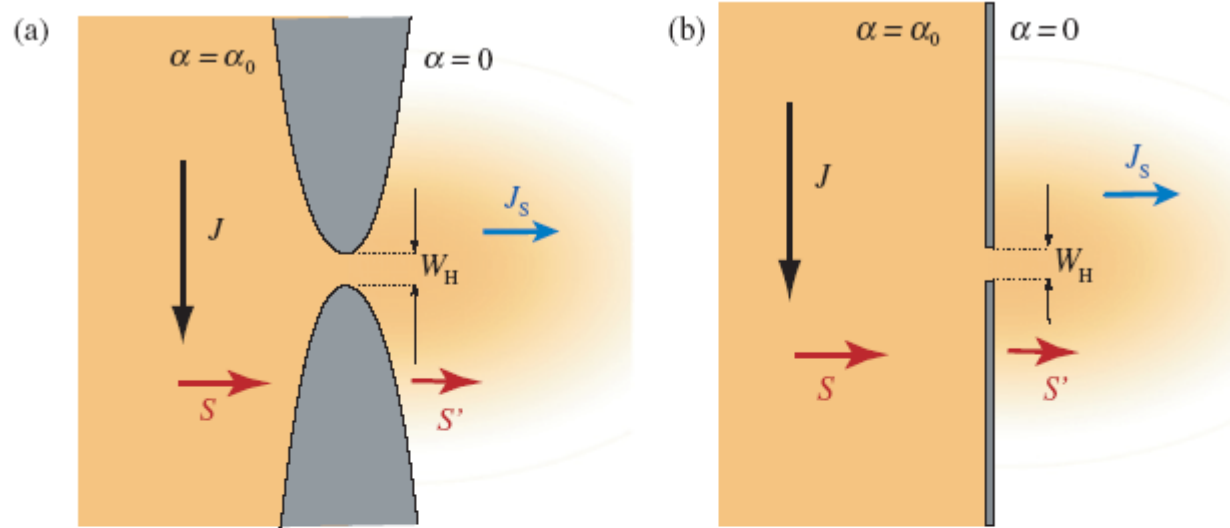
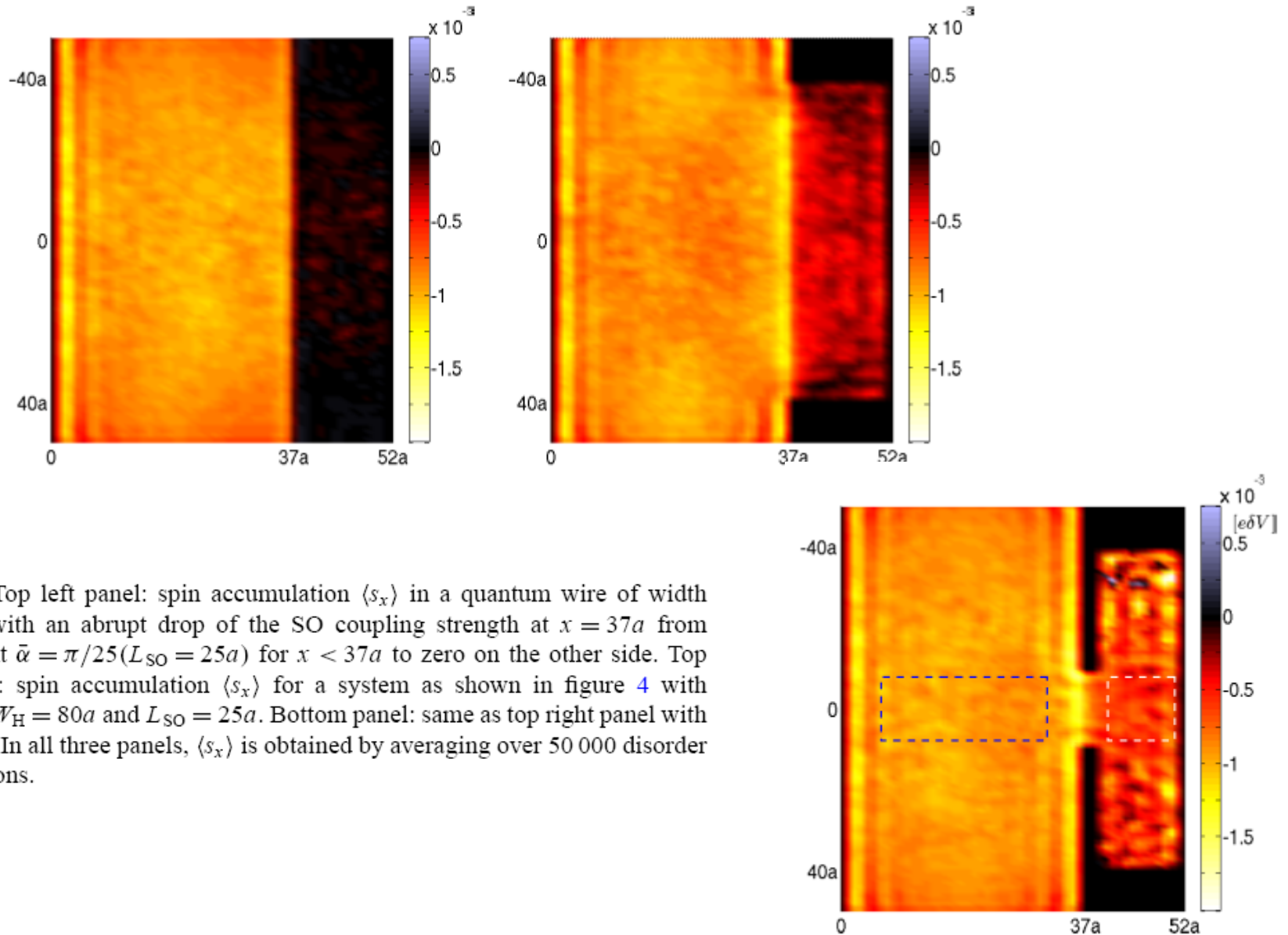


**Figure 3.** Geometry of the contact: (a) 2DEG with a constriction in the middle. On the left side there is an applied homogeneous current density which is modified near the opening. On the right side, the current density far away from the contact as well as the net charge current flowing from the left region to the right region is zero. However, there is a finite spin current and a finite spin accumulation in the right region. The respective mobilities of the left and right regions are assumed to be the same but the Rashba coefficients are different. (b) An idealized version of (a) used in the calculations of this section. The origin is chosen at the center of the opening with width  $W_H$ .



# Spin-Hall Effect in a non-uniform driving field



## Restoration of the SHE in a Rashba-type 2DEG by a nonuniform electric field ?

$$h_k = \alpha(\mathbf{k} \times \hat{z})$$

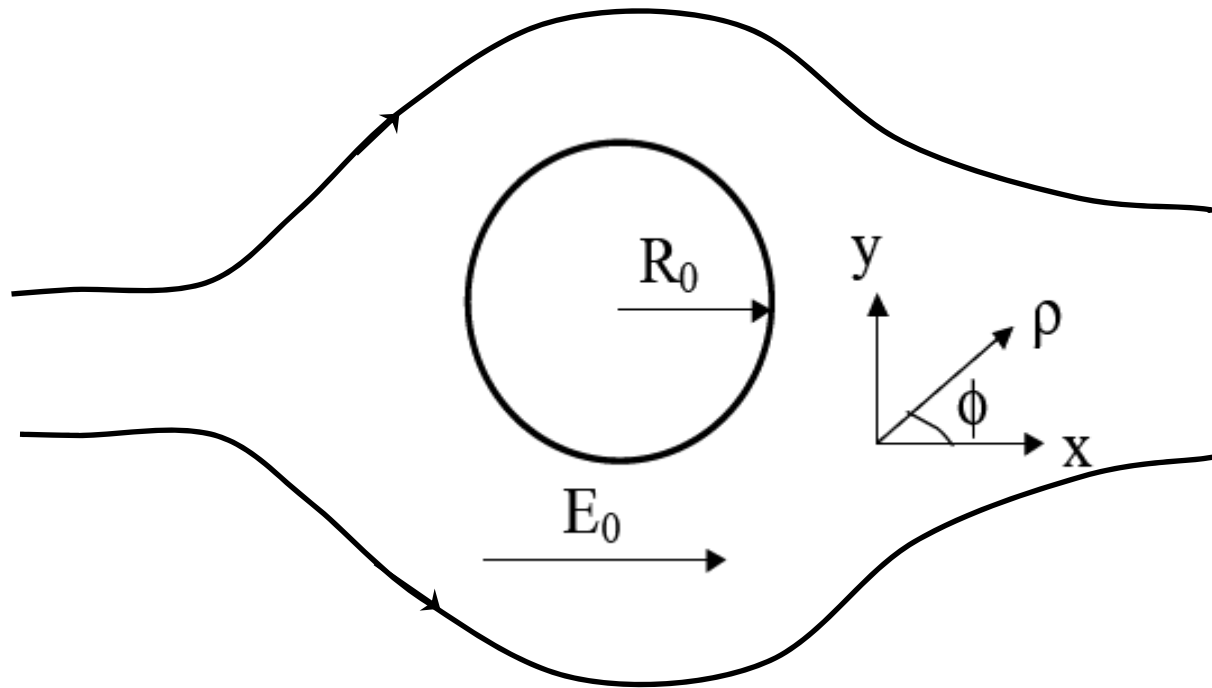
A spin diffusion equation for a nonuniform driving field:

$$\begin{cases} \left( D\nabla^2 - 2\frac{\xi^2}{\tau} \right) S_x + \left( 2\xi v_F \frac{\partial}{\partial x} \right) S_z - \xi^2 \alpha \frac{\partial}{\partial y} D_0^0 = 0 \\ \left( D\nabla^2 - 2\frac{\xi^2}{\tau} \right) S_y + \left( 2\xi v_F \frac{\partial}{\partial y} \right) S_z + \xi^2 \alpha \frac{\partial}{\partial x} D_0^0 = 0 \\ \left( D\nabla^2 - 4\frac{\xi^2}{\tau} \right) S_z - 2\xi v_F \frac{\partial}{\partial x} S_x - 2\xi v_F \frac{\partial}{\partial y} S_y = 0 \end{cases}$$

$$\xi = \alpha k_F \tau$$

$$D_0^0 = 2N_F e \varphi(r)$$

We consider a situation when the electric current flows around a hole in the Rashba-type 2DEG.



$$\varphi(r) = -E_0(r + R_0^2/r)\cos\phi$$

$$\mathbf{E} = -\nabla\varphi(r)$$

$$\begin{cases} \left( D\nabla^2 - 2\frac{\xi^2}{\tau} \right) S_x + \left( 2\xi v_F \frac{\partial}{\partial x} \right) S_z - \xi^2 \alpha \frac{\partial}{\partial y} D_0^0 = 0 \\ \left( D\nabla^2 - 2\frac{\xi^2}{\tau} \right) S_y + \left( 2\xi v_F \frac{\partial}{\partial y} \right) S_z + \xi^2 \alpha \frac{\partial}{\partial x} D_0^0 = 0 \\ \left( D\nabla^2 - 4\frac{\xi^2}{\tau} \right) S_z - 2\xi v_F \frac{\partial}{\partial x} S_x - 2\xi v_F \frac{\partial}{\partial y} S_y = 0 \end{cases}$$

$$h_k = \alpha(\mathbf{k} \times \hat{z})$$

$$\varphi(r) = -E_0(r + R_0^2/r)\cos\phi$$

$$D = v_F^2 \tau / 2$$

$$D_0^0 = 2N_F e \varphi(r)$$

$$\tilde{E} = eE_0 N_F \tau$$

**Total spin densities:**

$$S_i = S_i^b + S_i^p + \Delta S_i$$

$$\begin{cases} S_x^p = -\alpha \tilde{E} \frac{R_0^2}{\rho^2} \sin 2\phi \\ S_y^p = \alpha \tilde{E} \left( -1 + \frac{R_0^2}{\rho^2} \cos 2\phi \right) \\ S_z^p = 0 \end{cases}$$

$$\begin{cases} \nabla^2 (\Delta S_x) - 4\Delta S_x + 2(\nabla_+ + \nabla_-) \Delta S_z = 0 \\ \nabla^2 (\Delta S_y) - 4\Delta S_y - 2i(\nabla_+ - \nabla_-) \Delta S_z = 0 \\ \nabla^2 (\Delta S_z) - 8\Delta S_z - 2(\nabla_+ + \nabla_-) \Delta S_x + 2i(\nabla_+ - \nabla_-) \Delta S_y = 0 \end{cases}$$

$$\nabla_{\pm} = \partial/\partial x \pm \partial/\partial y$$

$$\Delta S_x = \sum_m A_m h_m^{(1)}(\gamma\rho) e^{im\phi}$$

$$\Delta S_y = \sum_m B_m h_m^{(1)}(\gamma\rho) e^{im\phi}$$

$$\Delta S_z = \sum_m C_m h_m^{(1)}(\gamma\rho) e^{im\phi}$$

$$\gamma = \pm 2i, \pm \sqrt{2 + 2i\sqrt{7}} \text{ and } \pm \sqrt{2 - 2i\sqrt{7}}$$

**Boundary condition:**  
**zero radial spin current at the hole boundary**

$$\begin{cases} -\frac{1}{2} (e^{-i\phi} \nabla_+ + e^{i\phi} \nabla_-) \Delta S_x - 2 \cos \phi \Delta S_z - 2\alpha \tilde{E} \frac{R_0^2}{\rho^3} \sin 2\phi \Big|_{\rho=R_0} = 0 \\ -\frac{1}{2} (e^{-i\phi} \nabla_+ + e^{i\phi} \nabla_-) \Delta S_y - 2 \sin \phi \Delta S_z + 2\alpha \tilde{E} \frac{R_0^2}{\rho^3} \cos 2\phi \Big|_{\rho=R_0} = 0 \\ -\frac{1}{2} (e^{-i\phi} \nabla_+ + e^{i\phi} \nabla_-) \Delta S_z + 2 \cos \phi \Delta S_x + 2 \sin \phi \Delta S_y \Big|_{\rho=R_0} = 0 \end{cases}$$

Compare with what we have previously for the spin current

$$I_y^i(\mathbf{r}) = -2D \frac{\partial S_i}{\partial y} - \frac{R^{ijy}}{\hbar} (S_j - S_j^b) + \frac{I_{sH}}{\hbar} \delta_{iz}$$

Total spin densities:

$$S_i = S_i^b + S_i^p + \Delta S_i$$

Bulk spin densities:

$$S_x^b = 0$$

$$S_y^b = -\frac{\alpha}{\hbar} e E N_F \tau$$

$$S_z^b = 0$$

Particular spin densities:

$$S_x^p = -\frac{\alpha}{\hbar} e E N_F \tau \left( \frac{R_0^2}{\rho^2} \sin 2\phi \right)$$

$$S_y^p = \frac{\alpha}{\hbar} e E N_F \tau \left( \frac{R_0^2}{\rho^2} \cos 2\phi \right)$$

$$S_z^p = 0$$

Physical parameters used for the following figures:

$$\alpha = 0.3 \times 10^{-12} \text{ eVm}$$

$$E = 40 \text{ mV}/\mu\text{m}$$

$$l_{\text{so}} = 3.77 \text{ } \mu\text{m}$$

$$l_{\text{e}} = 0.43 \text{ } \mu\text{m}$$

$$R_0 = l_{\text{so}}$$

Bulk spin densities:

$$S_x^b = 0$$

$$S_y^b = -\frac{\alpha}{\hbar} e E N_F \tau = -3.33 \text{ (1 / } \mu\text{m}^2\text{)}$$

$$S_z^b = 0$$

Total spin densities:

$$S_i = S_i^b + S_i^p + \Delta S_i$$

Particular spin densities:

$$S_x^p = -\frac{\alpha}{\hbar} e E N_F \tau \left( \frac{R_0^2}{\rho^2} \sin 2\phi \right) = -3.33 \left( \frac{R_0^2}{\rho^2} \sin 2\phi \right) \text{ (1 / } \mu\text{m}^2\text{)}$$

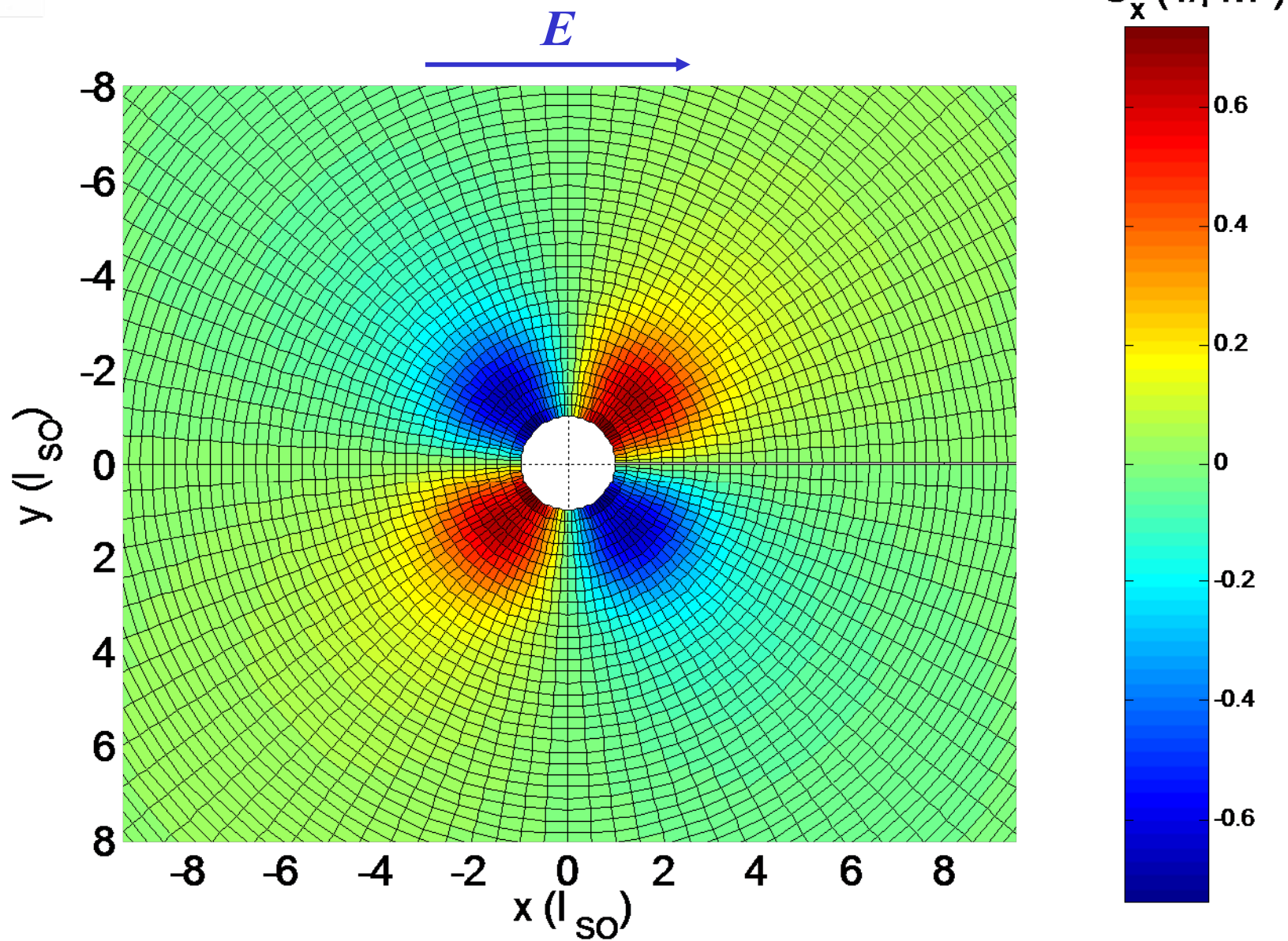
$$S_y^p = \frac{\alpha}{\hbar} e E N_F \tau \left( \frac{R_0^2}{\rho^2} \cos 2\phi \right) = 3.33 \left( \frac{R_0^2}{\rho^2} \cos 2\phi \right) \text{ (1 / } \mu\text{m}^2\text{)}$$

$$S_z^p = 0$$



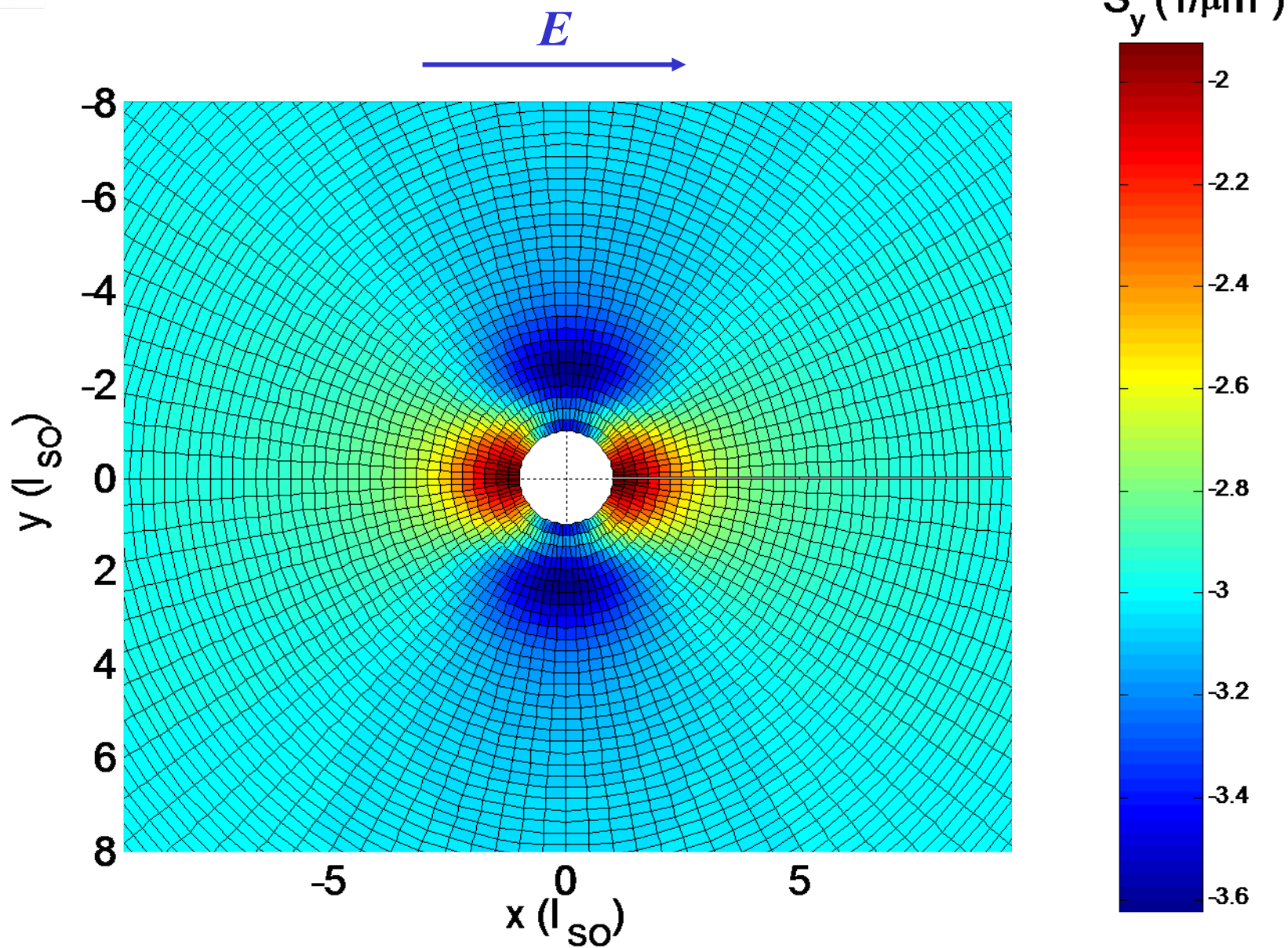
In-plane spin polarization:  $S_x$

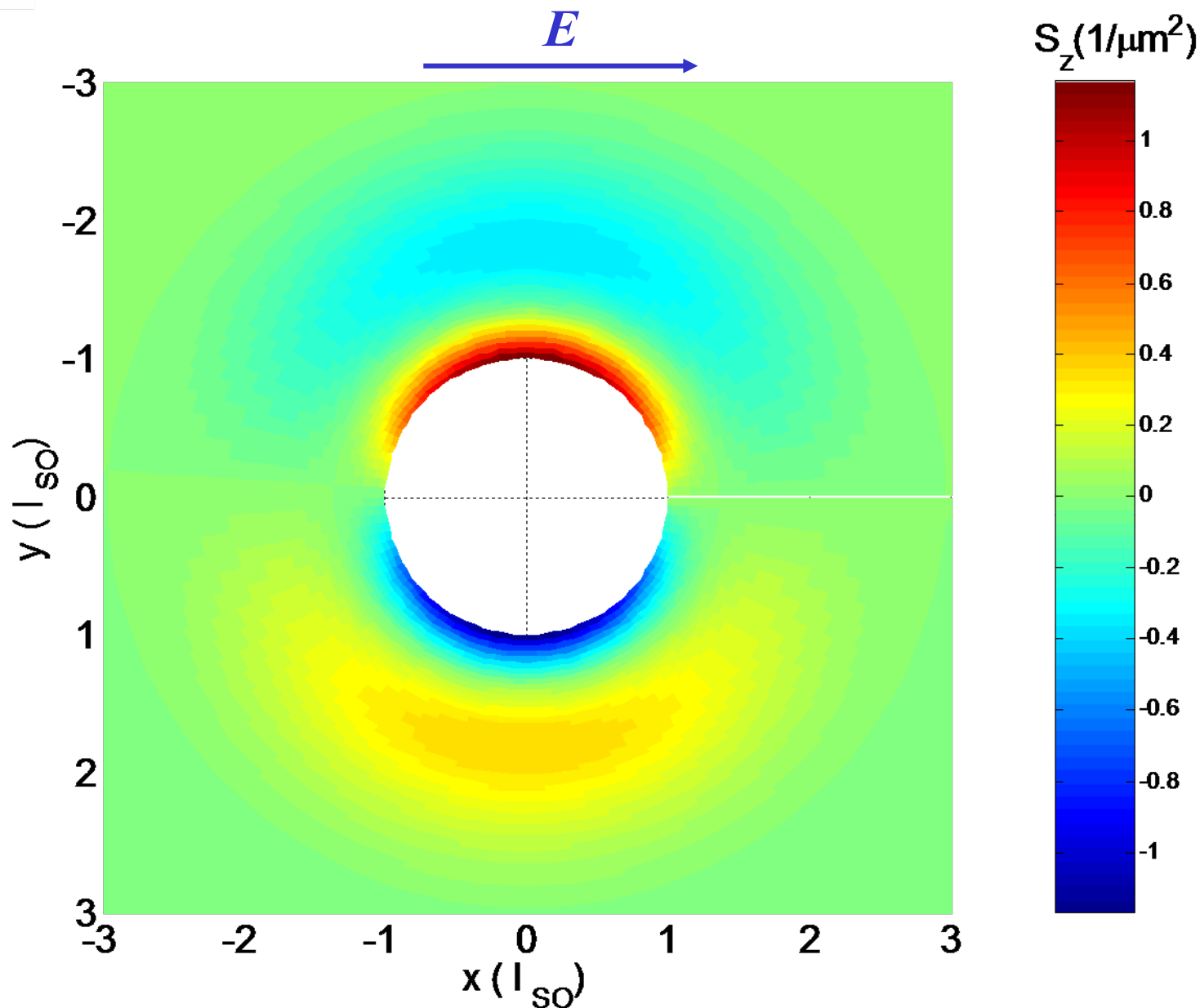
Nonuniform field



In-plane spin polarization:  $S_y$

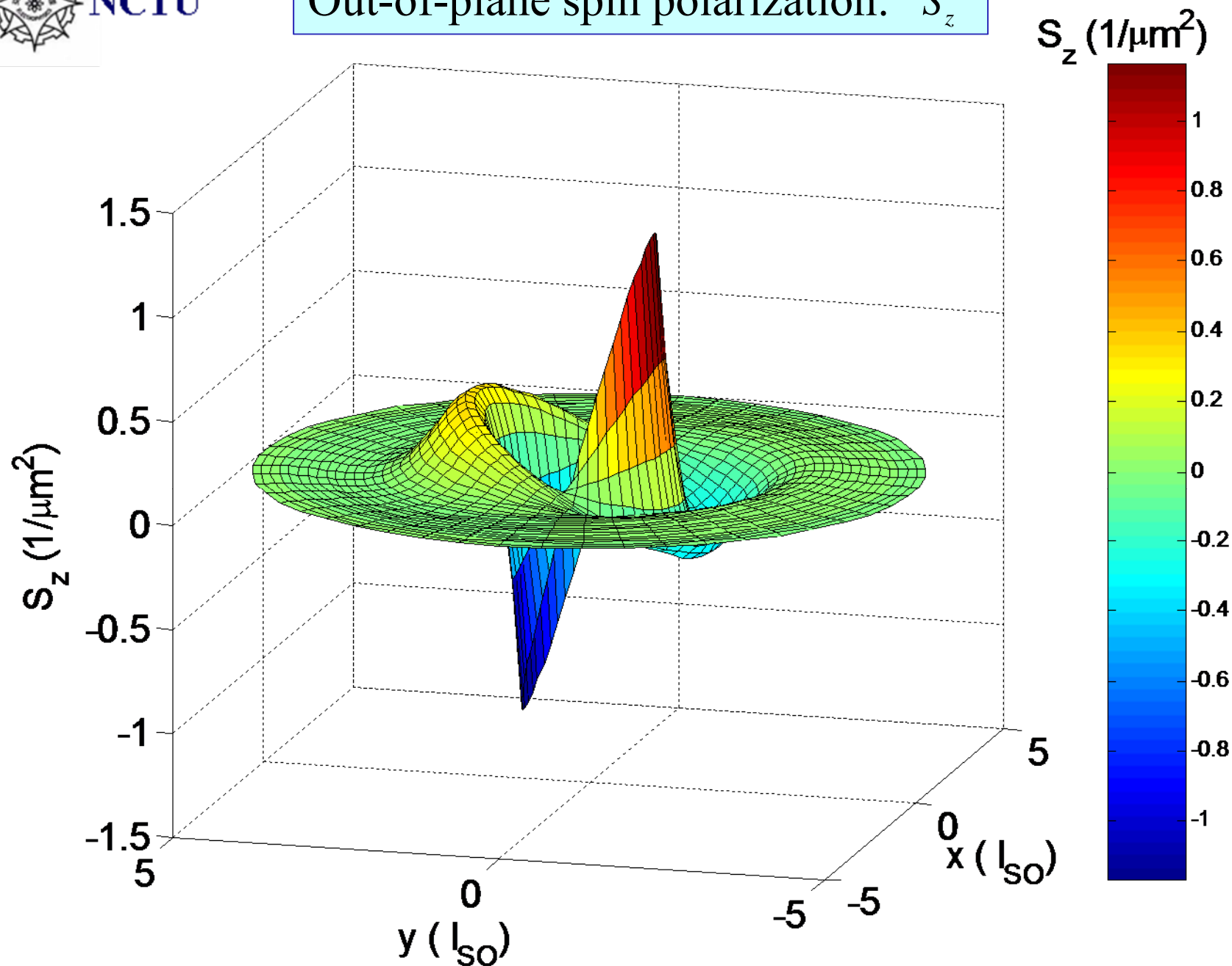
Nonuniform field





# Out-of-plane spin polarization: $S_z$

Nonuniform field



## Summary

We have shown that a Rashba-type SOI 2DEG supports Spin-Hall-type spin accumulation in simple background scatterers: if the driving field is nonuniform.

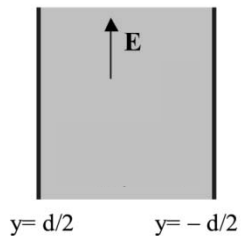
# Competition between SOIs

# Competing interplay between Rashba and cubic- $k$ Dresselhaus SOI

$$\begin{cases} \mathbf{h}_{\mathbf{k},1} = \alpha (k_y, -k_x) + \beta \kappa^2 (-k_x, k_y), & \tilde{\beta} (\equiv \beta \kappa^2) \\ \mathbf{h}_{\mathbf{k},3} = (\beta k_x k_y^2, -\beta k_y k_x^2). \end{cases}$$

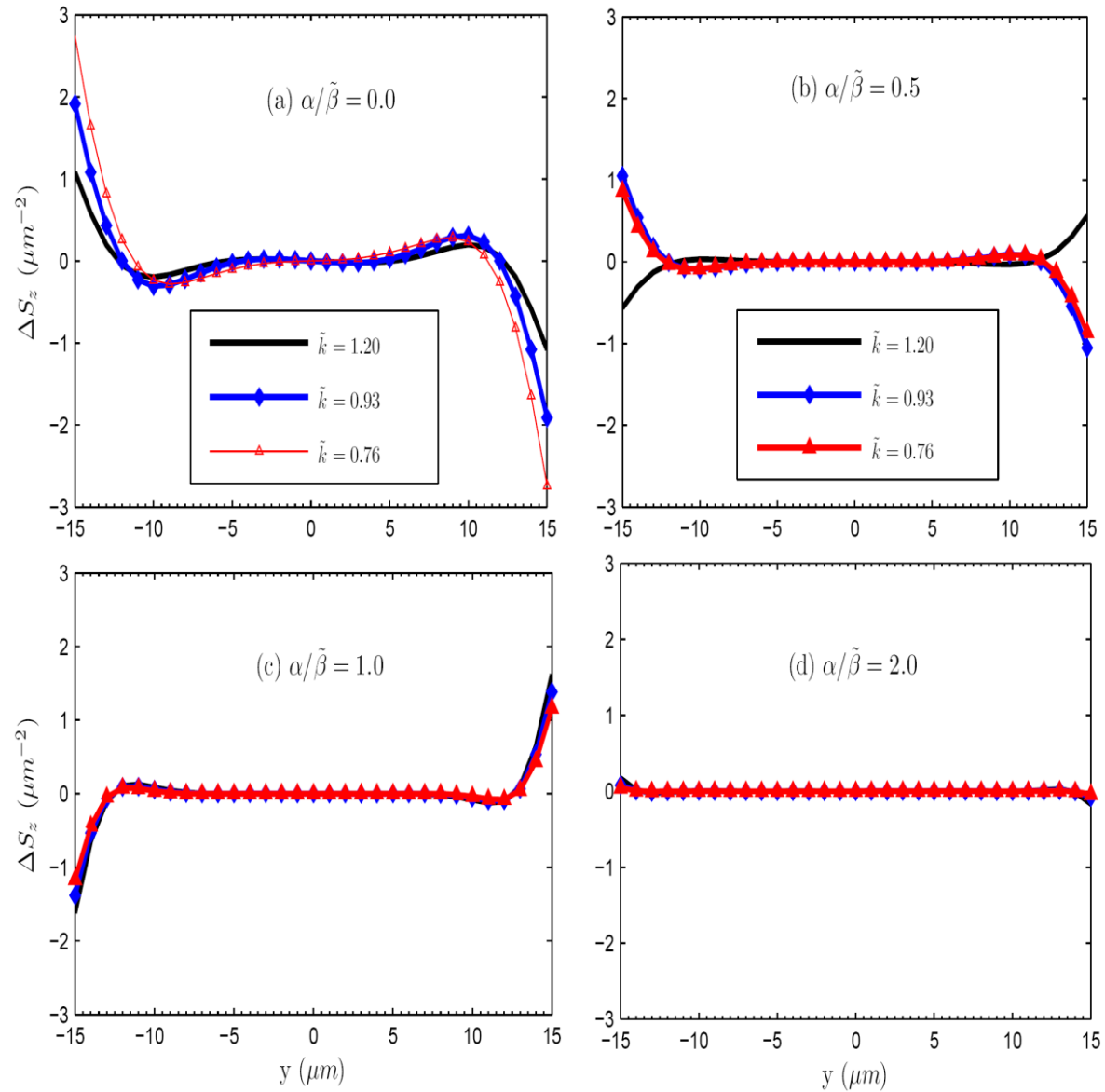
Spin diffusive equation for a semiconductor strip

$$\begin{cases} D \left( \frac{\partial^2}{\partial y^2} S_z \right) + \frac{R^{zx y}}{\hbar} \frac{\partial}{\partial y} S_x + \frac{R^{zy y}}{\hbar} \frac{\partial}{\partial y} S_y - \frac{\Gamma^{zz}}{\hbar^2} S_z = 0 \\ D \left( \frac{\partial^2}{\partial y^2} S_y \right) + \frac{R^{yz y}}{\hbar} \frac{\partial}{\partial y} S_z - \frac{\Gamma^{yy}}{\hbar^2} S_y - \frac{\Gamma^{yx}}{\hbar^2} S_x - \frac{C_x}{\hbar^2} = 0 \\ D \left( \frac{\partial^2}{\partial y^2} S_x \right) + \frac{R^{xz y}}{\hbar} \frac{\partial}{\partial y} S_z - \frac{\Gamma^{xx}}{\hbar^2} S_x - \frac{\Gamma^{xy}}{\hbar^2} S_y - \frac{C_y}{\hbar^2} = 0 \end{cases}$$



## Spatial profile of $\Delta S_z$

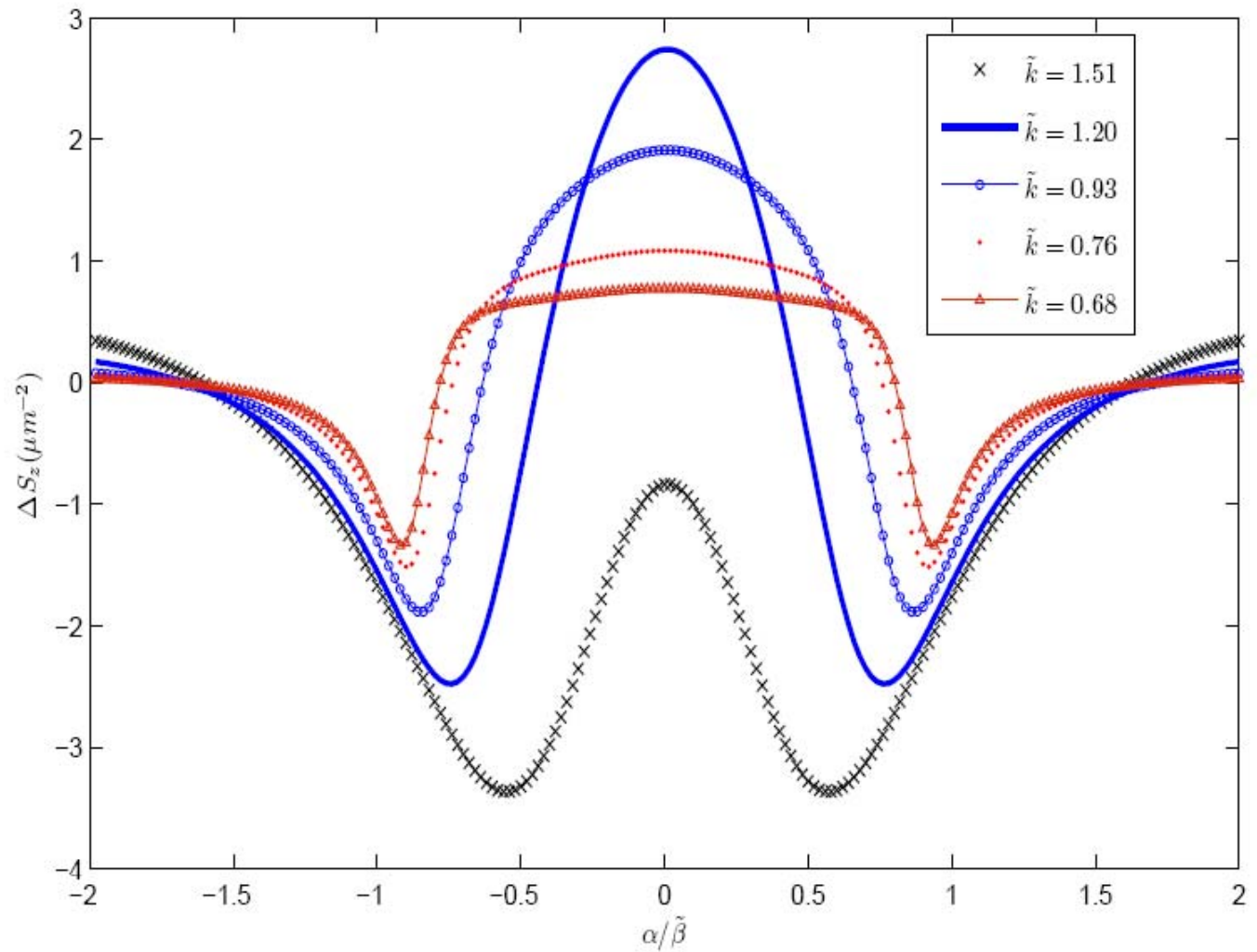
Spin accumulation  
is entirely suppressed  
when  $\alpha = 2\tilde{\beta}$



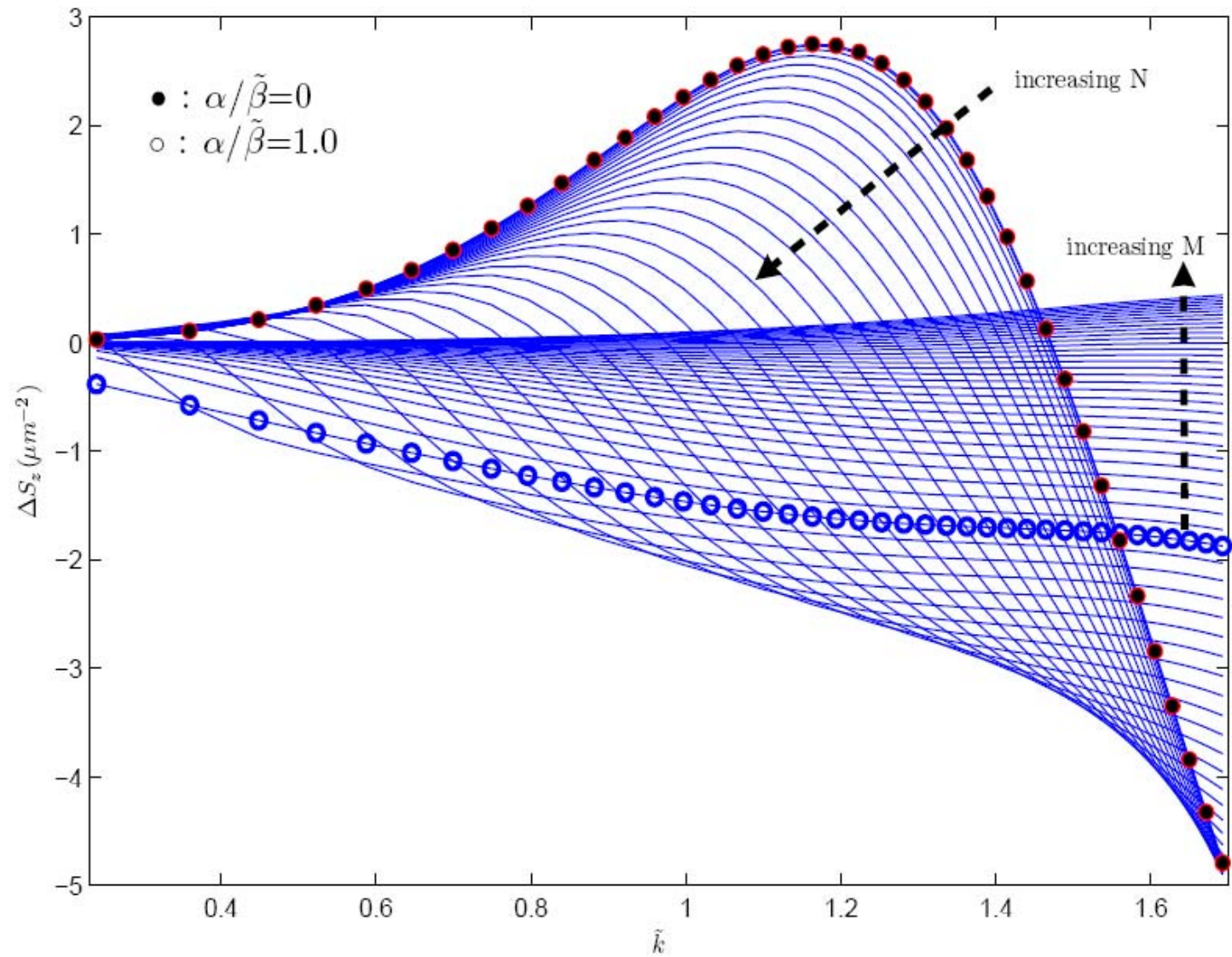


$\Delta S_z$  at sample edges vs  $\alpha/\tilde{\beta}$

Spin accumulation  
is essentially  
suppressed  
when  $\alpha = 2\tilde{\beta}$ .



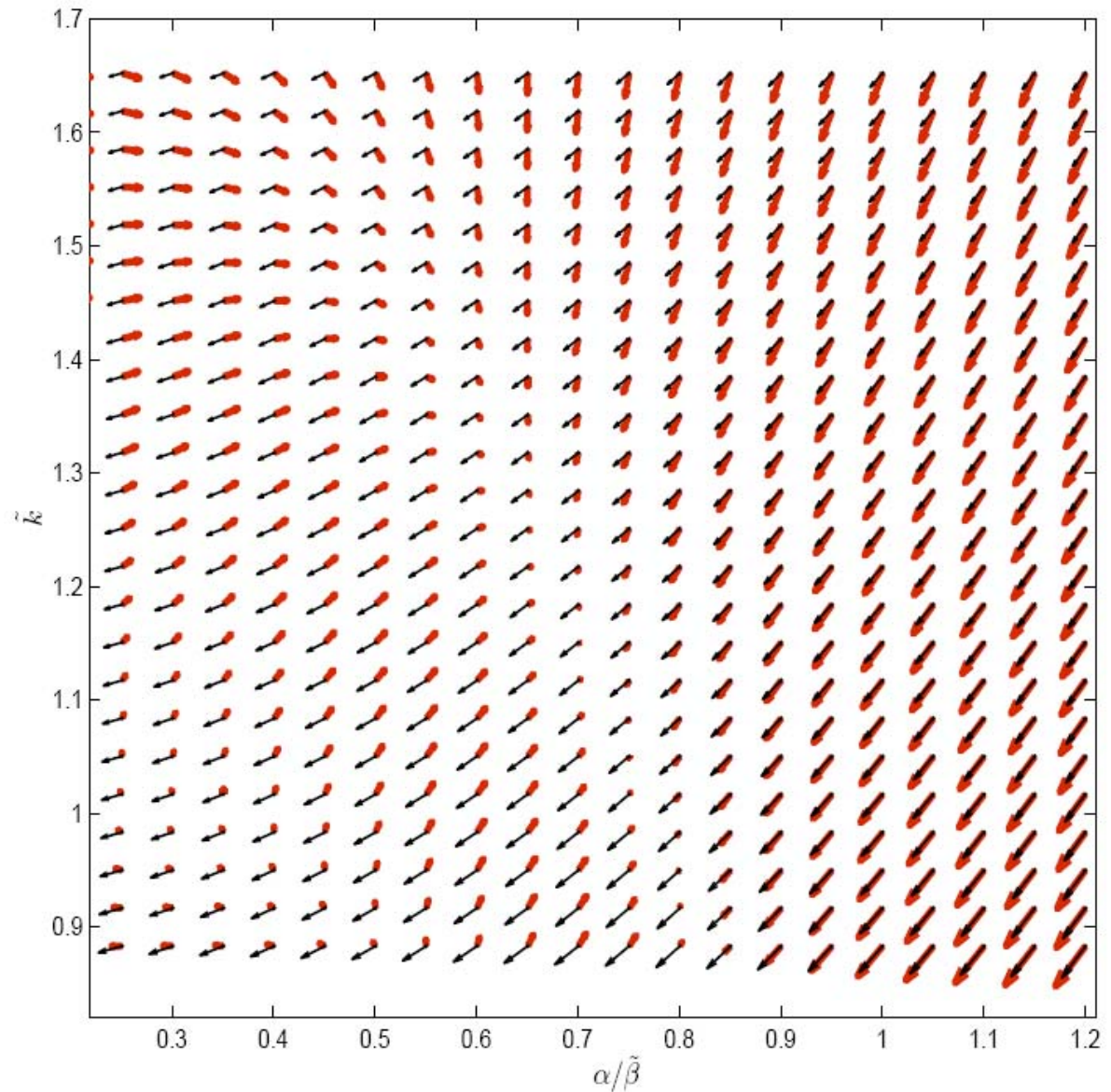
# $\Delta S_z$ at sample edges vs $\tilde{k}$



## Bulk spin polarization

Red arrows:  
contain full effects of  
Rashba and cubic- $k$   
Dresselhaus SOIs.

Black arrows:  
contain only effects of  
Rashba and linear- $k$   
Dresselhaus SOIs.

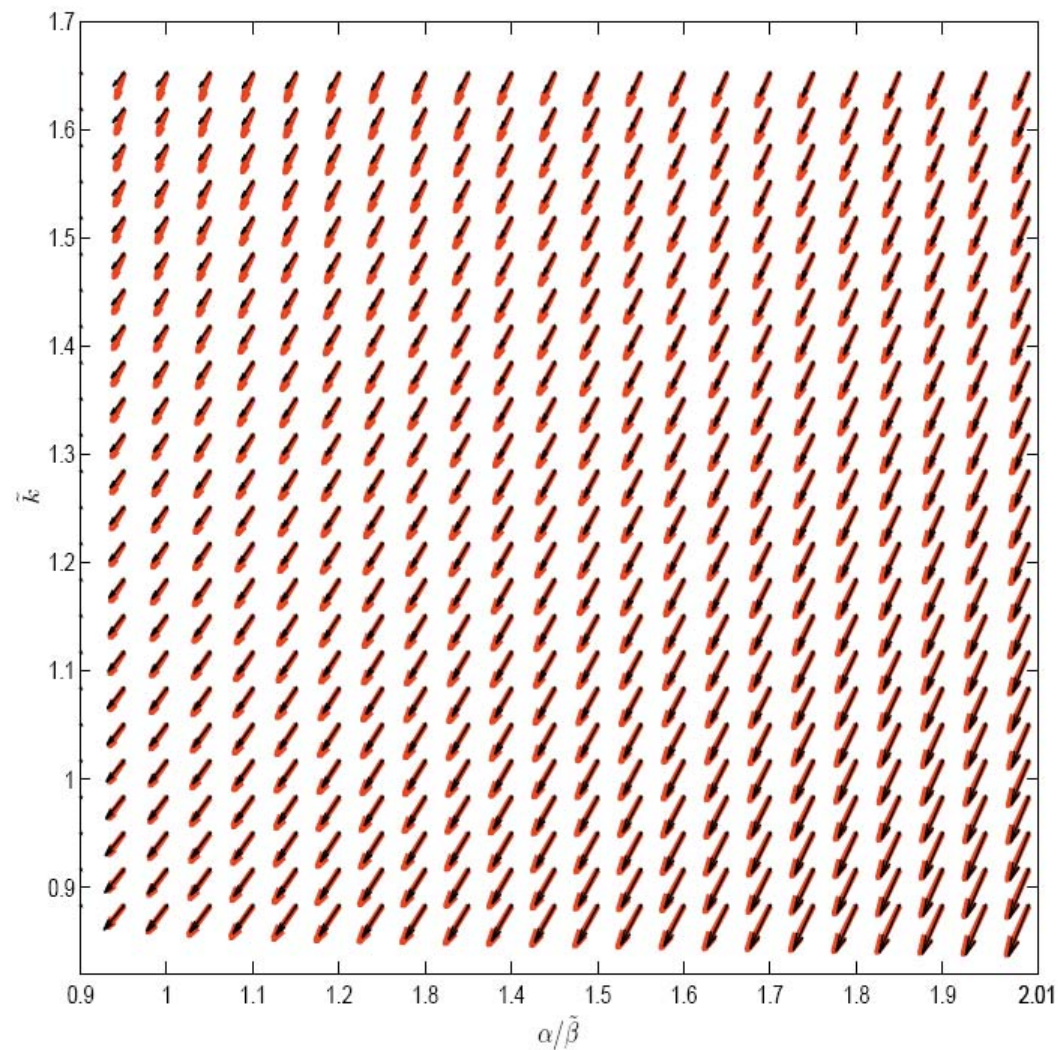




## Bulk spin polarization

Red arrows:  
contain full effects of  
Rashba and cubic- $k$   
Dresselhaus SOIs.

Black arrows:  
contain only effects of  
Rashba and linear- $k$   
Dresselhaus SOIs.



# Quantum Spin-Hall

# Quantum Spin Hall Effect and Topological Phase Transition in HgTe Quantum Wells

B. Andrei Bernevig,<sup>1,2</sup> Taylor L. Hughes,<sup>1</sup> Shou-Cheng Zhang<sup>1\*</sup>

We show that the quantum spin Hall (QSH) effect, a state of matter with topological properties distinct from those of conventional insulators, can be realized in mercury telluride–cadmium telluride semiconductor quantum wells. When the thickness of the quantum well is varied, the electronic state changes from a normal to an “inverted” type at a critical thickness  $d_c$ . We show that this transition is a topological quantum phase transition between a conventional insulating phase and a phase exhibiting the QSH effect with a single pair of helical edge states. We also discuss methods for experimental detection of the QSH effect.

$$\Psi = (|\Gamma_6, \frac{1}{2}\rangle, |\Gamma_6, -\frac{1}{2}\rangle, |\Gamma_8, \frac{3}{2}\rangle, |\Gamma_8, \frac{1}{2}\rangle, |\Gamma_8, -\frac{1}{2}\rangle, |\Gamma_8, -\frac{3}{2}\rangle)$$

$$H_{\text{eff}}(k_x, k_y) = \begin{pmatrix} H(k) & 0 \\ 0 & H^*(-k) \end{pmatrix},$$

$$H(k) = \varepsilon(k) + d_i(k)\sigma_i$$

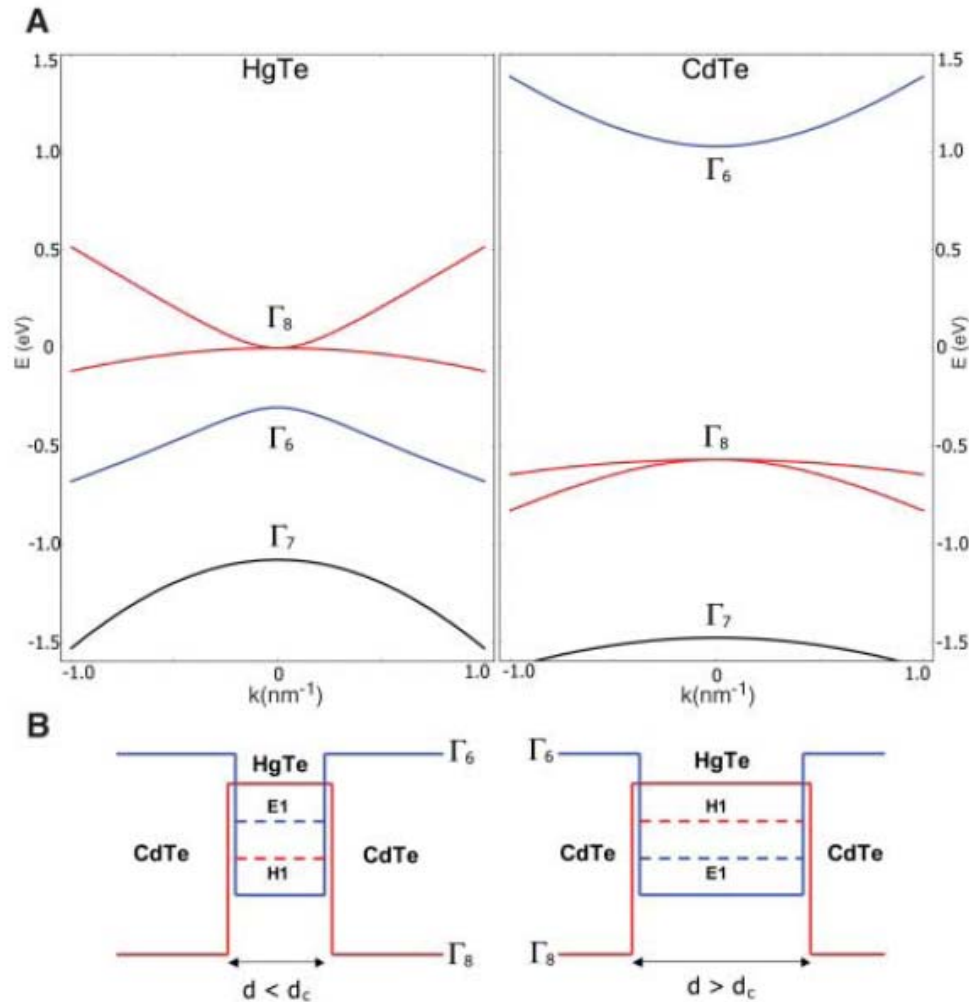


**Fig. 1. (A)** Bulk energy bands of HgTe and CdTe near the  $\Gamma$  point. **(B)** The CdTe-HgTe-CdTe quantum well in the normal regime  $E1 > H1$  with  $d < d_c$  and in the inverted regime  $H1 > E1$  with  $d > d_c$ . In this and other figures,  $\Gamma_8/H1$  symmetry is indicated in red and  $\Gamma_6/E1$  symmetry is indicated in blue.

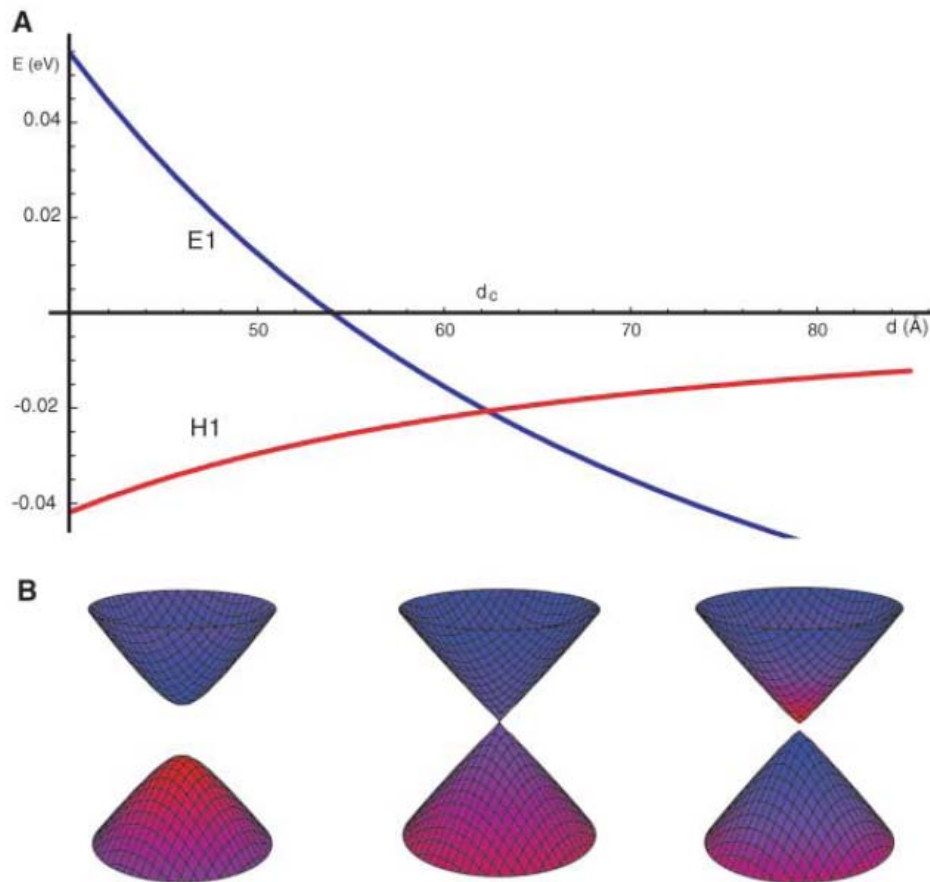
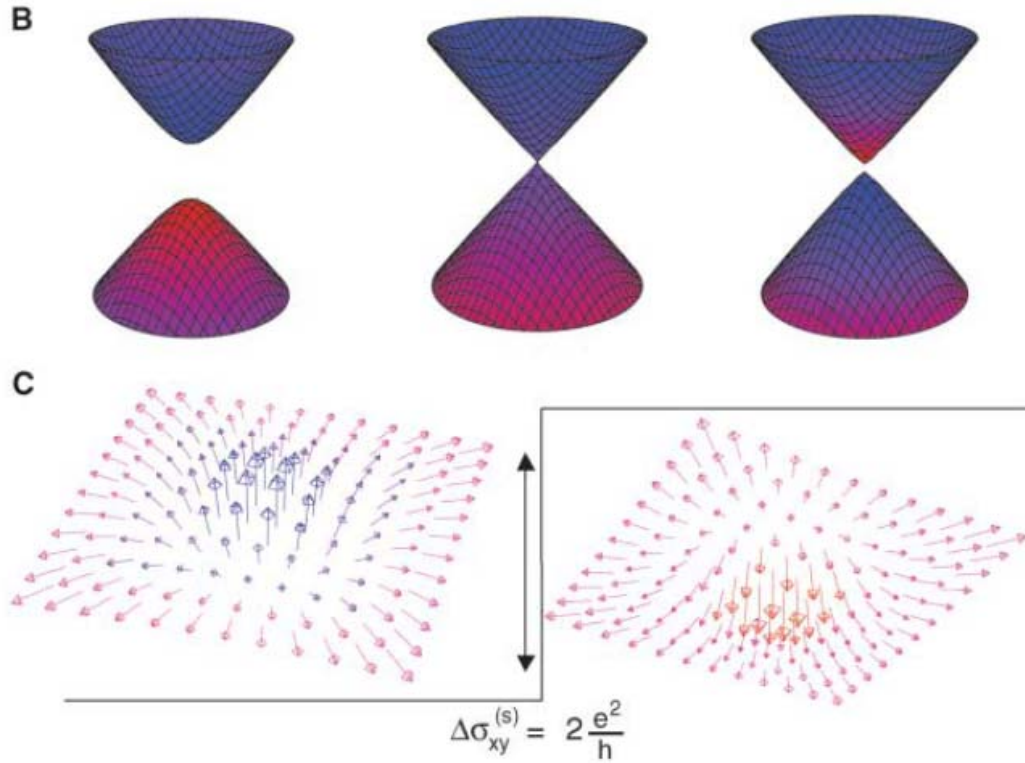


**Fig. 2.** (A) Energy of  $E1$  (blue) and  $H1$  (red) bands at  $k_{||} = 0$  versus quantum well thickness  $d$ . (B) Energy dispersion relations  $E(k_x, k_y)$  of the  $E1$  and  $H1$  subbands at  $d = 40, 63.5$ , and  $70$  Å (from left to right). Colored shading indicates the symmetry type of the band at that  $k$  point. Places where the cones are more red indicate that the dominant state is  $H1$  at that point; places where they are more blue indicate that the dominant state is  $E1$ . Purple shading is a region where the states are more evenly mixed. At  $40$  Å, the lower band is dominantly  $H1$  and the upper band is dominantly  $E1$ . At  $63.5$  Å, the bands are evenly mixed near the band crossing and retain their  $d < d_c$  behavior moving farther out in  $k$ -space. At  $70$  Å, the regions near  $k_{||} = 0$  have flipped their character but eventually revert back to the  $d < d_c$  farther out in  $k$ -space. Only this dispersion shows the meron structure (red and blue in the same band).





**(C)** Schematic meron configurations representing the  $d_i(k)$  vector near the  $\Gamma$  point. The shading of the merons has the same meaning as the dispersion relations above. The change in meron number across the transition is exactly equal to 1, leading to a quantum jump of the spin Hall conductance  $\sigma_{xy}^{(s)} = 2e^2/h$ . We measure all Hall conductances in electrical units. All of these plots are for  $\text{Hg}_{0.32}\text{Cd}_{0.68}\text{Te}$ -HgTe quantum wells.

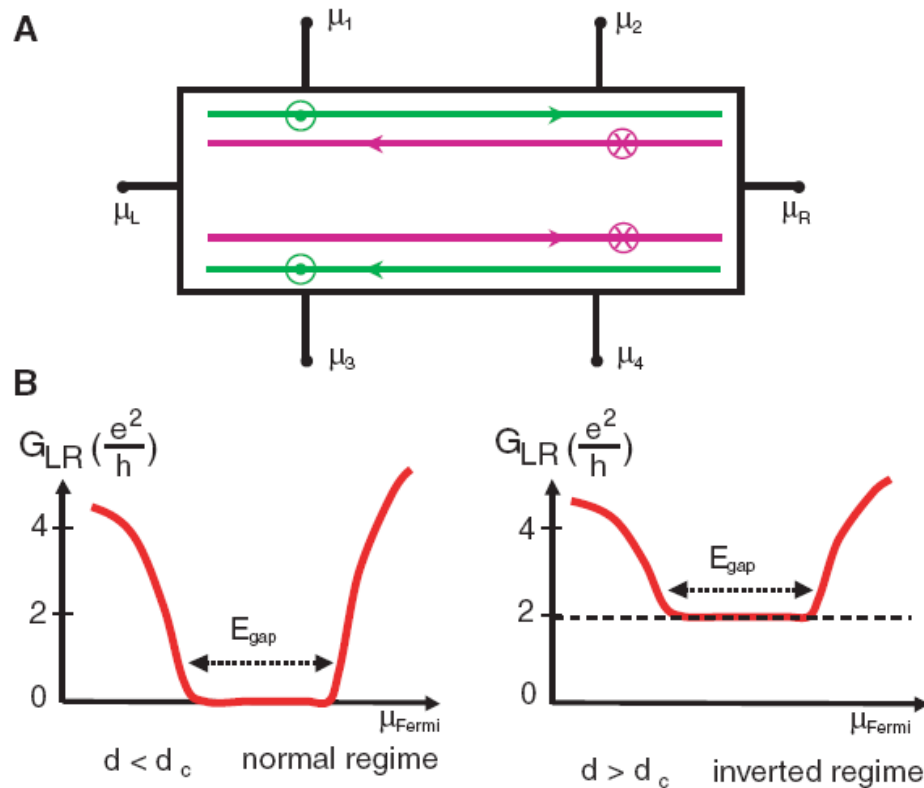
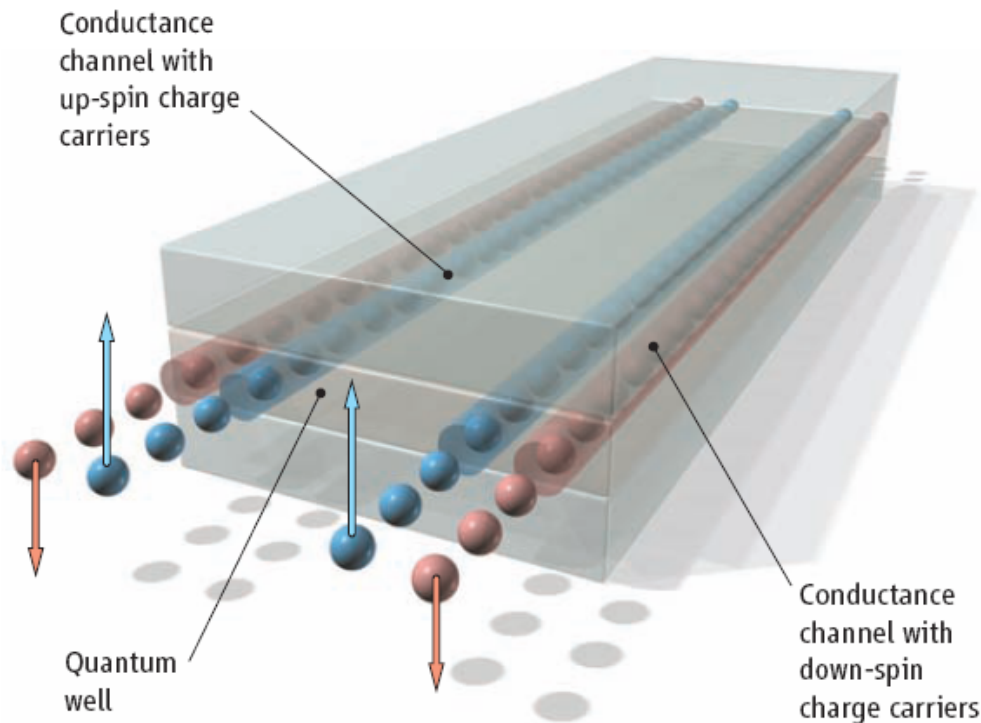


**Fig. 3. (A)** Experimental setup on a six-terminal Hall bar showing pairs of edge states, with spin-up states in green and spin-down states in purple. **(B)** A two-terminal measurement on a Hall bar would give  $G_{LR}$  close to  $2e^2/h$  contact conductance on the QSH side of the transition and zero on the insulating side. In a six-terminal measurement, the longitudinal voltage drops  $\mu_2 - \mu_1$  and  $\mu_4 - \mu_3$  vanish on the QSH side with a power law as the zero temperature limit is approached. The spin Hall conductance  $\sigma_{xy}^{(s)}$  has a plateau with the value close to  $2e^2/h$ .

# Quantum Spin Hall Insulator State in HgTe Quantum Wells

Markus König,<sup>1</sup> Steffen Wiedmann,<sup>1</sup> Christoph Brüne,<sup>1</sup> Andreas Roth,<sup>1</sup> Hartmut Buhmann,<sup>1</sup> Laurens W. Molenkamp,<sup>1\*</sup> Xiao-Liang Qi,<sup>2</sup> Shou-Cheng Zhang<sup>2</sup>



Schematic of the spin-polarized edge channels in a quantum spin Hall insulator.

Recent theory predicted that the quantum spin Hall effect, a fundamentally new quantum state of matter that exists at zero external magnetic field, may be realized in HgTe/(Hg,Cd)Te quantum wells. We fabricated such sample structures with low density and high mobility in which we could tune, through an external gate voltage, the carrier conduction from n-type to p-type, passing through an insulating regime. For thin quantum wells with well width  $d < 6.3$  nanometers, the insulating regime showed the conventional behavior of vanishingly small conductance at low temperature. However, for thicker quantum wells ( $d > 6.3$  nanometers), the nominally insulating regime showed a plateau of residual conductance close to  $2e^2/h$ , where  $e$  is the electron charge and  $h$  is Planck's constant. The residual conductance was independent of the sample width, indicating that it is caused by edge states. Furthermore, the residual conductance was destroyed by a small external magnetic field. The quantum phase transition at the critical thickness,  $d = 6.3$  nanometers, was also independently determined from the magnetic field-induced insulator-to-metal transition. These observations provide experimental evidence of the quantum spin Hall effect.

$$H_{\text{eff}}(k_x, k_y) = \begin{pmatrix} H(k) & 0 \\ 0 & H^*(-k) \end{pmatrix},$$

$$H = \varepsilon(k) + d_i(k)\sigma_i \quad (1)$$

where  $\sigma_i$  are the Pauli matrices, and

$$d_1 + id_2 = A(k_x + ik_y) \equiv Ak_+$$

$$d_3 = M - B(k_x^2 + k_y^2),$$

$$\varepsilon_k = C - D(k_x^2 + k_y^2). \quad (2)$$

## LETTERS

# Coupling of spin and orbital motion of electrons in carbon nanotubes

F. Kuemmeth<sup>1\*</sup>, S. Ilani<sup>1\*</sup>, D. C. Ralph<sup>1</sup> & P. L. McEuen<sup>1</sup>

Electrons in atoms possess both spin and orbital degrees of freedom. In non-relativistic quantum mechanics, these are independent, resulting in large degeneracies in atomic spectra. However, relativistic effects couple the spin and orbital motion, leading to the well-known fine structure in their spectra. The electronic states in defect-free carbon nanotubes are widely believed to be four-fold degenerate<sup>1–10</sup>, owing to independent spin and orbital symmetries, and also to possess electron–hole symmetry<sup>11</sup>. Here we report measurements demonstrating that in clean nanotubes the spin and orbital motion of electrons are coupled, thereby breaking all of these symmetries. This spin–orbit coupling is directly observed as a splitting of the four-fold degeneracy of a single electron in ultra-clean quantum dots. The coupling favours parallel alignment of the orbital and spin magnetic moments for electrons and antiparallel alignment for holes. Our measurements are consistent with recent theories<sup>12,13</sup> that predict the existence of spin–orbit coupling in curved graphene and describe it as a spin-dependent topological phase in nanotubes. Our findings have important implications for spin-based applications in carbon-based systems, entailing new design principles for the realization of quantum bits (qubits) in nanotubes and providing a mechanism for all-electrical control of spins<sup>14</sup> in nanotubes.

In this work we directly measure the intrinsic electronic spectrum by studying a single charge carrier, an electron or a hole, in an ultra-clean carbon nanotube quantum dot. Remarkably, we find that the expected four-fold symmetry and electron–hole symmetry are broken by spin–orbit coupling, demonstrating that the spin and orbital motion in nanotubes are not independent degrees of freedom. The observed spin–orbit coupling further determines the filling order in the many-electron ground states, giving states quite different from models based purely on electron–electron interactions.



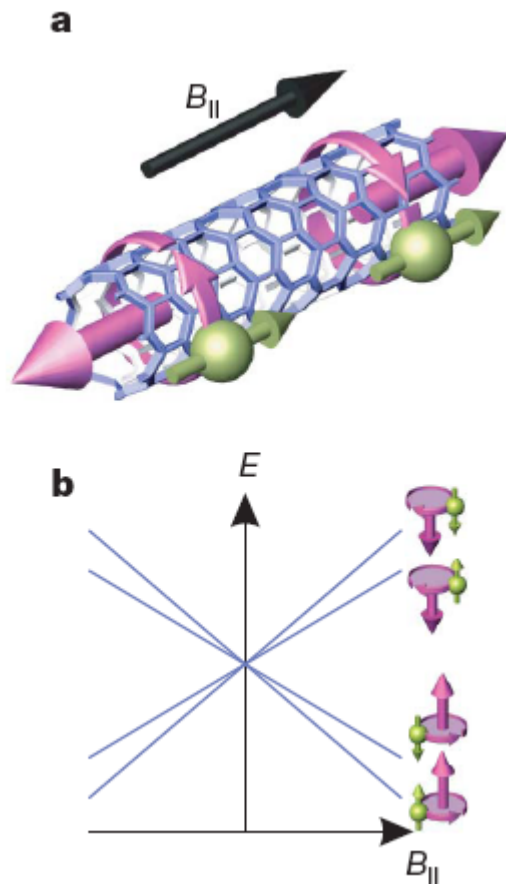
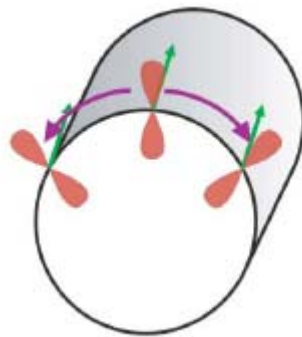
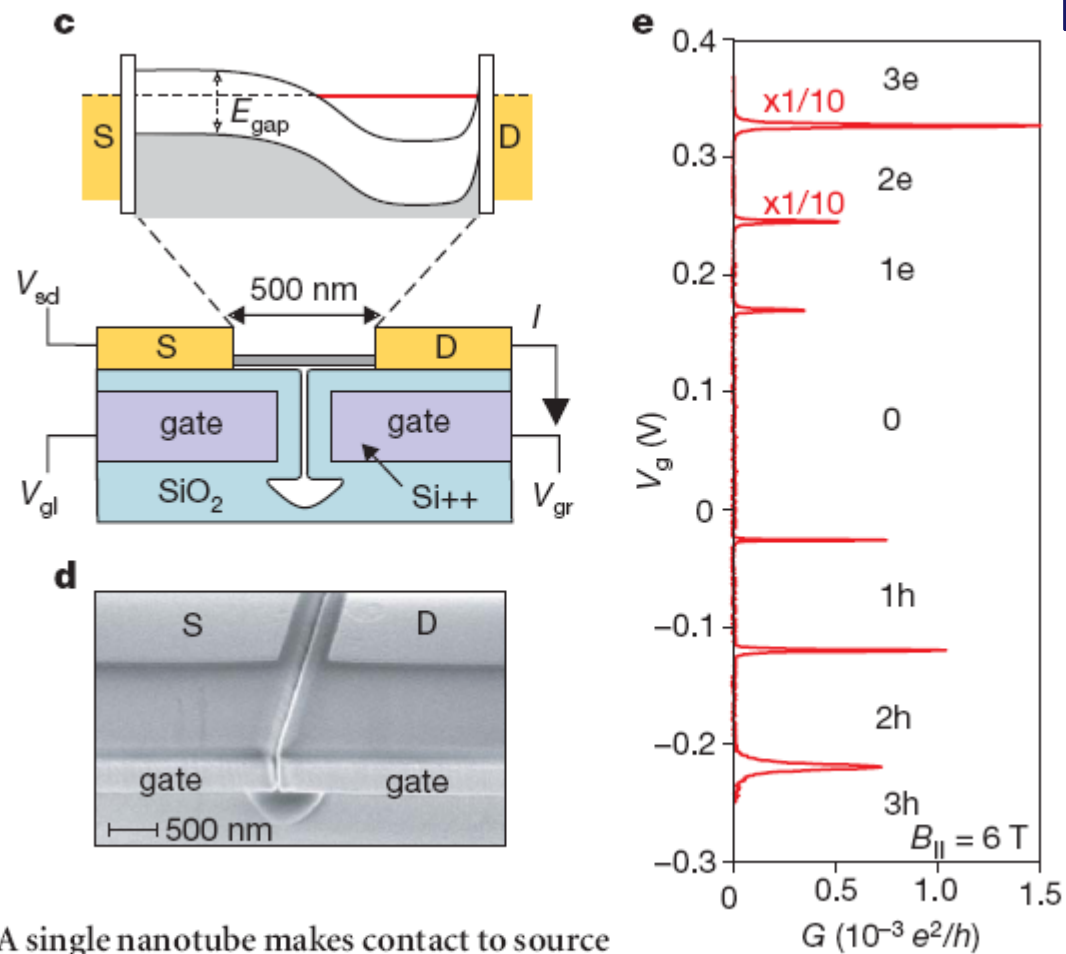


**Figure 1 | Few-electron carbon nanotube quantum dot devices.** **a**, Electrons confined in a nanotube segment have quantized energy levels, each four-fold degenerate in the absence of spin–orbit coupling and defect scattering. The purple arrow at the left (right) illustrates the current and magnetic moment arising from clockwise (anticlockwise) orbital motion around the nanotube. The green arrows indicate positive moments due to spin. **b**, Expected energy splitting for a defect-free nanotube in a magnetic field  $B_{\parallel}$  parallel to the nanotube axis in the absence of spin–orbit coupling: At  $B_{\parallel} = 0$  T, all four states are degenerate. With increasing  $B_{\parallel}$  each state shifts according to its orbital and spin magnetic moments, as indicated by purple and green arrows respectively.



**Theoretical model for spin–orbit interaction in nanotubes and the energy level spectroscopy of a single hole.** **a**, Schematic of an electron with spin parallel to the nanotube axis revolving around the nanotube circumference. The carbon  $p_z$  orbitals (red) are perpendicular to the surface. In the rest frame of the electron, the  $p_z$  orbital rotates around the spin.



respectively. **c**, Device schematic. A single nanotube makes contact to source and drain electrodes, separated by 500 nm, and is gated from below by two gate electrodes. The two gate voltages ( $V_{gl}$ ,  $V_{gr}$ ) are used to create a quantum dot localized above the right or left gate electrodes. The energy band diagram is shown for the first case. **d**, Scanning electron micrograph of the device, taken before nanotube growth to avoid damage to the nanotube. **e**, The measured linear conductance,  $G = dI/dV_{sd}$ , as function of gate voltage,  $V_g$ , for a dot localized above the right gate ( $B_{||} = 6$  T, temperature  $T = 30$  mK). The number of electrons or holes in the dot is indicated. The conductance of the top two peaks is scaled by 1/10.

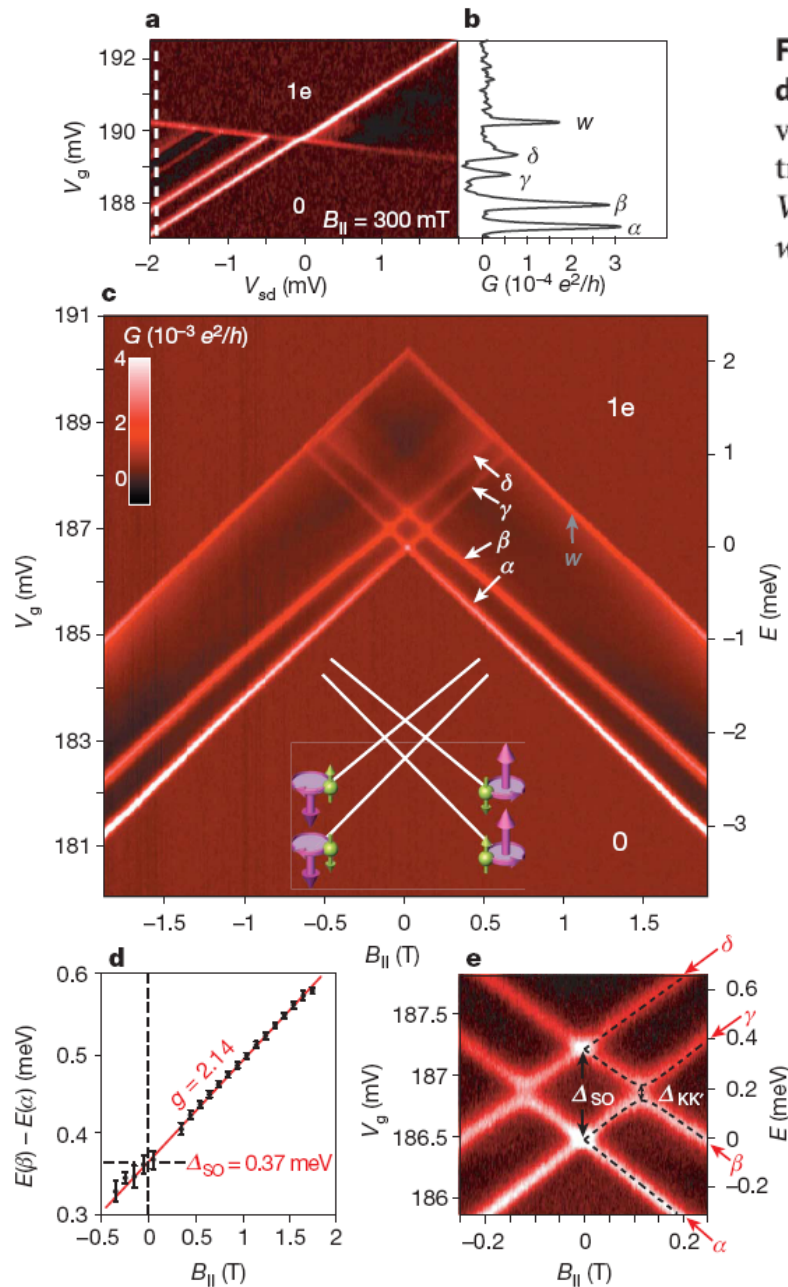


**Figure 2 | Excited-state spectroscopy of a single electron in a nanotube dot.** **a**, Differential conductance,  $G = dI/dV_{sd}$ , measured as function of gate voltage,  $V_g$ , and source-drain bias,  $V_{sd}$ , at  $B_{||} = 300$  mT, displaying transitions from zero to one electron in the dot. **b**, A line cut at  $V_{sd} = -1.9$  mV reveals four energy levels  $\alpha$ ,  $\beta$ ,  $\gamma$  and  $\delta$  as well as another peak  $w$  corresponding to the edge of the one-electron Coulomb diamond.

**c**,  $G = dI/dV_{sd}$  as a function of  $V_g$  and  $B_{||}$  at a constant bias  $V_{sd} = -2$  mV. The resonances  $\alpha$ ,  $\beta$ ,  $\gamma$ ,  $\delta$  and  $w$  are indicated. The energy scale on the right is determined by scaling  $\Delta V_g$  with the conversion factor  $\alpha = 0.57$  extracted from the slopes in **a**. Inset: orbital and spin magnetic moments assigned to the observed states. **d**, Extracted energy splitting between the states  $\alpha$  and  $\beta$  as a function of  $B_{||}$  (dots). The linear fit (red line) gives a Zeeman splitting with  $g = 2.14 \pm 0.1$ , and a zero-field splitting of  $\Delta_{SO} = 0.37 \pm 0.02$  meV (error bars, 1 s.d.). **e**, Magnified view of panel **c** showing the zero-field splitting due to spin-orbit interaction ( $\Delta_{SO}$ ) as well as finite-field anticrossing due to  $K$ - $K'$  mixing ( $\Delta_{KK'}$ ). Dashed lines show the calculated spectrum using  $\Delta_{KK'} = 65$   $\mu$ eV.



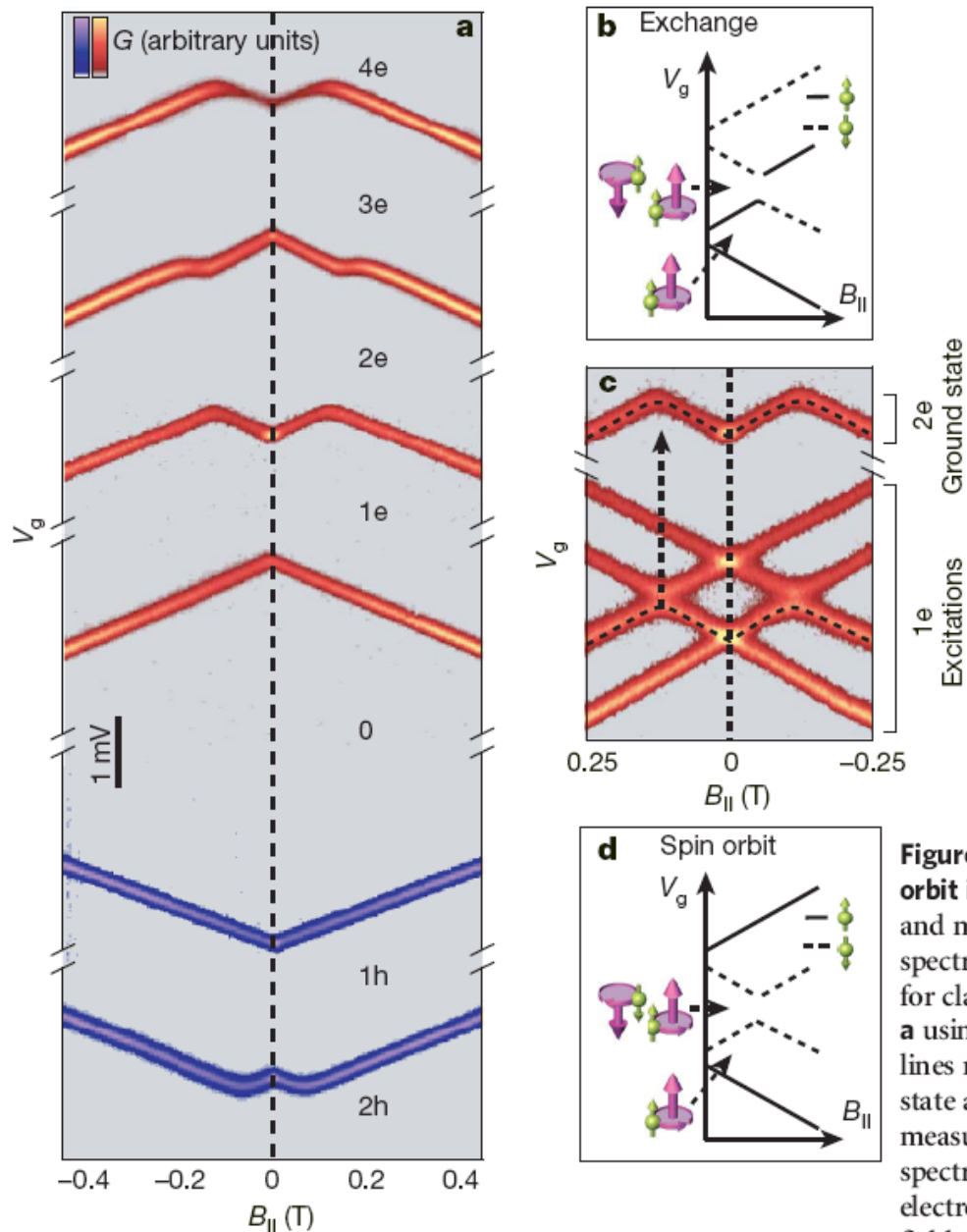


**Figure 3 | The many-electron ground states and their explanation by spin-orbit interaction.** **a**,  $G = dI/dV_{sd}$ , measured as a function of gate voltage,  $V_g$ , and magnetic field,  $B_{||}$ , showing Coulomb blockade peaks (carrier addition spectra) for the first four electrons and the first two holes (data are offset in  $V_g$  for clarity). **b**, Incorrect interpretation of the addition spectrum shown in **a** using a model with exchange interactions between electrons. Dashed/solid lines represent addition of down/up spin moments. The two-electron ground state at low fields, indicated at the left, is a spin triplet. **c**, Comparison of the measured two-electron addition energy from **a** with the one-electron excitation spectrum from Fig. 2e. **d**, Schematic explanation of the data in **a** using electronic states with spin-orbit coupling: The two-electron ground state at low fields, indicated on the left, is neither a spin-singlet nor a spin-triplet state.

**The End**